

Aus dem Institut für Physik der Universität Potsdam

# **Synchronization Transitions in Complex Systems**

## **Dissertation**

zur Erlangung des akademischen Grades  
Doktor der Naturwissenschaften  
(Dr. rer. nat.)  
in der Wissenschaftsdisziplin Theoretische Physik

eingereicht an der  
Mathematisch-Naturwissenschaftlichen Fakultät  
der Universität Potsdam

von  
**Dmitri Topaj**  
geboren am 23. März 1970 in St. Petersburg

Potsdam, im September 2001



# Kurzfassung

Gegenstand dieser Arbeit ist die Untersuchung generischer Synchronisierungsphänomene in interagierenden komplexen Systemen. Diese Phänomene werden u. a. in gekoppelten deterministischen chaotischen Systemen beobachtet. Bei sehr schwachen Interaktionen zwischen individuellen Systemen kann ein Übergang zum schwach kohärenten Verhalten der Systeme stattfinden. In gekoppelten zeitkontinuierlichen chaotischen Systemen manifestiert sich dieser Übergang durch den Effekt der Phasensynchronisierung, in gekoppelten chaotischen zeitdiskreten Systemen durch den Effekt eines nichtverschwindenden makroskopischen Feldes.

Der Übergang zur Kohärenz in einer Kette lokal gekoppelter Oszillatoren, beschrieben durch Phasengleichungen, wird im Bezug auf die Symmetrien des Systems untersucht. Es wird gezeigt, daß die durch die Symmetrien verursachte Reversibilität des Systems nichttriviale topologische Eigenschaften der Trajektorien bedingt, so daß das als dissipativ konstruierte System in einem ganzen Parameterbereich quasi-Hamiltonische Züge aufweist, d. h. das Phasenvolumen ist im Schnitt erhalten, und die Lyapunov-Exponenten sind paarweise symmetrisch.

Der Übergang zur Kohärenz in einem Ensemble global gekoppelter chaotischer Abbildungen wird durch den Verlust der Stabilität des entkoppelten Zustandes beschrieben. Die entwickelte Methode besteht darin, die Selbstkonsistenz des makroskopischen Feldes aufzuheben, und das Ensemble in Analogie mit einem Verstärkerschaltkreis mit Rückkopplung durch eine komplexe lineare Übertragungsfunktion zu charakterisieren. Diese Theorie wird anschließend für einige theoretisch interessanten Fälle verallgemeinert.





# Abstract

Subject of this work is the investigation of generic synchronization phenomena in interacting complex systems. These phenomena are observed, among all, in coupled deterministic chaotic systems. At very weak interactions between individual systems a transition to a weakly coherent behavior of the systems can take place. In coupled continuous time chaotic systems this transition manifests itself with the effect of phase synchronization, in coupled chaotic discrete time systems with the effect of non-vanishing macroscopic mean field.

Transition to coherence in a chain of locally coupled oscillators described with phase equations is investigated with respect to the symmetries in the system. It is shown that the reversibility of the system caused by these symmetries results to non-trivial topological properties of trajectories so that the system constructed to be dissipative reveals in a whole parameter range quasi-Hamiltonian features, i. e. the phase volume is conserved on average and Lyapunov exponents come in symmetric pairs.

Transition to coherence in an ensemble of globally coupled chaotic maps is described with the loss of stability of the disordered state. The method is to break the self-consistency of the macroscopic field and to characterize the ensemble in analogy to an amplifier circuit with feedback with a complex linear transfer function. This theory is then generalized for several cases of theoretic interest.



# Contents

<b>1</b>	<b>Introduction</b>	<b>1</b>
1.1	Describing complex systems . . . . .	2
1.1.1	System and environment . . . . .	2
1.1.2	Determinism, uncertainty and complexity . . . . .	3
1.1.3	Deterministic chaos as source of complexity . . . . .	5
1.1.4	Entropy production vs. emergence of order . . . . .	8
1.1.5	Synchronization as emergence of order . . . . .	9
1.1.6	Modelling synchronization effects in complex systems . . . . .	10
1.2	Complete and weak synchronization . . . . .	11
1.2.1	Topological view on the onset of synchronization . . . . .	12
1.2.2	Statistical approach to the onset of synchronization . . . . .	13
1.3	Phase of a signal and phase synchronization . . . . .	14
1.3.1	Phase equations around stable periodic solutions . . . . .	14
1.3.2	Phase synchronization by external force and mutual synchronization . . . . .	17
1.3.3	Phase synchronization in presence of noise . . . . .	18
1.3.4	Phase synchronization of chaotic systems . . . . .	19
1.4	Summary . . . . .	21
<b>2</b>	<b>Synchronization vs. reversibility in an oscillator lattice with nearest-neighbor coupling</b>	<b>23</b>
2.1	Introduction . . . . .	23
2.2	The phase lattice model and its properties . . . . .	24
2.2.1	Basic model . . . . .	24
2.2.2	Properties of the model . . . . .	25
2.2.3	Small and large couplings . . . . .	26
2.2.4	Clustering hierarchy . . . . .	27
2.2.5	Quasi-Hamiltonian dynamics for small couplings . . . . .	30
2.3	Reversibility of regular and chaotic regimes . . . . .	32
2.3.1	Three oscillators . . . . .	32
2.3.2	Reversibility . . . . .	33
2.3.3	Reversibility of the oscillator lattice . . . . .	35
2.3.4	Three coupled oscillators revisited . . . . .	36
2.3.5	Four coupled oscillators . . . . .	36
2.3.6	Large number of oscillators . . . . .	40
2.4	Destruction of reversibility . . . . .	41
2.4.1	Non-uniform frequency distribution . . . . .	41
2.4.2	Non-symmetric coupling function . . . . .	45
2.4.3	On $P$ -symmetric solutions and their destruction . . . . .	47
2.5	Summary . . . . .	51

<b>3</b>	<b>Transition to coherence in globally coupled maps</b>	<b>53</b>
3.1	Introduction . . . . .	53
3.1.1	Formulation of the problem . . . . .	54
3.1.2	Finite-size effects . . . . .	54
3.2	Linear stability analysis . . . . .	55
3.2.1	Breaking self-consistency condition . . . . .	55
3.2.2	Linearization . . . . .	56
3.2.3	On "good" and "bad" maps . . . . .	56
3.2.4	Ensemble as a linear filter . . . . .	57
3.2.5	Stability of a linear filter . . . . .	57
3.2.6	Stability of a feedback loop . . . . .	59
3.3	Linear response of chaotic maps . . . . .	60
3.3.1	Method 1: static response of the $p$ -iterate . . . . .	60
3.3.2	Method 2: spectral decomposition . . . . .	61
3.4	Transition to coherence in coupled Bernoulli maps . . . . .	62
3.4.1	The system . . . . .	62
3.4.2	Calculation of transfer function: method 1 . . . . .	63
3.4.3	Calculation of transfer function: method 2 . . . . .	67
3.4.4	Transition points . . . . .	68
3.4.5	Numerics . . . . .	69
3.4.6	Discrete Hopf bifurcation at $\varepsilon_{c1}$ . . . . .	69
3.4.7	Asymmetric subcritical bifurcation at $\varepsilon_{c2}$ . . . . .	71
3.5	Extensions of the theory . . . . .	74
3.5.1	Dynamics with additive noise . . . . .	74
3.5.2	Complex dynamical dependence on the mean field . . . . .	75
3.5.3	Ensembles of non-identical systems . . . . .	78
3.6	Possible further extentions . . . . .	82
3.6.1	Structurally unstable systems . . . . .	82
3.6.2	Continuous time systems . . . . .	84
3.7	Summary . . . . .	85
	<b>Résumé</b>	<b>87</b>
	<b>Acknowledgements</b>	<b>91</b>
	<b>Bibliography</b>	<b>93</b>

*Unter System ... soll jedes Wirklich-Seiende verstanden werden, das sich in einer äußerst komplexen, veränderlichen, im Ganzen nicht beherrschbaren Umwelt identisch hält.*

*(Niklas Luhmann)*

# Chapter 1

## Introduction

Is Plato's Demiurge needed to create Cosmos out of Chaos? Is a Hobbes' dictator needed to establish a civil order out of the ground state anarchy? Or is it cabbalistic Allmighty whose emanations from an undefinable Ein-Soph state into the present form of the world we now call Genesis (or, maybe, quantum-mechanical measurement)? Since the antique atomism it has been a fundamental problem of natural philosophy to discover how order arises from irregular microscopic states of matter. There had to be either some higher force or some coherence in the individual irregular dynamics for macroscopic order to be explained.

On the other hand, nature was regarded in the sense of Newtonian dynamics as a huge closed conservative and deterministic system. Given an initial state the whole evolution in nature could be tracked forward and backward in time by a Laplacian demon. Thus there was no place for any irregularity in the dynamics of a closed system. Every irregularity had therefore to be ascribed either to the openness of the system or to insufficient knowledge of its initial state. This classical picture was destroyed by Poincaré who recognized that no calculable solutions exist for the locally well-defined 3-body-problem of celestial mechanics. Later on the Birkhoff and Smale mathematically proved the possibility for solutions of problems of classical mechanics to be deterministically chaotic, i. e. unpredictable on large time scales.

Microscopically regular dynamics can thus cause chaos on larger scales. Macroscopically regular dynamics can be caused in its turn by microscopically irregular motion. The first observation leads to the necessity to redefine and to deeper understand complexity. The second one attracts scientific attention to synchronization phenomena.

First discovered by Huygens in the middle of the 17th century synchronization is now known to appear in a vast number of scientific disciplines: in physics and life sciences, in mechanical and electrical engineering, in chemistry and acoustics, in economy and sociology etc. Huygens [43] observed that two pendulum clocks became completely synchronized when placed on a common console. At the end of the 19th century Rayleigh [83] described the effect of mutual damping of slightly detuned organ pipes due to interactions. In the 1940s the effect of synchronization of mechanical rotators [12] was found. The first steps in the theoretic description of the effect of synchronization were made in the works of Appleton [3] and Van der Pol [22]. In the 1980s the effect of synchronization in chaotic systems was found (cf. [71]),

giving rise to an intensive research in this field.

This work on generic synchronization phenomena in complex deterministic dynamical systems is organized as follows: in the rest of this chapter the concepts of complex systems and synchronization as well as the theoretical approach in studying these phenomena are introduced, then typical kinds of interactions between elements of a complex system and different types of synchronization, i. e. complete, weak and phase synchronization are discussed in more details. Chapter 2 is devoted to the effect of phase synchronization in lattices of dissipative chaotic systems with nearest-neighbor couplings. Synchronization phenomena in a reduced system of phase equations are investigated with respect to the symmetries of the dynamics. In Chapter 3 a transition to coherence in globally coupled discrete chaotic dynamical systems is described. An analytic approach to the problem of finding the transition point is derived.

## 1.1 Describing complex systems

There exists a deep controversy concerning what one means while speaking about complex systems. Without intention to stick with this discussion we want to clarify now what is understood under complex systems in the framework of this thesis.

### 1.1.1 System and environment

A system is an entity consisting of some elements obeying some inherent rules and interacting with each other and with the rest of the world. Not every collection of elements, rules and interactions can be meaningfully called a system. Persistence at least in one constituent of the above definition is usually required. One can speak about a system consisting of the same elements, or a system of changing elements obeying the same dynamic equations, or a system with changing elements and mutating rules but behaving with a certain constancy in its environment.

In this sense the concept of system is a concept of an artificial reduction of complexity of the world when trying to describe its certain aspect. This concept is therefore subjective. Essentially, environment objectively exists (in a materialistic philosophy) while a system only exists as observation of a system, i. e. distinguishing between system and its environment. A system can be studied, its environment not. Otherwise one would have to enlarge the system definition for relevant aspects of the environment.

As the environment cannot be studied assumptions on its interaction with the system under investigation have to be made. If no interaction between a system and its environment takes place then this system is called closed, otherwise it is called open. For an open system all external forces must be considered as given and can be modelled with regular, irregular or even random terms in corresponding dynamical equations.

Elements constituting the system can also be treated as systems, which is the reductionist paradigm of classical science. The most fundamental elements in this hierarchy are usually

assumed to have the simplest inherent dynamical laws, continuous or discrete. These dynamical laws can be deterministic or contain stochastic terms, their dynamics can also be regular or chaotic.

### 1.1.2 Determinism, uncertainty and complexity

Saying that a system is complex means implicitly that contemporary science cannot handle all its aspects. Otherwise this complexity would be trivial in the reductionist approach. The current definition of complex systems as systems with nonlinear or/and stochastic terms in their mathematical formulation is well established due to lack of knowledge how to deal with generic nonlinear systems. Complexity means inability to understand and to predict, which makes this term anthroposophic and reflexive. It is the man's problem, not that of the nature.

Hence it is the question of our subjective selfdefinition how to deal with complexity, i. e. after having realized that there are no exact synopsis and prognosis. The two opposing metaphysical doctrines of the 19th century, determinism of Laplace [56] and tychism of Peirce [68] put the blame for it on the two different parties. Pierce stated that it is the nature itself that is ruled by the "law of chance" while Laplace argued that the nature can be exactly described and predicted if an exact knowledge about its initial state and dynamical rules is provided. The Laplacian determinism which dominated the natural sciences for a century means that no matter how many variables one needs to completely describe a system (a direct product of all variables needed for a complete description of a system is called phase space of a dynamical system), obtaining exact information about the dynamical rules and just one state at any time moment gives complete information about the past and the future states of the system. These states are lying on a path (trajectory) in the phase space which is defined by its any point because (the principle of causality) trajectories in the phase space cannot intersect.

Introducing complexity, one admits the limitedness of one's knowledge, accuracy and rationality. This means that one usually calls a system complex if either its initial state or its dynamical rule or the formalism of describing it are not exact but possibly contain some errors (note that our mathematics is not free of paradoxes as well – of course, one could equally blame the nature and/or our way of thought for it).

Therefore the probabilistic approach to complex systems is unavoidable, either in describing initial conditions (with letting dynamical rules remain deterministic) or in admitting stochastic terms in the equations of motion. In fact, these two approaches, deterministic and stochastic dynamics, are not completely antagonistic. Ergodic theory of complex systems [97, 26, 18] unifies them. To some extent, the probabilistic theory of a complex deterministic system can be understood as a coarse-grained description of its temporal evolution.

If the dynamic rules are deterministic and no nonlinearity enters the corresponding mathematical model then its solution can be written in a trivial way as superposition of solutions of its constituting elements. In linear systems errors in the definition of the initial condition can be easily handled so that the complexity related to these errors does not grow with time.

Complex systems are therefore often defined as systems of many interacting nonlinear el-

## CHAPTER 1. INTRODUCTION

ements, or as systems of many nonlinearly interacting elements, or as systems of many interacting elements with complex external forces. The dynamics generated by complex systems can be itself either regular, e. g. periodic or quasiperiodic, or irregular, e. g. intermittent, chaotic or stochastic.

In the framework of stochastic models even linear equations are not easy to deal with and thus should be called complex. In this work we restrict ourselves to deterministic dynamical equations only.

The question is now how to quantify complexity. While there are still many different approaches to this problem (cf. [6]) it is clear that the measure of complexity should be a measure of inexactness, or after Ruelle [91] "a measure of randomness in the system". The corresponding physical quantity is entropy.

If possible states of a system are taken by the system with some probability then the information entropy  $H$ , i. e. the mean uncertainty of this probability distribution is given [95] by

$$H = - \langle \log p \rangle$$

Here  $\langle \cdot \rangle$  means averaging over accessible phase space, in the case of a continuous probability distribution this reads

$$H = - \int p(x) \log p(x) dx$$

The information entropy corresponds to the amount of information additionally needed to resolve uncertainty in order to specify exactly in which state the system is at a given time.\*

To quantify the complexity of the time evolution of a complex system one can use the concept of entropy of a finite symbolic sequence (cf. [25]). Imagine the phase space of a dynamical system partitioned in some way into  $M$  regions. Each region is assigned a symbol  $a_k$  (like  $A, C, G, T$  with  $M = 4$  in the coding of DNA). Then every trajectory in the phase space is represented by a sequence of visited symbols  $\{A_k\}$  like

$$\dots, C, A, C, G, A, T, T, T, G, C, A, \dots$$

For every sequence, finite or infinite, one can define the probability  $p_n(A_1, A_2, \dots, A_n)$  to find the given subsequence (block)  $\{A\}_n = (A_1, A_2, \dots, A_n)$  of the length  $n$ .

The entropy per block of the length  $n$  is then

$$H_n = - \sum_{\forall \{A\}_n} p_n(\{A\}_n) \log p_n(\{A\}_n)$$

The uncertainty of the symbol following the block is

---

\*Note that the information entropy is not a covariant quantity, it varies with transformations of phase space variables. Contrary to this, a transformation entropy  $K\{p(x), \hat{p}(x)\}$  (the information gain) of a transition from one probability distribution  $p(x)$  to another one  $\hat{p}(x)$  is covariant

$$K\{p(x), \hat{p}(x)\} = - \int p(x) \log \frac{p(x)}{\hat{p}(x)} dx$$



$$h_n = H_{n+1} - H_n$$

The entropy of the source  $h$  of the sequence is defined by

$$h = \lim_{n \rightarrow \infty} h_n = \lim_{n \rightarrow \infty} H_n/n \quad (1.1)$$

For a very broad class of generating processes (ergodic processes) was shown [49] that

$$H_{n+1} \geq H_n \quad \text{and} \quad \frac{H_{n+1}}{n+1} \leq \frac{H_n}{n} \quad (1.2)$$

This ensures existence of the limit (1.1). The value  $h$  (measured in bits per time) is the asymptotic rate of entropy production in the system with time (i. e. with adding the next symbol to the sequence) so that the total uncertainty in a complex system asymptotically grows with time, if  $h > 0^\dagger$ .

Note that entropy as a measure of complexity can be used independently of the nature of the process that generates the symbolic sequence. And one can expect that complex sequences are generated in every non-linear system which is large enough. This enlightens the historical fact that general systems theories and theories of complex systems arose independently in different fields of science in the first three decades of the 20th century. In the second part of the 20th century concepts of complexity and complex systems were applied in practically every scientific discipline (cf. [7]).

E. g. in theoretical biology the principal ideas of what was called the "theory of complex systems" was developed by Berthalanffy [106], in economics by Hayek [41], in the theory of state and governmental management by Bogdanov [14]. A discussion on complexity can also be found in Bakhtine's works on linguistics of that time [9]. In the 60s these or similar ideas were developed in chemistry by Prigogine [34] and in sociology by Luhmann [60] and advanced later in the 70s in numerous works on Haken's synergetics [40].

In some disciplines the measure of complexity  $h$  could be directly calculated. For instance, Shannon [96] himself calculated the entropy of printed English texts. Investigations of texts in different languages and music pieces [44] followed, having led to a sort of quantitative theory of aesthetic values [92]. Investigation of properties of biosequences (cf. [28]) developed itself to an independent science of mathematical evolution (cf. [27]).

To understand generic effects in complex systems models that are known to generate typical (in the sense of asymptotic entropy production) complex dynamics are usually investigated – so-called deterministic chaotic systems.

### 1.1.3 Deterministic chaos as source of complexity

A dynamical rule of a complex system can be described by an evolution operator  $F^{t_1, t}$  which transforms the state of the system at some time  $t_1$  as described by a point  $x(t_1)$  in the ( $n$ -dimensional) phase space into the state  $x(t_2)$  at another time  $t_2 = t_1 + t$ . If time is continuous

---

<sup>†</sup>From the equations (1.2) follows directly  $h \geq 0$ , which corresponds to the second principle of equilibrium thermodynamics.

## CHAPTER 1. INTRODUCTION

then the evolution operator describes for every initial point in the phase space a continuous trajectory, if time is discrete then the evolution is a directed graph (described by a map).

Of course, it is always possible to reduce a trajectory to a directed graph by considering discretized times (so-called stroboscopic map). If the evolution operator is given by a set of ordinary differential equations then it describes a flow in the phase space, its stroboscopic maps are all invertible. This is ensured by the fact that trajectories in the phase space cannot intersect<sup>‡</sup>. General maps in discrete time dynamics are not necessarily invertible.

Assume that the dynamics of the system is bounded. Then this implies existence of so-called non-wandering points in the phase space; most of trajectories starting from any vicinity of such a point either never leave this vicinity (stable fixed point) or will return into this vicinity at some later time (oscillating dynamics). The set of all non-wandering points that is stable in some sense is called attractor of the system. If dynamics of the systems is bounded then every trajectory will enter a vicinity of some non-wandering point in a finite transient time.

That means that bounded dynamics will almost always end up on an attractor which may have the dimension equal or less than the dimension of the underlying phase space. In dissipative systems evolution should contract the phase space<sup>§</sup> so that one expects that the attractor (i. e. the set of non-wandering points) has a smaller dimension than the dimension of the embedding phase space.

Not all points in the phase space are visited equally often. This fact can be reflected in a coarse-grained description by means of the probability (density)  $\rho(x, t)$  of finding the trajectory at the point  $x$  at a given time  $t$  if no information on the initial conditions is available. With the evolution operator  $F^{t_1, t}$  acting in the phase space a corresponding operator acting in the space of probability functions can be defined, so-called Frobenius-Perron operator defined by the integral equation

$$\rho(x, t_1 + t) = \int \delta(x - F^{t_1, t}y) \rho(y, t_1) dy \quad (1.3)$$

Note that a certain trajectory does not have to visit all the non-wandering points, i. e. it does not have to cover the whole attractor. For instance, this is the case if a non-wandering point is itself periodic. Nor all trajectories, which visit a vicinity of a non-wandering point, visit it with the same frequency (same probability).

If these probabilities are the same for a whole set of trajectories (as defined with their initial conditions) having the dimension of the underlying phase space then this probability distribution is called natural measure of a point on the attractor. Almost every initial probability distribution will converge in the sense of the Frobenius-Perron equation (1.3) to this natural measure. A trajectory from this set is called typical with respect to the natural measure.

If a dynamical system is autonomous, i. e. the dynamic equations are not explicitly time-

---

<sup>‡</sup>In singular points some trajectories, so-called separatrices, can intersect each other but this intersection takes infinite time. Thus all stroboscopic maps of flows defined for finite time intervals are still invertible.

<sup>§</sup>We will see later on that the same system of equations can demonstrate dissipative and conservative behavior at different parameter values. Therefore dissipativity should be understood as a property of the dynamics but not that of the equations of motion.

## 1.1. DESCRIBING COMPLEX SYSTEMS

dependent, and mixing, then the Frobenius-Perron operator does not depend on  $t_1$  and the solution of (1.3) should converge to an invariant (time-independent) distribution  $\rho(x)$ .

A system is called ergodic if average properties of a trajectory are the same as averaged properties of the attractor, i. e. for any observable  $q(x)$  holds [15]

$$\lim_{T \rightarrow \infty} \frac{1}{T} \int_0^T q(F^t x) dt = \int q(x) \rho(x) dx \quad (1.4)$$

Chaoticity means sensitive dependence of trajectories on the attractor on small perturbations. It is quantified with the construction of the Lyapunov exponent.

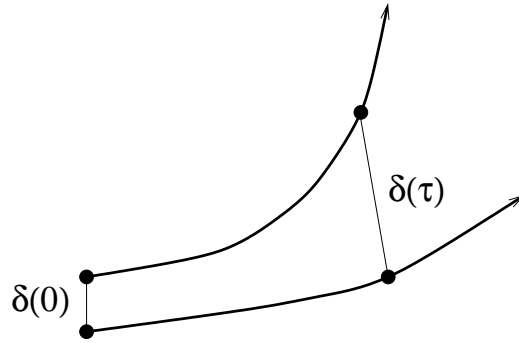


Figure 1.1: Divergence of two close trajectories. An initial perturbation  $\delta(0)$  typically grows exponentially with time in a chaotic system.

Let a dynamical system be described by a  $n$ -dimensional ordinary differential equation<sup>¶</sup>.

$$\dot{x} = f(x, t) \quad (1.5)$$

Consider a solution of the equation (1.5) starting in  $x(0)$  and another solution of the same equation starting in a close point  $x(0) + \delta(0)$  with  $|\delta| \ll 1$ . From (1.5) a linearized equation for the difference vector  $\delta(t)$  between these two solutions can be derived.

$$\dot{\delta} = \frac{\partial f(x, t)}{\partial x} \delta \quad (1.6)$$

At every point of the phase space the matrix  $\frac{\partial f(x, t)}{\partial x}$  stretches the vector  $\delta$  in directions of its eigenvectors by the corresponding eigenvalues. Thus the perturbation vector  $\delta(\tau)$  at a time  $\tau$  is formed from  $\delta(0)$  through the integration along the unperturbed trajectory  $x(t)$ , so to say, by successive stretchings with locally defined matrices  $\frac{\partial f(x, t)}{\partial x}$ . With the assumption that the norm of the local stretching matrices fluctuates around some mean value the length of the vector  $\delta$  scales asymptotically with time as

$$|\delta(\tau)| \sim |\delta(0)| e^{\lambda \tau}$$

For different initial perturbations  $\delta(0)$  the number  $\lambda$  can be different being determined by the direction of  $\delta(0)$ . All these numbers are called Lyapunov exponents of the solution

<sup>¶</sup>In the case of a mapping the whole argumentation is analogous.

## CHAPTER 1. INTRODUCTION

$x(t)$  of the system (1.5). Altogether there are  $n$  Lyapunov exponents which can be positive or negative. A dynamical system is usually called chaotic if there is an ergodic set in which a typical trajectory has at least one positive Lyapunov exponent. Then initially close trajectories typically diverge exponentially with time. Of course, there are such degenerative initial conditions that the corresponding difference vector  $\delta(0)$  is orthogonal to the direction of the stretching but they form a set of zero measure.

In the language of symbolic sequences produced by initially close trajectories this means that there always exists a probability that two sequences with identical histories will generate different symbols in the next time step. The uncertainty  $h_{KS}$  of a next symbol (or, more exactly, its supremum over all partitions of the phase space) if all the past symbols  $A_{-t}$ ,  $t = 1, \infty$ , are known is called Kolmogorov-Sinai entropy (production rate) of a dynamical system [51, 52].

Intuitively, two trajectories can only quit visiting the same symbols by escaping from each other in an unstable direction. The corresponding connection between Kolmogorov-Sinai entropy and Lyapunov exponents has been derived [70] under the assumption that the natural probability measure is smooth in the unstable directions<sup>||</sup> to be just the sum of positive Lyapunov exponents

$$h_{KS} = \sum_{\lambda_i > 0} \lambda_i \quad (1.7)$$

Kolmogorov-Sinai entropy  $h_{KS}$  is zero for regular (periodic or quasiperiodic) bounded dynamics and infinite in stochastic systems (cf. [58]). In deterministic chaotic systems the entropy production rate is finite, which makes them especially useful in modelling of complexity production and reduction.

### 1.1.4 Entropy production vs. emergence of order

The second principle of thermodynamics postulates convergence of every large closed system to the state of maximal entropy, the equilibrium. This corresponds to the irreversibility of the evolution in a closed system, the system (when described with some macroscopic variable) tends to the state of maximal probability, the attractor. Fluctuations around the attractor are of the order  $\frac{1}{\sqrt{N}}$  with  $N$  being the number of the systems in ensemble.

The attractor is stable. The initial state of the system gets forgotten with approaching the attractor so that the attractor in a large closed system corresponds to the state of maximal macroscopic symmetry. For a measured symbolic sequence in any macroscopic variable

---

<sup>||</sup>Under more general assumptions an inequality was shown [90] to hold

$$h_{KS} \leq \sum_{\lambda_i > 0} \lambda_i$$

Generally can be written [36, 26]

$$h_{KS} = \sum_{\lambda_i > 0} d_i \lambda_i$$

Numbers  $d_i$  are called partial information dimensions of the attractor (cf. [58]).

## 1.1. DESCRIBING COMPLEX SYSTEMS

this means that the asymptotic entropy production rate  $h$  is zero. In fact, this implicitly means that coupling together a large number of chaotic systems would only generate trivial dynamics in any macroscopic variable (up to the finite size effects). In general, producing entropy in the system should move it, according to the classical thermodynamics, to a trivial (disordered) state.

However, this does not hold in every system. Imagine that such an open system and the boundary conditions are chosen that the temperature of the system remains constant. Then the equilibrium state of the system is defined by the extremum of its free energy  $F = E - TS$  but not extremum of its entropy  $S$ , with  $E$  being the energy and  $T$  the temperature. As discussed in [81], the equilibrium is the result of competing minimizing the energy and maximizing the entropy, i. e. at small temperatures one observes highly organized structures (with small energy and entropy) and for large temperature the entropy dominates and the system converges to a disordered state.

One sees that even in the framework of Boltzmann's equilibrium thermodynamics ordered states are possible, though these states have to be static and hence cannot explain dynamical growth of complexity and self-organized structures. To explain the dynamical complexity and emergence of order in oscillating complex systems, i. e. systems far from equilibrium one has to consider systems where the equilibrium state is unstable or does not exist at all.

Physically, this is generally the case in dissipative dynamical systems under permanent input of energy. Their dynamics is far from equilibrium and, while they produce entropy, the produced entropy is "exported" and highly organized structures can arise.

### 1.1.5 Synchronization as emergence of order

Interacting nonlinear systems as well as nonlinearly interacting systems can demonstrate dynamics which is more complex than the dynamics of these systems in absence of interactions. In the language of Haken's synergetics [40], a system is more than just a sum of its parts. But also the contrary is possible, and the interplay of individual systems reduces total complexity of the solution. E. g. coupling together two chaotic systems can produce periodic or even constant dynamics.

Synchronization is the situation when interactions make dynamics of individual systems similar in a certain sense, which surely is form of reduction of complexity. Freely translated from Greek, synchronization means "sharing common time" by different processes, due to interactions. Systems which are not synchronous in absence of interactions reveal some coherence in their dynamics while being coupled together. Usually one formalizes this by introducing a coupling parameter and analyzing bifurcations in the dynamics of the system with changing coupling strength. According to the type of coupling synchronization between closed complex systems and synchronization between a complex system and external forces can be studied.

To characterize synchronism of different processes a corresponding macroscopic observable has to be defined. This makes synchronization a very general phenomenon. This observable has the meaning of an order parameter and is often directly connected to some measure

of complexity or its reduction.

### 1.1.6 Modelling synchronization effects in complex systems

From what has been said a possible way to investigate typical synchronization effects in complex systems is to construct typical models of a complex system consisting of complex (chaotic) subsystems. The subsystems, if uncoupled, produce chaotic dynamics, described by some dynamical equations. These equations can be continuous or discrete both in space and time.

A variety of intriguing effects in space-continuous complex systems described with partial differential equations are known like different types of turbulence [54], localization [24], dendritic growth [93] and roughening interfaces [75], or self-organized criticality [8].

In general, partial differential equations are much more difficult to analyze than ordinary differential equations. That is why coupled lattices of chaotic dynamical systems gained much scientific attention. Such a lattice can be understood as a discretization of a corresponding continuous space problem. The dynamics of each element in the lattice is given by a set of simple dynamical rules which can be continuous or discrete in time. One looks for generic effects, i. e. these effects should be non-specific for a definite choice of the dynamical laws and should hold for every typical complex (chaotic) systems.

The hope is that the results from coupled lattices can then be applied to continuous space systems by going over to the thermodynamic limit of infinitely many grid points on a lattice in a given bounded space interval\*\*.

The interactions between systems in the lattice are described by a coupling function (depending on the other systems in the lattice). Different types of coupling are investigated, e. g. nearest-neighbor or global coupling. A nearest-neighbor coupling models partial differential equations with local terms up to the second spatial derivatives only. A global coupling corresponds to a situation where the spatial dynamics produces a mean field equally acting in all points of the continuum. The action of the coupling can be isotropic or directed which is defined by the way how contributions of the neighbors enter the interaction term. In the case of one-dimensional lattices (chains) of coupled chaotic systems one speaks of unidirectional coupling if it contains contributions of elements from one side only and of bidirectional coupling if elements from the left and the right act symmetrically.

Another important aspect in modelling complex systems with lattices of chaotic elements of a finite size is the question of boundary conditions. Analogously to the continuous case different situations are possible while one usually restricts oneself in the fundamental questioning to either periodic or free boundary conditions.

If the dynamics on the attractor of an individual system in the lattice is oscillatory then one can analyze typical return times into a vicinity of a point on the attractor. In the synchronized state these return times have to be coherent in some sense.

Thus an outline of a synchronization research can be summarized as follows: one simulates a complex system with a lattice of discrete or continuous low-dimensional dynamical

---

\*\*This optimism, however, is damped by some results [18] showing that this thermodynamic limit can be non-equivalent to the underlying continuous problem.

equations generating oscillatory (regular or chaotic) trajectories and interacting with each other through a chosen coupling function. For each system an observable describing its temporal behavior is defined. In the disordered state the values of these variables are different. In the synchronized state the observables show a coherent pattern.

There were found different types of synchronization in lattices of coupled chaotic systems. Now we want to discuss them in more details. In the rest of this introductory chapter we will follow the recently published monograph [71] where the theoretical concepts of synchronization are formulated and the state of the art in the current research on synchronization is given.

## 1.2 Complete and weak synchronization

We start with considering two replica of some  $N$ -dimensional complex system (in the sense of complex dynamics) which are dissipatively coupled together. The most obvious kind of synchronization between these two systems, solutions of which  $x(t)$  and  $y(t)$  are different in absence of interactions, is when interactions make the solutions completely coincide. Without synchronization the dynamics takes place in a  $2N$ -dimensional phase space, in the synchronous regime the dynamics is restricted to the  $N$ -dimensional diagonal subspace  $x = y$ . This effect is called complete synchronization.

Continuous time systems can always be reduced to mappings by discretizing with an appropriate stroboscopic or Poincaré map. Thus, to illustrate features of complete synchronization let us consider two identical maps  $M : x(t) \mapsto x(t+1)$  multiplicatively coupled through the linear dissipative coupling operator  $L = \begin{pmatrix} 1-\varepsilon & \varepsilon \\ \varepsilon & 1-\varepsilon \end{pmatrix}$

$$\begin{pmatrix} x(t+1) \\ y(t+1) \end{pmatrix} = L \circ M \begin{pmatrix} x(t) \\ y(t) \end{pmatrix} = \begin{pmatrix} 1-\varepsilon & \varepsilon \\ \varepsilon & 1-\varepsilon \end{pmatrix} \cdot \begin{pmatrix} f(x(t)) \\ f(y(t)) \end{pmatrix} = \begin{pmatrix} (1-\varepsilon)f(x(t)) + \varepsilon f(y(t)) \\ (1-\varepsilon)f(y(t)) + \varepsilon f(x(t)) \end{pmatrix} \quad (1.8)$$

First note that the diagonal state  $x = y$  is always a solution. However, if the coupling is switched off,  $\varepsilon = 0$ , this solution is degenerate. Contrary to this, if  $\varepsilon = 1/2$  then the right hand sides of (1.8) are identical for  $x$  and  $y$ , and every solution converges to the diagonal after one time step. Obviously, this diagonal state can be either stable or unstable at different couplings  $\varepsilon$ .

It is possible to find the critical coupling  $\varepsilon_c \in [0, 1/2]$  where transition to complete synchronization takes place, i. e. the diagonal state becomes stable to small perturbations for  $\varepsilon > \varepsilon_c$ . Denoting with  $U = \frac{x+y}{2}$  and  $V = \frac{x-y}{2}$  the variables along and transverse to the diagonal respectively one can rewrite (1.8) in terms of longitudinal and transverse components of the dynamics.

$$\begin{aligned} U(t+1) &= \frac{f(U(t)+V(t)) + f(U(t)-V(t))}{2} \\ V(t+1) &= \frac{f(U(t)+V(t)) - f(U(t)-V(t))}{2} (1 - 2\varepsilon) \end{aligned} \quad (1.9)$$

Linearizing around the diagonal  $V(t) = 0$  we obtain linear mappings for small perturbation vectors  $u$  and  $v$  in the diagonal and the transversal subspaces.

$$\begin{aligned}
 u(t+1) &= f'(U(t)) \cdot u(t) \\
 v(t+1) &= (1 - 2\varepsilon) f'(U(t)) \cdot v(t) \\
 U(t+1) &= f(U(t))
 \end{aligned}
 \tag{1.10}$$

Mathematically, the equations (1.10) is a skew system. The dynamical equation for the underlying mapping drives equations for perturbations. Moreover, perturbations in the diagonal subspace and transverse perturbations do not interact and they are governed by the same equation up to the constant factor  $1 - 2\varepsilon$ . This means that every transverse Lyapunov exponent  $\lambda_{\perp} = \lambda_v$  is connected to the corresponding Lyapunov exponent of an uncoupled map  $\lambda = \lambda_u$ .

$$\lambda_{\perp} = \ln|1 - 2\varepsilon| + \lambda
 \tag{1.11}$$

The completely synchronized state  $x \equiv y$  becomes stable in the sense of average decay of perturbations when  $\lambda_{\perp} = 0$ , i. e. for  $\varepsilon > \varepsilon_c = (1 - e^{-\lambda})/2$ . However, topologically the transition to complete synchronization is a bit more complicated.

### 1.2.1 Topological view on the onset of synchronization

We proceed further with the assumption on the underlying map  $f(\cdot)$  to be one-dimensional and chaotic. Consider a  $T$ -periodic orbit  $x^*(t)$  inside the attractor. Because the mapping is chaotic this orbit is unstable along the diagonal (synchronized) subspace with the multiplier  $\mu_u = \prod_{t=1}^T f'(x^*(t))$ ,  $|\mu| > 1$ . The multiplier in the direction transverse to the synchronization diagonal is  $\mu_v = (1 - 2\varepsilon)\mu_u$ . This defines a bifurcation of the given periodic orbit that takes place at

$$\varepsilon_c(x^*) = \frac{1 - |\mu_u|^{-1}}{2}
 \tag{1.12}$$

Generally this critical value  $\varepsilon_c(x^*)$  can be different for different periodic orbits inside chaos,  $\varepsilon_c^{\min} \leq \varepsilon_c(x^*) \leq \varepsilon_c^{\max}$ . Therefore, topologically the transition of a chaotic attractor containing periodic orbits with different instability thresholds  $\varepsilon_c(x^*)$  takes place in a whole interval in  $\varepsilon$ . The value  $\varepsilon_c$  as defined by the transverse Lyapunov exponent belongs to the interval  $[\varepsilon_c^{\min}, \varepsilon_c^{\max}]$  as well.

Thus there are four regimes:

- **strong synchronization**

$\varepsilon > \varepsilon_c^{\max}$ : all periodic trajectories are transversally stable, this means that the (still chaotic) synchronized state  $V = 0$  is stable and attracts all points from its neighborhood;

- **weak synchronization**

$\varepsilon_c < \varepsilon < \varepsilon_c^{\max}$ : there are unstable periodic orbits but the chaotic attractor on the synchronization diagonal is stable on average, almost all points from a vicinity of the diagonal  $V = 0$  are attracted to it (but now there exist trajectories that run off this vicinity);



## 1.2. COMPLETE AND WEAK SYNCHRONIZATION

- weak asynchronous state  
 $\varepsilon_c^{max} < \varepsilon < \varepsilon_c$ : while still there are transversally stable periodic orbits, the synchronization diagonal is now unstable in the Lyapunov sense;
- strongly asynchronous state  
 $\varepsilon < \varepsilon_c^{max}$ : all periodic orbits are unstable, both in the diagonal subspace and in the transversal subspace.

One sees now that the diagonal subspace can be stable on average but still contain unstable orbits. Moreover, these unstable orbits can also be dense in this synchronization subspace. Therefore, this subspace cannot be properly called attractor in the topological sense, i. e. that the attractor consists of non-wandering point such that all trajectories starting from a certain open vicinity of this point return to this vicinity.

As transversally unstable orbits can be dense in the synchronization subspace any vicinity of any point in this subspace can in principle contain escaping points. Instead of the topologically defined attractor as a compact set with such an open vicinity that all points in this vicinity do not escape it (cf. [48]) the term of attractor is here to be understood in the sense of a probabilistic definition [63]. In this probabilistic definition an attractor is the smallest closed set attracting a set of initial points of strictly positive measure.

### 1.2.2 Statistical approach to the onset of synchronization

As seen in the topological description of the previous section, the averaged stability can deviate from the stability of individual trajectories. Averaging over the attractor discards all the fine topological structure; that is why synchronization can be described within a statistical approach, i. e. when considering the onset of synchronization as being noise-driven.

Let us introduce new notations

$$w = |v|, \quad z = \ln w$$

Now the equation (1.10) reads

$$w(t+1) = w(t)e^{\lambda_{\perp}} e^{g(U(t))} \quad (1.13)$$

Here the function  $g(\cdot)$  is

$$g(U(t)) = \ln |f'(t)| - \lambda$$

In the language of  $z$  it reads

$$z(t+1) = z(t) + \lambda_{\perp} + g(U(t)) \quad (1.14)$$

The equation (1.14) is linear which makes the further analysis simple. Formally writing the solution for large times  $T$ , one obtains

$$z(T) - z(0) - \lambda_{\perp} T = \Lambda T \quad (1.15)$$

## CHAPTER 1. INTRODUCTION

The value  $\Lambda$  is the finite-time Lyapunov exponent, shifted by  $\lambda$  and thus converging to zero for large  $T$

$$\Lambda = \frac{1}{T} \sum_{t=0}^{T-1} \ln |f'(t)| - \lambda \quad (1.16)$$

In other words, dynamics in  $z$  consists of the drift with constant velocity  $\lambda_{\perp}$  and a fluctuating part described by  $\Lambda$ . If  $\lambda_{\perp} > 0$  then  $z \rightarrow \infty$  and the synchronization diagonal is unstable. If  $\lambda_{\perp} < 0$  then it is stable.

Of course, fluctuations of the finite-time Lyapunov exponent  $\Lambda$  are not uncorrelated because they are generated by a deterministic dynamical system. But applying the central limit theorem one can consider  $\Lambda$  as a noisy term [66, 65, 19] with the Gaussian probability with a certain diffusion constant  $D$

$$p(\Lambda, T) \sim e^{-\frac{\Lambda^2 T}{2D}}$$

As  $z$  is linearly connected to  $\Lambda$ , it grows diffusively with

$$\langle (z - \langle z \rangle)^2 \rangle \sim DT \quad (1.17)$$

Near the transition to synchronization the value of the transverse Lyapunov exponent  $\lambda_{\perp}$  is small so that fluctuations dominate. Due to the diffusion (1.17) the distribution of  $z$  flattens with time, therefore very large and very small  $z$  become probable. This effect is called on-off intermittency [31, 32, 114]. In the time series of  $w$  this corresponds to randomly appearing bursts with very large amplitudes.

Compared to the topological description the statistical description represents an approach to complex systems where the averaged equations are deterministic and fine structures are described by noisy terms <sup>††</sup>.

### 1.3 Phase of a signal and phase synchronization

Another type of synchronization is so-called phase synchronization [72, 87, 88]. Intuitively, synchronization between two systems takes place when both systems evolve along trajectories on their attractors in a certain concordance. To quantify this concordance the notation of phase is introduced in order to reduce the full dynamics to relevant phase equations [62, 54].

Phase can be defined as the variable along the trajectory in a corresponding local coordinate frame.

---

<sup>††</sup>Bifurcations in chaotic systems seem to always admit two different descriptions: one in the framework of the statistical approach and another through tracking topological changes in the corresponding attractor. E. g. in [115] bifurcations in multiplicatively coupled maps were described as crisis, i. e. an abrupt change in the topology of the attractor, while in [55] was shown that all observed phenomena can equally be described in terms of on-off intermittency.

### 1.3.1 Phase equations around stable periodic solutions

For instance, given a dissipative autonomous system of ordinary differential equations  $\dot{x} = f(x)$  in a general  $N$ -dimensional phase space with a simple periodic limit cycle, its phase  $\varphi$  is postulated to change monotonously in time gaining  $2\pi$  by each rotation.

$$\dot{\varphi} = \omega = 2\pi/T \quad (1.18)$$

This uniformly rotating phase can be obtained from any angle variable  $\theta$  through the transformation

$$\varphi = \int_0^\theta \dot{\theta}^{-1} d\theta \quad (1.19)$$

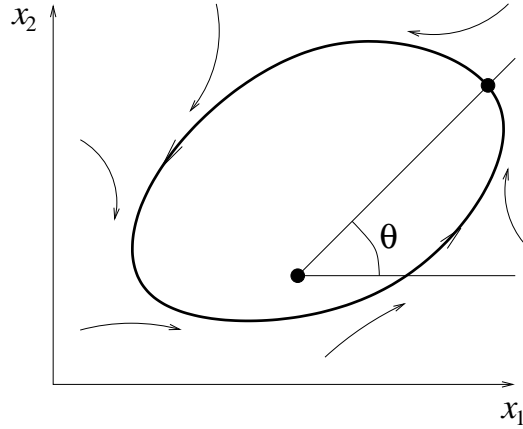


Figure 1.2: Phase of a limit cycle as defined by an arbitrary angle variable.

The most important property of phase is that it is neutrally stable. Perturbations in phase neither decay nor grow with time. This corresponds to the time shift invariance of autonomous dynamical systems. If some function  $x(t)$  is a solution then for every time shift  $\tau$  the function  $x(t + \tau)$  is a solution as well.

Interactions with other systems giving rise to synchronization modify solution of the system. Assuming that these interactions are small, one can describe this situation with the equation

$$\dot{x}_k = f_k(x_k) + \varepsilon g_k(x_1, \dots, x_M, t) \quad (1.20)$$

Altogether there are  $M$   $N$ -dimensional systems weakly interacting with each other through the coupling functions  $g_k(\cdot)$ . In the simplest case the equations (1.20) can be replaced with equations where the systems is driven by an external force.

$$\dot{x}_k = f_k(x_k) + \varepsilon p_k(x_k, t) \quad (1.21)$$

The external force drives the trajectory away from the limit cycle. However, as this force

CHAPTER 1. INTRODUCTION

is  $\varepsilon$ -small and the limit cycle is stable, the perturbed solution still lies in the vicinity of the limit cycle, perturbations transverse to the cycle are small. In contrast to this, perturbations along the cycle, i. e. perturbations in phase due to the action of  $p_k(\cdot)$  can be large.

It is possible to construct a continuation of a uniformly rotating phase variable as defined by the equations (1.18)-(1.19) into the vicinity of a stable limit cycle by means of so-called isochrones [111, 112, 38, 54]. A stroboscopic map with the period of the limit cycle  $\Phi(x) : x(t) \mapsto x(t + T)$  is attracting to the limit cycle, the latter is the set of fixed points of  $\Phi(x)$ . The set of preimages of a point  $x^*$  belonging to the limit cycle as defined by the map  $\Phi(x)$  is called isochrone, it is  $(N - 1)$ -dimensional hypersurface crossing the limit cycle in  $x^*$ . It is always possible to define monotonously rotating phase on the limit cycle according to the equation (1.19). By demanding that the phase is constant on each isochrone one defines monotonously rotating phase in the whole neighborhood of the limit cycle where isochrones exist.

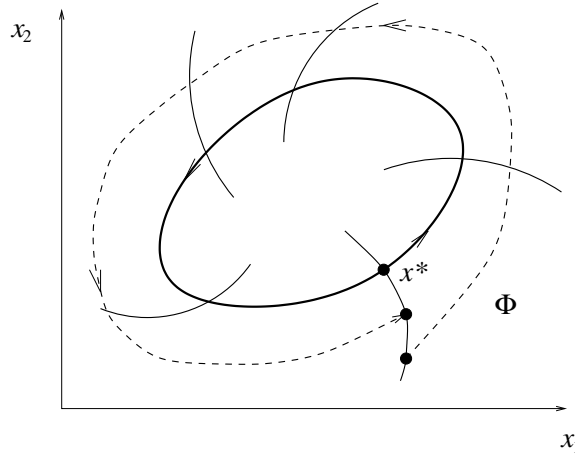


Figure 1.3: Construction of isochrones in the vicinity of a limit cycle.

With this definition for the phase the equation (1.19) is valid in some vicinity of the limit cycle in absence of interactions,  $\varepsilon = 0$  (here the map  $\Phi(x)$  and, consequently, all isochrones are defined with respect to the unperturbed dynamics).

$$\dot{\varphi}(x) = \omega$$

Or, as phase is per definition a smooth function of the variables  $x$ ,

$$\sum \frac{\partial \varphi}{\partial x_k} \dot{x}_k = \omega$$

With this interaction-free definition of the phase the phase equation (1.18) in the perturbed case (1.21) reads

$$\dot{\varphi}(x) = \omega + \varepsilon \sum \frac{\partial \varphi}{\partial x_k} p_k(x, t)$$

As the second term is proportional to  $\varepsilon$  and deviations of  $x$  from the limit cycle  $x_0$  are small

### 1.3. PHASE OF A SIGNAL AND PHASE SYNCHRONIZATION

as well so up to the first order of  $\varepsilon$  one can neglect these deviations to obtain with denoting

$$Q(\varphi, t) = \sum \frac{\partial \varphi(x_0(\varphi))}{\partial x_k} p_k(x_0(\varphi), t)$$

$$\dot{\varphi}(x) = \omega + \varepsilon Q(\varphi, t) \quad (1.22)$$

As the limit cycle can be parametrized with the phase  $\varphi$  the equation for the phase is now in a closed form with  $Q(\cdot)$  being  $2\pi$ -periodic in  $\varphi$ . Note that the same line of argumentation is applicable if the cycle is fully unstable. In this case the whole derivation holds after inverting time.

#### 1.3.2 Phase synchronization by external force and mutual synchronization

By taking the stroboscopic map with the period  $T$  of the perturbation  $Q(\varphi, t)$  in the equation (1.22) we obtain a one-to-one correspondence between  $\varphi(t)$  and  $\varphi(t + T)$ , the so-called circle map:

$$\varphi_{n+1} = \varphi_n + \mu + \varepsilon F(\varphi_n) \quad (1.23)$$

We have denoted here  $\mu = \omega T$ . The dynamics of the circle map (1.23) can be characterized by the rotation number, the average phase shift per one iteration (one period of the external force):

$$\rho = \lim_{n \rightarrow \infty} \frac{\varphi_n - \varphi_0}{2\pi n} = \lim_{t \rightarrow \infty} \frac{(\varphi(t) - \varphi(0))T}{t} = \frac{\Omega}{\omega} \quad (1.24)$$

The rotation number is shown (cf. [48]) to be independent of the initial point  $\varphi_0$ . The number  $\Omega$  is the observed frequency (average velocity of phase rotation)

$$\Omega = \lim_{t \rightarrow \infty} \frac{\varphi(t) - \varphi(0)}{t} \quad (1.25)$$

According to the Denjoy theorem [21], if the rotation number  $\rho$  is irrational then the circle map (1.23) can be transformed with an appropriate substitution  $\varphi = g(\theta)$  to the circle shift  $\theta_{n+1} = \theta_n + 2\pi\rho$ . The solution of the circle shift is trivial so that the solution of the circle map is quasi-periodic for any  $2\pi$ -periodic function  $g(\cdot)$ :

$$\varphi_n = g(\varphi_0 + 2\pi\rho n) \quad (1.26)$$

On a periodic trajectory the rotation number is rational  $\rho = q/p$ . For the fixed point  $\varphi_p = \varphi_0 + 2\pi q$  of the  $p$ -iterate of the circle map one can write up to the order of  $\varepsilon$  (with denoting

$$F_p(\varphi_n) = \frac{1}{p} \sum_{k=0}^{p-1} F(\varphi_n + 2\pi \frac{q}{p} k)$$

$$\varepsilon F_p(\varphi_n) = \omega_0 T - 2\pi \frac{q}{p} \quad (1.27)$$

The equation (1.27) has a solution if  $\omega T - 2\pi \frac{q}{p} \in \mathfrak{R}F_p$ , this defines the synchronization regions in the  $(\mu, \varepsilon)$ -plane, so-called Arnold tongues [4]. In the case of the sine circle map

## CHAPTER 1. INTRODUCTION

( $F(\varphi) = \sin \varphi$ ) these synchronization regions have width  $\Delta\mu$  with the scaling  $\Delta\mu \sim \varepsilon^p$  [5] (because the function  $F_p$  is obtained by an averaging along a trajectory, it is small for large  $p$ ). Inside the Arnold tongues the system described in absence of the external force with the phase equation  $\dot{\varphi} = \omega$  is  $\frac{q}{p}$ -synchronized to the external force. In the figure 1.4 (adopted from [71], p. 227) the Arnold tongues corresponding to small  $q$  and  $p$  are shown.

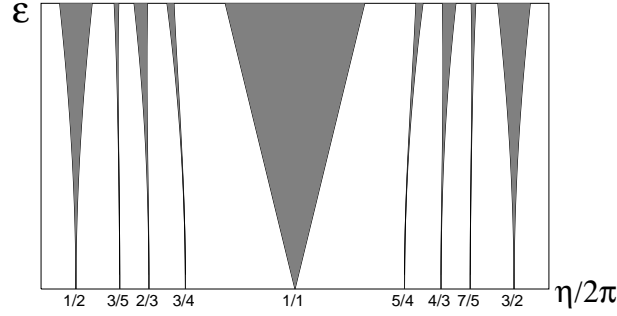


Figure 1.4: Major Arnold tongues in the sine circle map.

If no external forces are acting on the system, but instead the synchronization is caused by the interactions between two or more coupled systems then the approach is analogous. Let us consider two systems described with the closed phase equations

$$\begin{cases} \dot{\varphi}_1 = \omega_1 + \varepsilon Q_1(\varphi_1, \varphi_2) \\ \dot{\varphi}_2 = \omega_2 + \varepsilon Q_2(\varphi_1, \varphi_2) \end{cases} \quad (1.28)$$

In the zero approximation the phases rotate with the unperturbed frequencies  $\omega_1$  and  $\omega_2$ . Writing the coupling functions  $Q_{1,2}$  in the Fourier representation, e. g.  $Q_1 = \sum_{k,l} a_1^{k,l} e^{i(k\varphi_1 + l\varphi_2)}$ , we note that all terms correspond to fast rotations except the terms that fulfill the resonance condition  $k\omega_1 + l\omega_2 \approx 0$ .

Assuming that the natural frequencies are close to the resonance  $n\omega_1 \approx m\omega_2$ , we can write with denoting  $\nu = n\omega_1 - m\omega_2$  and  $q(\psi) = \sum_j (na_1^{nj, -mj} e^{ij\psi} - ma_2^{mj, -nj} e^{-ij\psi})$  the averaged equation of one variable  $\psi = n\varphi_1 - m\varphi_2$ , that is the equation of the circle map:

$$\dot{\psi} = \nu + \varepsilon q(\psi) \quad (1.29)$$

Inside the synchronization region (Arnold tongue) the constant relation  $\frac{\Omega_1}{\Omega_2} = \frac{m}{n}$  between the observed frequencies of the oscillators holds, this effect is called frequency locking due to interactions.

### 1.3.3 Phase synchronization in presence of noise

In order to be able to deal with complex systems that generally allow a coarse-grained description only let us now spell a couple of words on synchronization in presence of noise. The natural way to describe mutual synchronization of noisy oscillators is to include a noise term in the equation (1.29):

### 1.3. PHASE OF A SIGNAL AND PHASE SYNCHRONIZATION

$$\dot{\psi} = \nu + \varepsilon q(\psi) + \xi(t) \quad (1.30)$$

The theory of synchronization of noisy oscillators is well established [100, 61] and should not be repeated here. A simple physical interpretation of the Langevin dynamics (1.30) can be given as a random walk of a zero-mass particle in an effective one-dimensional potential  $V(\psi) = -\nu\psi - \varepsilon \int^\psi q(x) dx$ . This situation is illustrated in the figure 1.5 (adopted from [71], p. 262). Synchronization corresponds to the minima of the potential, the desynchronized state to the potential without minima.

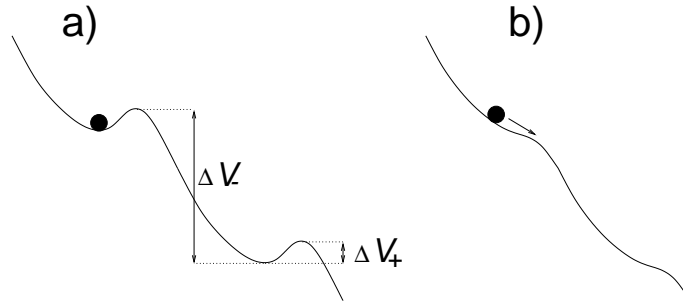


Figure 1.5: Phase as a particle in a potential. (a) The minima of the potential correspond to the synchronization, due to the noise the particle can overcome the barrier and a  $2\pi$  phase slip occurs. (b) Outside the synchronization region the particle slides down.

In the synchronized state the action of noise can push the phase out of the minimum of the potential, the phase will make a so-called phase slip to the next minimum. If the noise is unbounded then there always is probability of such slips at any non-zero noise intensity. In the diagram for the frequency difference  $\Omega_\psi = \langle \dot{\psi} \rangle$  vs. the mismatch  $\nu$  of the natural frequencies, shown in the figure 1.6 (adopted from [79]), no synchronization plateau like that of the noise-free case can exist even at very small noise intensity. Another situation is when the noise is bounded, now at small noise intensity the particle cannot overcome the barrier and the synchronization plateau still exists at small mismatch  $\nu$ .

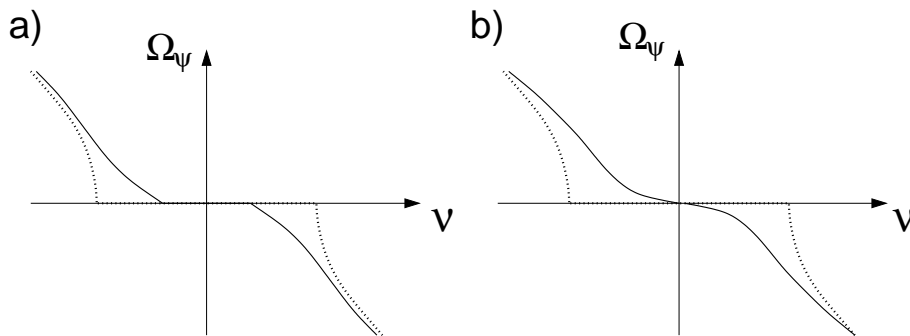


Figure 1.6: Synchronization plateau, frequency difference vs. mismatch for (a) bounded and (b) unbounded noise. With the dotted curves the synchronization region without action of noise is shown.

### 1.3.4 Phase synchronization of chaotic systems

The formalism of isochrones around fully stable or fully unstable periodic solutions does not work for the saddle-type periodic orbits. This is a very typical situation in chaotic dynamics, the closure of an attractor contains infinitely many unstable saddle-type periodic orbits of different periods. Every typical trajectory on a chaotic attractor wanders from one unstable periodic orbit to another, the period cannot be properly defined.

Thus the first obstacle in extending the phase equation approach on chaotic systems is the problem of definition of the phase itself. A reasonable definition of the phase of a chaotic system should correspond to the shift along the trajectory in the local coordinates and hence ensure marginal stability and zero Lyapunov exponent. For the periodic orbits embedded in chaos this definition also has to reduce to the usual one.

One way to define phase of a chaotic solution is the concept of analytic signal [33, 67, 82, 98, 13] based on the Hilbert transform. Given a signal  $s(t)$ , we assume time  $t$  to be complex. Then such an imaginary part  $\tilde{s}(t)$  is looked for that the full complex signal  $S(t) = s(t) + i\tilde{s}(t)$  is an analytic function of complex  $t$ . By this analyticity condition  $\tilde{s}(t)$  is uniquely defined from the given signal  $s(t)$  to be the Hilbert transform of  $s(t)$

$$\tilde{s}(t) = \frac{1}{\pi} \lim_{T \rightarrow \infty} \int_{-T}^T \frac{s(\tau)}{t - \tau} d\tau$$

The instantaneous phase  $\varphi(t)$  and amplitude  $A(t)$  of the process  $s(t)$  are unambiguously defined as the argument and the amplitude of the complex signal  $S(t) = s(t) + i\tilde{s}(t) = A(t)e^{i\varphi(t)}$ . The main advantage of defining the phase of a signal by the Hilbert transform is that it is defined in the unique way. The problem is that the signal used to define the phase can be chosen in different ways in a dynamical system.

Another approach [77] to define phase is to define an appropriate Poincaré section, i. e. such a hypersurface in the phase space that all trajectories on the attractor cross it. Every isochrone of the case of a periodic limit cycle can serve as Poincaré section. Then every crossing of a Poincaré section can be understood as one rotation and thus should correspond to the  $2\pi$ -shift in phase. A definition of phase can now be set by the requirement that phase grows monotonously between two consequent crossings. The definition of the phase with a Poincaré section is not unique as well, it depends on the choice of the section.

$$\varphi(t) = 2\pi \frac{t - t_n}{t_{n+1} - t_n} + 2\pi n, \quad t_n \leq t < t_{n+1} \quad (1.31)$$

Sometimes one can find such a projection of the attractor on some plain that in this plain the projections of (chaotic) trajectories are close to a limit cycle. This means that one can introduce an angle variable as in the figure 1.2 so that the phase can be introduced according to the equation (1.19). Also this definition is not unique because the projection can be made in different ways.

Although there is no unique definition of the phase of a chaotic system, one sees that all three above definitions are equivalent in the sense that in a long time average their growth



rates are the same. Therefore every of these definitions can be used in practical calculations. With using the definition via Poincaré maps, one can represent the dynamics of the amplitude (vector) and the phase between two subsequent Poincaré crossings in the form [72]

$$\begin{aligned} A_{n+1} &= M(A_n) \\ \dot{\phi} &= \omega + F(A_n) \end{aligned} \tag{1.32}$$

The equation (1.32) is similar to the equation of a periodic oscillator driven by a noisy term, the term  $F(A_n)$  is chaotic and can be understood as some effective noise. Therefore, the dynamics of phase in a chaotic system is generally diffusive with some diffusion constant  $D$ .

$$\langle \varphi(t) - \varphi(0) - \omega t \rangle \sim Dt$$

## 1.4 Summary

Large complex systems are called complex because they are difficult to describe with a full accuracy. In order to describe them a probabilistic approach in the sense of averaged properties is unavoidable.

Complexity can be quantified with Kolmogorov-Sinai entropy of the dynamics of the system. For regular dynamics it is zero, for stochastic dynamics infinite. In deterministic chaotic systems this entropy is finite. When linear deterministic systems are coupled linearly, then the complexity neither falls nor grows, this situation is trivial in the reductionist approach. To reveal non-trivial effects in deterministic complex system either the individual systems or the coupling have to be non-linear, complex systems can be modelled with lattices of interacting dynamical systems.

Introducing interactions between individual systems can increase or decrease complexity of the whole system. As the dynamics of a large non-linear system cannot be decomposed in terms of its constituting subsystems and studied independently for each such subsystem, complexity typically grows with increasing system size and stronger interactions between subsystems. However, also the opposite effect is possible, stronger interactions can cause simpler dynamics in a large complex systems.

Synchronization is the effect where an increasing coupling strength makes the dynamics of interacting systems timely coherent. Most obvious this effect is in the case of complete synchronization where interactions make the dynamics of individual systems completely coincide, and a number of subsystems of a large complex system form a cluster of completely same dynamics so that the dimensionality of the whole system is reduced according to the size of the cluster. The threshold of this transition is defined by the stability condition for the cluster solution, stability can be understood within the topological or the statistical approaches, these approaches are two alternative ways to describe large complex (ergodic) dynamical systems.

Less strong is the effect of phase synchronization of oscillating systems which is characterized by emerging coherence in the speed of oscillations (e. g. the same mean rotation number per time unit) while the amplitude dynamics remains almost unchanged as compared with

## CHAPTER 1. INTRODUCTION

the interaction-free case. In the case of continuous time systems the phase can be defined as the variable along the trajectory in the local coordinate frame, for oscillating dynamics in absence of interactions it can be defined to be rotating with a constant velocity, specific for each subsystem. Dynamics in dissipative systems in presence of interactions can be described for small coupling with closed equations in phases only. The reason is that phase is neutrally stable while the amplitude dynamics is dissipative.

The definition of the phase is not unique but for analyzing the transition to coherence all definitions should be equivalent in terms of long time averages. For general (chaotic) oscillating dynamics the phase can be introduced by Hilbert transform, in the vicinity of a stable limit cycle by the construction of isochrones, by Poincaré sections, or, sometimes, by an angle variable if some projection of the dynamics is close to a limit cycle.

In this work the transition to coherence at small couplings is investigated. In the next chapter transition to coherence in a lattice of dynamical systems with nearest-neighbor coupling described by closed phase equations is discussed with respect to the symmetries in the system. Then the corresponding effect in discrete chaotic systems, i. e. the transition to coherence in populations of chaotic maps coupled through a mean field is investigated.

## Chapter 2

# Synchronization vs. reversibility in an oscillator lattice with nearest-neighbor coupling

In this chapter we consider a lattice of coupled oscillating systems described by the phase equations showing a hierarchical transition to synchronization through successive formation of synchronization clusters. We demonstrate that there also exists a competing effect caused by the symmetries in the lattice, which makes the latter reveal not dissipative but rather Hamiltonian-in-mean features.

### 2.1 Introduction

The synchronization transitions in lattices of coupled oscillators with nearest-neighbors coupling have attracted a lot of attention recently. Such lattices appear, e. g., in laser arrays [35], Josephson junctions [16], phase locked loops [1, 20], and even in piano strings [107]. Although particular dynamical systems describing these lattices are quite different, there are many general features that can be described already in the framework of the simplest model of coupled phase equations [54, 29, 53, 85] as described in the introductory chapter. Indeed, because the phase of a self-sustained oscillator is free and the amplitude is relaxing to a particular value, small coupling influences the phases only.

The same description can be used for coupled chaotic oscillators as well. Here the phase  $\varphi_k$  of an individual oscillator is free corresponding to a zero Lyapunov exponent; in absence of interactions it rotates with the natural angular velocity  $\omega_k$  specific for this oscillator (plus chaotic fluctuations). Effect of the coupling is phase synchronization of chaotic oscillators [72, 77, 78].

In the case of many coupled oscillators, between the limiting cases of full synchronization (when all oscillators have the same angular velocity) and complete desynchronization (all the frequencies are different) one encounters regimes of partial synchronization. For a lattice such a state appears in the form of synchronization clusters, when neighboring or even non-neighboring oscillators form groups having the same average frequency  $\langle \dot{\varphi} \rangle$ . In general, the

transition from a non-synchronous to a synchronous state can be described as formation and merging of clusters.

Particular features of this process depend on the coupling and on the distribution of natural frequencies. Typically, one assumes that the coupling is attracting, i. e. it tends to equalize the phases of interacting oscillators. More variative is the distribution of frequencies, here two types of models attracted special interest. In papers [2, 116] a random distribution of natural frequencies was considered. Here one can make only statistical predictions on the transition. In [29] a linear distribution of the natural frequencies in a one-dimensional lattice have been studied. It was motivated by experimental observations of formation of clusters in mammalian intestinal smooth muscle [23]. Also boundary conditions are of relevance. These are typically chosen to be free or periodic. These two types of boundary conditions are not equivalent even in the thermodynamic limit, which will be discussed later on. Below only the case of free boundary conditions is investigated.

## 2.2 The phase lattice model and its properties

Here we describe the phase lattice model, reduce it to a closed system in phase differences, and briefly outline its general properties.

### 2.2.1 Basic model

An individual system is described with a phase variable  $\varphi_k$ , it rotates with a constant natural frequency  $\omega_k$ . The coupling of nearest neighbors is implemented via a coupling function  $f$  that depends on the phase differences. As a result, we obtain a set of ordinary differential equations (cf. [1, 54, 29])

$$\left\{ \begin{array}{l} \dot{\varphi}_1 = \omega_1 + \varepsilon f(\varphi_2 - \varphi_1) \\ \dots\dots\dots \\ \dot{\varphi}_k = \omega_k + \varepsilon f(\varphi_{k-1} - \varphi_k) + \varepsilon f(\varphi_{k+1} - \varphi_k) \\ \dots\dots\dots \\ \dot{\varphi}_N = \omega_N + \varepsilon f(\varphi_{N-1} - \varphi_N) \end{array} \right. \quad (2.1)$$

Here  $\varepsilon$  is the coupling constant, it is assumed to be the same for all oscillator pairs. Furthermore we assume  $f(0) = 0$  and  $f'(0) > 0$ . In this case the coupling function tends to equalize the phases of neighbor systems. In other words, this coupling corresponds to a discrete diffusion operator so that it is expected to act dissipatively. To see this, one can expand the right hand side of the equations (2.1) assuming  $\varphi_{k+1} - \varphi_k$  to be small. This yields  $\varepsilon f'(0)(\varphi_{k+1} - 2\varphi_k + \varphi_{k-1})$  which is the discrete form of the second spatial derivative. As the individual systems in the lattice (2.1) are defined modulo  $2\pi$ , the coupling function  $f(\varphi)$  also has to be  $2\pi$ -periodic,  $f(\varphi) = \sum(a_k \sin k\varphi + b_k \cos k\varphi)$ .





## 2.2. THE PHASE LATTICE MODEL AND ITS PROPERTIES

In the case of free boundary conditions and the nearest-neighbor coupling this is equivalent to the condition  $\varepsilon_c = \max_{\forall k} \left| \sum_{m=1}^k \omega_m \right|$  which was derived in [42]. In this case the eigenvalues of  $A_{(N \times N)}$  can be expressed [1] in terms of the second-order Chebyshev polynomials.

It is worth noting that properties of the system strongly depend on symmetry properties of the vector  $\Delta$ , the function  $f(\cdot)$  (or the symmetry of its range) and the coupling matrix  $A$  which is given by the geometry of the problem.

Thus, a stable phase-locked solution exists for large enough couplings. From the consideration above it is also clear, how it loses its stability. This happens when for some  $m^*$  the solutions of (2.7) cease to exist via a saddle-node bifurcation. Typically, beyond this transition the variable  $\psi_{m^*}$  rotates while other phase differences remain bounded. This corresponds to the splitting of the lattice (2.1) in two clusters  $k \leq m^*$  and  $k > m^*$ .

The limiting situations described above suggest that there exists a hierarchy of transitions from the completely phase-locked state at large  $\varepsilon$  to the quasiperiodic state at small  $\varepsilon$ . A scenario depends on the frequencies  $\omega_k$ . Here we focus on a particular case of linearly distributed natural frequencies in the lattice. As have been discussed in [29], it corresponds to a real experimental situation of mammalian intestinal smooth muscle [23]. The results for this particular case are presented in [103], here we discuss them in more detail.

### 2.2.4 Clustering hierarchy

Further in this chapter we consider the particular case of a linear distribution of natural frequencies in (2.1). This means that all frequency differences  $\Delta_k$  in (2.2) are equal. Rescaling the time we can set these differences to unity, thus the resulting system has only one parameter – the coupling constant  $\varepsilon$ . Of course, this specific choice  $\Delta_k = 1$  introduces some new symmetries into the system; below we will see that they strongly influence the dynamics. Furthermore, we use the coupling function  $f(\psi) = \sin \psi$ . This simplest choice also brings additional symmetries, to be discussed below.

Note that the equations (2.1) are autonomous. Additionally they are invariant with respect to an equal shift in all variables  $\varphi_k$  (because of the possibility of reduction to the closed equations in differences  $\psi_k = \varphi_{k+1} - \varphi_k$ ). This means that non-constant solutions of the equations (2.1) are neutrally stable for perturbations along them (in time) as well as for rotations as a whole (shift of all phases), and two Lyapunov exponents are zero in the interval  $\varepsilon \in [0, \varepsilon_c]$ . Above  $\varepsilon_c$  the solution is constant in time. Therefore only one Lyapunov exponent corresponding to the rigid rotation still has to be zero.

The main quantities of interest are the observed frequencies of the oscillators defined as the mean rotation velocities  $\Omega_k = \langle \dot{\varphi}_k \rangle$ . For the oscillators forming a cluster of synchronization these frequencies coincide. Thus, an appearance of a cluster can be easily seen from the bifurcation diagram  $\Omega_k$  vs  $\varepsilon$ . We present these diagrams for several values of the chain length  $N$  in the figure 2.1.

The synchronization diagrams reveal several features.

(i) With increasing  $\varepsilon$  the oscillators successively group into clusters of equal frequencies. The last transition to a single cluster occurs at  $\varepsilon_c$ , which can be calculated according to the

CHAPTER 2. SYNCHRONIZATION VS. REVERSIBILITY

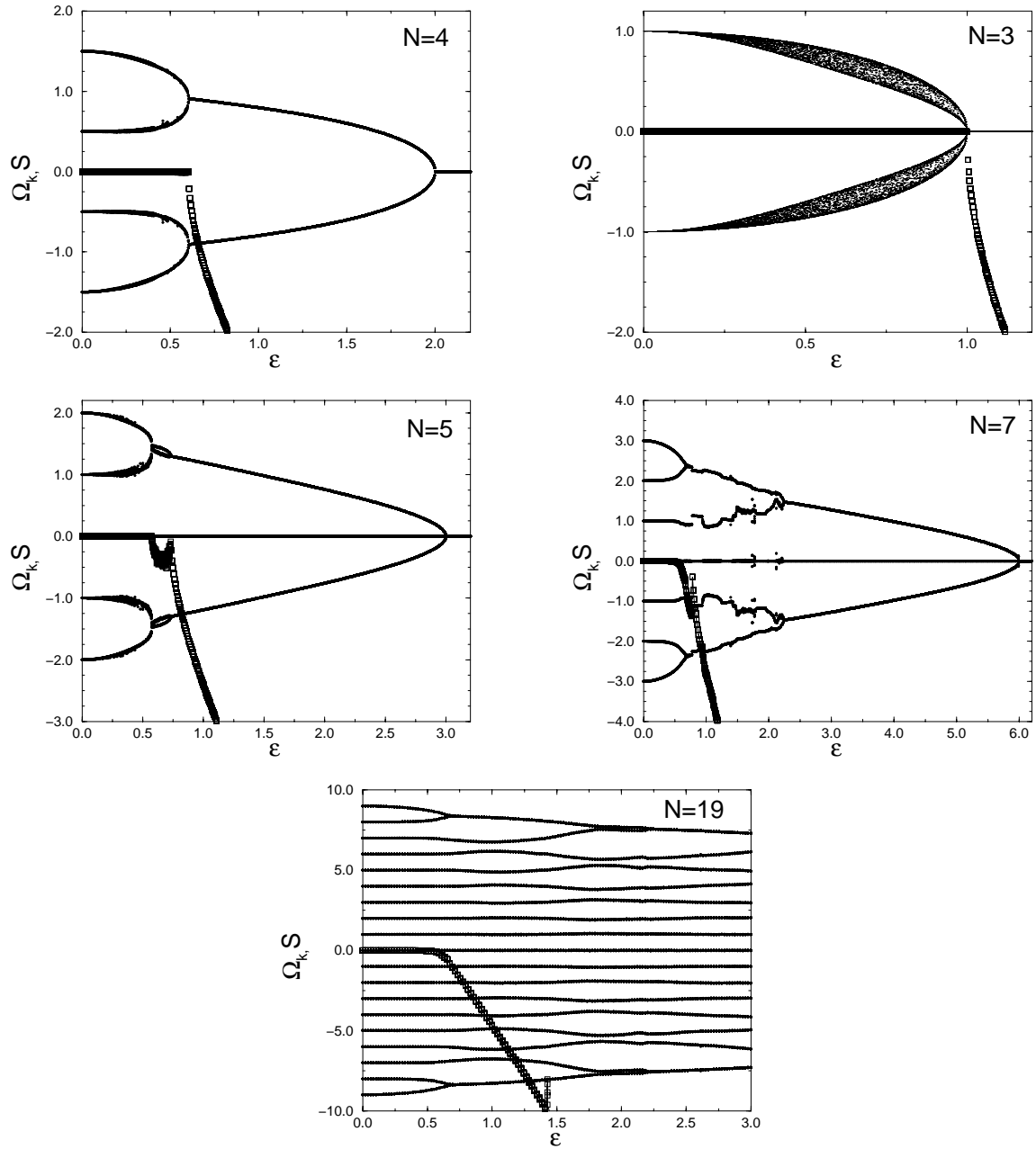


Figure 2.1: Observed frequencies  $\Omega_k$  vs. coupling strength  $\epsilon$  for oscillator chains of different length. The bifurcation diagrams were produced by choosing randomly 10 initial points for each  $\epsilon$  and plotting the resulting frequencies with dots on one graph. The smeared regions that are seen for small  $\epsilon$  indicate the dependence of the frequencies on the initial conditions. On these graphs also the average expansion rate  $S$  (see eq. (2.11)) of the phase volume is shown with squares.



## 2.2. THE PHASE LATTICE MODEL AND ITS PROPERTIES

equations (2.7) and (2.8) above as

$$\varepsilon_c = \begin{cases} N^2/8 & \text{even } N \\ (N-1)(N+1)/8 & \text{odd } N \end{cases} \quad (2.10)$$

When approaching the thermodynamic limit  $N \rightarrow \infty$  the critical coupling  $\varepsilon_c$  diverges quadratically, in the thermodynamic limit there are no fixed point solutions.

(ii) There are regions of frequency locking, e. g. around  $\varepsilon = 0.8$  in the chain of  $N = 7$  phase oscillators in the figure 2.1.

In the figure 2.2 a closer look at the bifurcation diagram in the case of  $N = 7$  oscillators with numerically calculated Lyapunov exponents is presented. In the frequency locking regions at  $\varepsilon \approx 0.8$  and  $\varepsilon \approx 1.3$  the frequencies are  $\Omega_1 = \Omega_2 = 2\Omega_3$ ,  $\Omega_4 = 0$ ,  $2\Omega_5 = \Omega_6 = \Omega_7 = -\Omega_1$ . In the language of phase differences  $\psi_k = \varphi_{k+1} - \varphi_k$  this means that (except for the clusters  $\Omega_1 = \Omega_2$ ,  $\Omega_6 = \Omega_7$ ) the relative phase differences  $\psi_k$  all grow with the same velocity. Both regions are then a sort of 1:1 frequency locking\*.

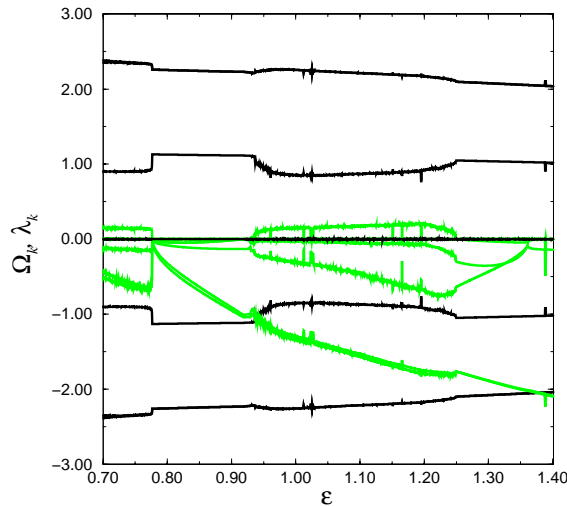


Figure 2.2: Phase locking regions,  $N = 7$ . Mean rotation velocities and calculated Lyapunov exponents (in grey) are shown.

The frequency locking windows correspond to existence of stable periodic solutions which is supported by the observation that all but two Lyapunov exponents are negative in these windows (remember, two Lyapunov exponents are always zero at  $\varepsilon < \varepsilon_c$ ), while beyond them there are positive Lyapunov exponents too so that the lattice is in a chaotic state.

(iii) In some regions of  $\varepsilon$  the diagram is “smeared”. Most visible is this region for the case of three oscillators. In the smeared region the averaged frequency depends on initial conditions, what means that the system does not have a single attractor, but, presumably,

\*One could argue that this situation can also be called as 2:1 locking in the sense of  $\varphi_k$ . However, shifting all the natural frequency  $\omega_k$  by an arbitrary constant would destroy the relations  $\Omega_1 = \Omega_2 = 2\Omega_3$  but the relations for the differences  $\Omega_2 - \Omega_3 = \Omega_3 - \Omega_4 = \Omega_4 - \Omega_5$  would still be valid.

many invariant states. Note that these regions mostly appear in small lattices at small couplings, prior to the first clustering. The discussion of this state is the main purpose of the analysis below [103].

### 2.2.5 Quasi-Hamiltonian dynamics for small couplings

To reveal the dynamics of the lattice, we have calculated the Lyapunov exponents. The calculations of the exponents give the results shown in the figure 2.3. For small couplings we always numerically obtain a sign-symmetric picture of the exponents: they appear in pairs having the same absolute value and opposite signs (additionally, some Lyapunov exponents can be zero). This means that the phase volume is conserved on time average: its mean divergence

$$S = \sum_k \left\langle \frac{\partial \dot{\psi}_k}{\partial \psi_k} \right\rangle = -2\varepsilon \sum_k \langle f'(\psi_k) \rangle \quad (2.11)$$

is the sum of the Lyapunov exponents, and it vanishes. We have checked this by calculating the average (2.11) directly, and found it to be nearly zero (apart from statistical fluctuations). These results are presented in the figure 2.1 (see also detailed calculations in the figure 2.11).

The symmetrical Lyapunov exponents and the conservation of the phase volume are the hallmarks of the Hamiltonian dynamics. Thus we call the dynamics of the lattice at small couplings quasi-Hamiltonian.

In particular, any element of the phase volume  $V = \int \prod dp_k dq_k$  in Hamiltonian systems is conserved (Liouville theorem)

$$\dot{V} = \left\{ \int \prod_k dp_k dq_k, H \right\} = 0 \quad (2.12)$$

Moreover, in Hamiltonian systems Lyapunov exponents always come in symmetric pairs  $\pm\lambda$  [59]. Here a similar structure of Lyapunov exponents is observed, at least in the parameter region of small  $\varepsilon$ .

Obviously, as seen in the figures 2.1 and 2.3, the system (2.3) does not necessarily show dissipative behavior as understood in terms of the phase space contraction. In other words,  $\sum \lambda_k < 0$  is not always valid. This sum is the trace of the right side matrix in the linearized version of (2.3), written for a variation vector  $\delta$  and averaged over a trajectory:

$$\begin{aligned} \dot{\delta}_k &= \varepsilon \sum A_{km} f'(\psi_m) \delta_m, \quad \text{or} \\ \dot{\delta} &= A(\psi) \cdot \delta, \quad \text{with} \quad \text{Sp}A(\psi) = -2\varepsilon \sum f'(\psi_k) \end{aligned}$$

While the sum of the Lyapunov exponents is  $S = \langle \text{Sp}A \rangle$ , the time dependent function of the motion  $\text{Sp}A(\psi(t))$  is interesting by itself. It gives the local phase space volume element expansion rate at every trajectory point  $\psi(t)$ . In a Hamiltonian system this expansion rate equals to zero.

Figures 2.4 and 2.5 show the time dependence of  $\text{Sp}A(t)$  for a chain of four oscillators at different  $\varepsilon$ . Remarkable is the behavior of the system at small  $\varepsilon$ . While numerically  $\sum \lambda_k = \langle \text{Sp}A \rangle = 0$  which resembles the features of Hamiltonian systems, the phase space volume is

## 2.2. THE PHASE LATTICE MODEL AND ITS PROPERTIES

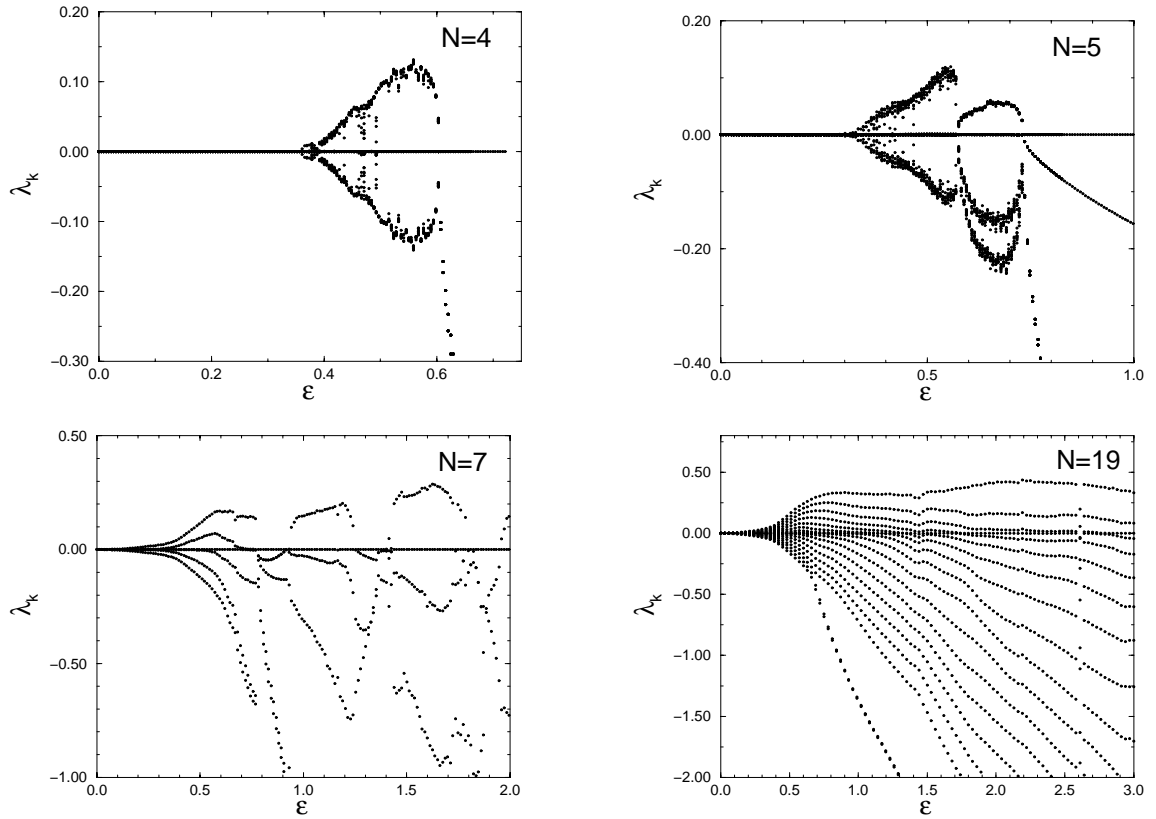


Figure 2.3: Lyapunov exponents vs. coupling strength  $\epsilon$  for the same lattices as in the figure 2.1 (the case  $N = 3$  is not shown, here all Lyapunov exponents vanish for  $\epsilon < 1$  and two are negative for  $\epsilon > 1$ ).

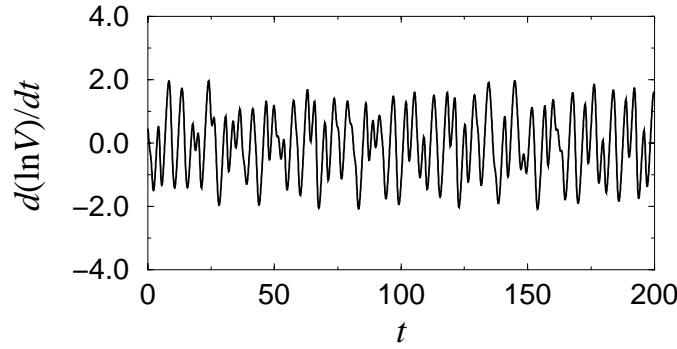


Figure 2.4: The local phase space volume element expansion rate  $\frac{d \ln V}{dt} = \text{Sp}A(t)$  at  $\varepsilon = 0.40$  as the function of time, four oscillators,  $N = 4$ ,  $\langle \text{Sp}A \rangle = \sum \lambda_k \approx 0$ . In a Hamiltonian system phase space volume is conserved, here this would give  $\frac{d}{dt} \ln V = \langle \text{Sp}A \rangle = 0$ .

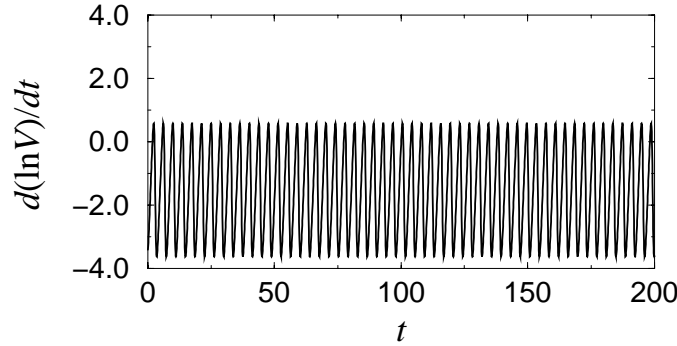


Figure 2.5: The same at  $\varepsilon = 0.70$ , the mean value  $\langle \text{Sp}A \rangle = \sum \lambda_k = -1.5439 < 0$ .

not an integral of motion, it is time-dependent through the instant vector  $\psi(t)$ , and so may be periodic, quasiperiodic, or chaotic. Thus the system (2.6) constructed to be dissipative reveals for a definite coupling strength range not only no dissipative but rather Hamiltonian-in-mean features. It is this Hamiltonian-in-mean kind of behavior that will be further addressed as quasi-Hamiltonian.

## 2.3 Reversibility of regular and chaotic regimes

In this section we will demonstrate that the origin of the quasi-Hamiltonian behavior lies in the reversibility of the system (2.2).

### 2.3.1 Three oscillators

We start with the simplest case of a chain consisting of three oscillators with the vector of frequency differences  $\Delta = \begin{pmatrix} 1 \\ 1 \end{pmatrix}$ . The system (2.6) is two-dimensional:

$$\begin{cases} \dot{\psi}_1 = 1 - 2\varepsilon \sin \psi_1 + \varepsilon \sin \psi_2 \\ \dot{\psi}_2 = 1 - 2\varepsilon \sin \psi_2 + \varepsilon \sin \psi_1 \end{cases} \quad (2.13)$$

### 2.3. REVERSIBILITY OF REGULAR AND CHAOTIC REGIMES

One can substitute  $x = (\psi_1 + \psi_2)/2$  and  $y = (\psi_1 - \psi_2)/2$  into (2.13) and divide one equation by the other to get one non-autonomous ordinary differential equation with the only parameter  $\varepsilon^{-1} > 1$ .

$$\frac{dy}{dx} = -\frac{3 \sin y \cos x}{\varepsilon^{-1} + \sin x \cos y} \quad (2.14)$$

Or, with denoting  $s = x - \frac{\pi}{2}$

$$\frac{dy}{ds} = \frac{3 \sin y \sin s}{\varepsilon^{-1} - \cos s \cos y} \quad (2.15)$$

The right hand side of the equation (2.15) is odd with respect to  $s$ . This means that every solution  $y(s)$  of the equation (2.15) is  $s$ -even. In particular  $y(-\pi) = y(\pi)$ , and, as  $\dot{y}(s) = \dot{y}(s + 2\pi)$ , every solution has to be  $2\pi$ -periodic as seen in the figure 2.6.

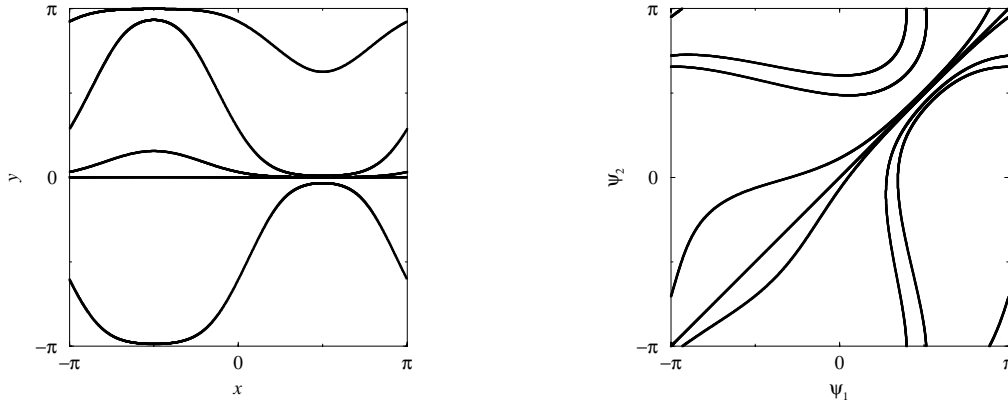


Figure 2.6: Numerical solutions of (2.14) for different initial conditions in  $x$ - $y$  and  $\psi_1$ - $\psi_2$  diagrams, they are all periodic with different periods.  $\varepsilon = 0.29$ .

As a consequence the Lyapunov exponent corresponding to a shift in  $y(0)$  also vanishes. Hence, all three Lyapunov exponents are zero below  $\varepsilon_c = 1$  and the system shows not dissipative but rather conservative behavior in the whole range  $\varepsilon \in [0, 1]$ . Observed velocities  $\Omega_k = \langle \dot{\phi}_k \rangle$  can vary in dependence on the initial condition  $y(0)$ , which is confirmed in the figure 2.1, where initial conditions at different  $\varepsilon$  were randomly chosen.

As seen, in a chain of three oscillators the degenerative dependence on the threshold velocities  $\Omega_k$  from initial conditions is present due to the symmetry in the frequency mismatch between neighbors and the specific choice  $f(\psi) = \sin \psi$ . Let us now generalize this observation for larger chains.

#### 2.3.2 Reversibility

Our explanation of the quasi-Hamiltonian behavior is based on the specific symmetry of the equations (2.1). Namely, the specific symmetries discussed above cause reversibility of the dynamics (see [94, 86] for mathematical definitions).

Reversibility means that there exists an involution  $\mathbf{R} : \Psi \mapsto \Psi$  (involution means that  $\mathbf{R}^2$  is identical transformation;  $\Psi$  here denotes the set of variables  $\Psi = (\psi_1, \dots, \psi_n)$ ) which together with the time reversal transformation  $\mathbf{T} : t \mapsto -t$  leaves the system invariant. Reversibility yields that the trajectories of a dynamical system come in symmetric pairs. Indeed, for every point of the phase space  $\Psi(0)$  there is the symmetric point  $\mathbf{R}\Psi(0)$ , and the trajectory  $\Psi(t)$  starting from  $\Psi(0)$  is symmetric to the trajectory  $\mathbf{R}\Psi(-t)$  running backward in time and starting from  $\mathbf{R}\Psi(0)$ . In the terms of trajectory stability, these symmetric trajectories have inverse Lyapunov spectra, because the Lyapunov exponents change sign with the time inversion and are invariant under any change of variables [64].

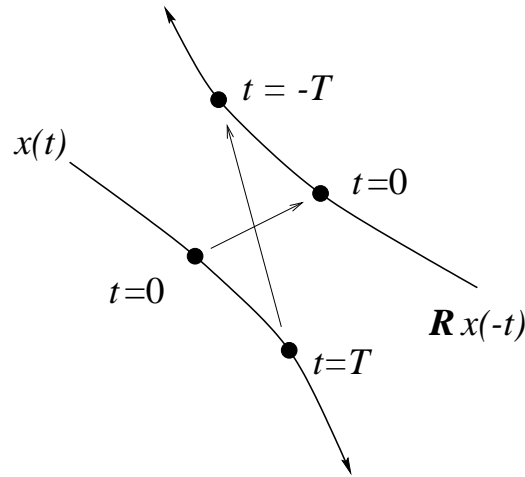
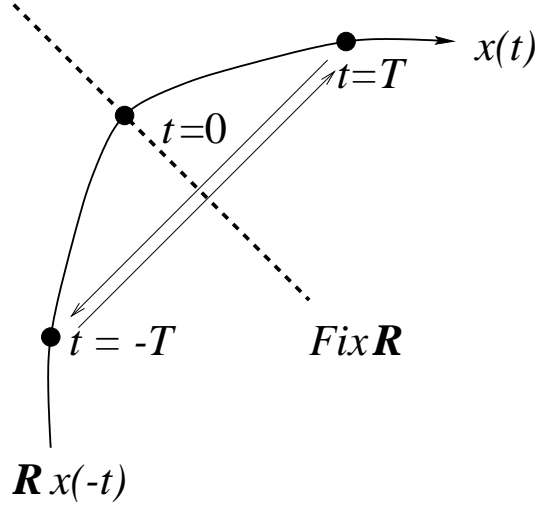


Figure 2.7: The reversibility symmetry, all trajectories come in pairs.

The fact that a system is reversible (i. e. it possesses an involution as described above) still does not say anything on the dissipativity/conservativity of the observed dynamics; it means only that if there is an attractor, there should be the corresponding symmetric repeller. Particularly important is the case where some symmetric trajectories coincide, i. e. if the involution  $\mathbf{R}$  transforms a trajectory to itself. It will be the case if this trajectory crosses the set  $Fix\mathbf{R}$  of the invariant points of the involution ( $\Psi \in Fix\mathbf{R}$  means that  $\mathbf{R}\Psi = \Psi$ ). Such a trajectory we call reversible. If we set  $\mathbf{R}\Psi(0) = \Psi(0)$  (crossing of  $Fix\mathbf{R}$  happens at time  $t = 0$ ) then for a reversible trajectory holds  $\mathbf{R}\Psi(T) = \Psi(-T)$ .

Note that if a reversible trajectory crosses the set  $Fix\mathbf{R}$  twice then it is periodic. Setting  $\mathbf{R}\Psi(0) = \Psi(0)$  and  $\mathbf{R}\Psi(T) = \Psi(T)$ , one notices immediately that  $\mathbf{R}\Psi(-T) = \Psi(-T) = \mathbf{R}\Psi(T)$  holds too. The trajectory has the period of  $2T$ . Properties of periodic reversible trajectories are like of those in Hamiltonian systems: the Lyapunov exponents are sign-symmetric and the phase space volume in their vicinity is conserved on average (in particular, the local Poincaré map is area-preserving).

In general, reversible trajectories may be non-periodic, and coexist with non-reversible ones. Here we can distinguish two cases. A reversible non-periodic trajectory can connect an attractor and a repeller, being heteroclinic. Note that even in this case the phase space in the vicinity of this trajectory is conserved on average, if averaging is understood in the sense of a principal value as integration from  $-T$  to  $T$  with  $T \rightarrow \infty$ .


 Figure 2.8: Reversible trajectories cross the invariant set  $Fix\mathbf{R}$ .

Otherwise, a reversible trajectory can be non-wandering<sup>†</sup>, in particular, it can repeatedly return to a vicinity of the set  $Fix\mathbf{R}$ . In the latter case the average properties have to be qualitatively similar to those of periodic reversible trajectories, and in particular the Lyapunov exponents are sign-symmetric. This property is very important if we consider complex (quasiperiodic or chaotic) invariant sets.

If such a set is ergodic, and at least one typical trajectory belonging to it is reversible and non-wandering, then the invariant measure is  $\mathbf{R}$ -symmetric and the dynamics of the system is quasi-Hamiltonian on this set. Note that this property does not require any symplectic structure and hence does not depend on evenness/oddness of the underlying phase space.

We now argue, that in order for periodic and non-wandering reversible trajectories to exist, the set  $Fix\mathbf{R}$  should be large enough. Let us consider the evolution of  $Fix\mathbf{R}$  in time. A reversible periodic trajectory exists if the sets  $F^t(Fix\mathbf{R})$  and  $Fix\mathbf{R}$  intersect, where  $F^t$  is the evolution operator of the dynamical system. This intersection generally can occur in a  $n$ -dimensional phase space if the topological dimension of  $Fix\mathbf{R}$  is large enough, at least  $[n/2]$ , i.e.  $n/2$  for even and  $(n-1)/2$  for odd  $n$ , the dimension of  $F^t(Fix\mathbf{R})$  being then  $[n/2] + 1$ .

Basing on the continuity arguments, we obtain the same estimate for a general existence of non-wandering trajectories, because in the latter case the distance between  $F^t(Fix\mathbf{R})$  and  $Fix\mathbf{R}$  has to nearly vanish at some times. Contrary to this, if the dimension of the set  $Fix\mathbf{R}$  is small, generally there are no non-wandering reversible trajectories. From these arguments it follows, that not all possible involutions  $\mathbf{R}$  can explain the quasi-Hamiltonian behavior, but only those having a high-dimensional invariant set  $Fix\mathbf{R}$ .

### 2.3.3 Reversibility of the oscillator lattice

We now proceed with applying this concept to the lattice of  $n$  oscillators (2.2). The involution yielding reversibility here is

<sup>†</sup>In the sense that its every point is non-wandering.

$$\mathbf{R} : \psi_k \mapsto \pi - \psi_{n-k} \quad (2.16)$$

One can see that this transformation can be represented as the product  $\mathbf{R} = \mathbf{P} \circ \mathbf{Q}$  of two involutions:

$$\mathbf{P} : \psi_k \mapsto \psi_{n-k} \quad (2.17)$$

and

$$\mathbf{Q} : \psi_k \mapsto \pi - \psi_k \quad (2.18)$$

These transformations reflect the symmetry of the distribution of the natural frequencies ( $\mathbf{P}$  requires  $\Delta_k = \Delta_{n-k}$ ) and the symmetry of the coupling function  $f(\cdot)$  ( $\mathbf{Q}$  requires that the odd function  $f$  has only odd harmonics in its expansion in sine Fourier series) as well as the specific geometry of the lattice given by the matrix  $A$  in the matrix formulation (2.4). Involution (2.16) has an invariant set  $\psi_k + \psi_{n-k} = \pi$  of dimension  $[n/2]$ , thus we can expect periodic and non-wandering reversible trajectories to exist. This is not the case for the involution  $\mathbf{Q}$ : its invariant set  $\psi_k = \pi/2$  is one point.

Below we consider implications of the reversibility described for some particular lattices.

### 2.3.4 Three coupled oscillators revisited

Involution (2.16) for the system (2.13) has invariant line  $\text{Fix}\mathbf{R} : \psi_1 + \psi_2 = \pi$ , or  $x = \pi/2$  in the language of the section 2.3.1.

Because  $\dot{x} = 1 - \varepsilon \sin x \cos y > 0$  when  $\varepsilon < \varepsilon_c = 1$ , it is clear that on the two-dimensional phase plane  $(\psi_1, \psi_2)$  every (rotating) trajectory crosses this line many times (more than once), thus all trajectories are periodic and reversible, and the desynchronized state is quasi-Hamiltonian. We show the phase portrait in the figure 2.9. It represents a typical for an integrable Hamiltonian system family of periodic orbits. These orbits have different periods, and this explains the diversity of frequencies ("smeariness") in the figure 2.1. A difference to Hamiltonian phase portraits can be also easily seen: because the phase volume is conserved in average, but not locally, different regions on the phase plane are filled with different densities. The transition to clusters occurs via an inverse saddle-node bifurcation, at which stable and unstable points appear at  $\psi_1 = \psi_2 = \pi/2$  from the condensation of trajectories.

### 2.3.5 Four coupled oscillators

The system of four coupled oscillators reads

$$\begin{cases} \dot{\psi}_1 = 1 - 2\varepsilon \sin \psi_1 + \varepsilon \sin \psi_2 \\ \dot{\psi}_2 = 1 - 2\varepsilon \sin \psi_2 + \varepsilon \sin \psi_1 + \varepsilon \sin \psi_3 \\ \dot{\psi}_3 = 1 - 2\varepsilon \sin \psi_3 + \varepsilon \sin \psi_2 \end{cases} \quad (2.19)$$

Applying the involution (2.16), we obtain that the set  $\text{Fix}\mathbf{R}$  is the line  $\psi_1 + \psi_3 = \pi, \psi_2 = \pi/2$ . The phase trajectories in a three-dimensional phase space generally do not intersect a given



### 2.3. REVERSIBILITY OF REGULAR AND CHAOTIC REGIMES

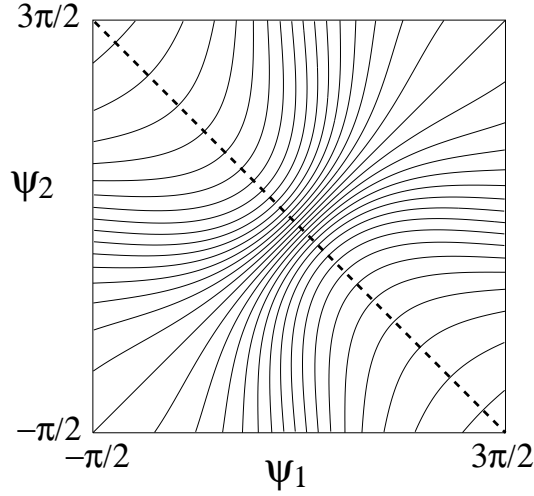


Figure 2.9: The phase portrait of the system (2.13). The line  $Fix\mathbf{R}$  is shown as bold dashed one; it is crossed by all trajectories.

line, so we cannot expect reversibility for all trajectories. In this case we observe a non-trivial transition from the quasi-Hamiltonian to the dissipative dynamics, to be described below.

To visualize the dynamics we constructed the Poincaré maps. The Poincaré section was chosen by the condition  $\psi_2 = \pi/2$  so that the invariant set of the involution is the line  $\psi_1 + \psi_3 = \pi$  on this plane. The Poincaré maps for different values of parameter  $\varepsilon$  are presented in the figure 2.10. They are constructed by iterations of initial points lying on the line  $\psi_1 + \psi_3 = \pi$ , i. e. belonging to  $Fix\mathbf{R}$ .

To verify whether the dynamics is quasi-Hamiltonian or not, we calculated the average divergence of the phase volume  $S$  over a very large time (up to  $T = 1.5 \times 10^7$ ). Only the values of  $S$  that are nearly the same for the averaging times  $T/2$  and  $T$  have been considered to be distinguishable from zero. The data is presented in the figure 2.11 together with the calculations for larger lattices.

(i) Quasiperiodic dynamics for small  $\varepsilon$ :

In the case shown in the figure 2.10a the dynamics appears to be quasiperiodic, and the phase space appears to be foliated by tori. All these tori cross the line  $Fix\mathbf{R}$ , thus on each torus there is a reversible non-wandering trajectory. This ensures reversibility of the tori, and the whole dynamics is quasi-Hamiltonian. The average divergence  $S$  in this case is indistinguishable from zero.

(ii) Mixed quasi-Hamiltonian dynamics:

In the case shown in the figure 2.10b the dynamics appears to be quasi-Hamiltonian with chaotic and quasiperiodic components. In some components images of  $Fix\mathbf{R}$  appear to be dense. This allows us to speak of “reversibility in average”. Note, that due to ergodicity the mean frequency is the same for all typical trajectories in the chaotic sea, but has different values for different tori. Thus, the mean frequency depends on initial conditions. On the other hand, there are components having no overlap with images of  $Fix\mathbf{R}$ , they are nevertheless symmetric with regard to the involution.

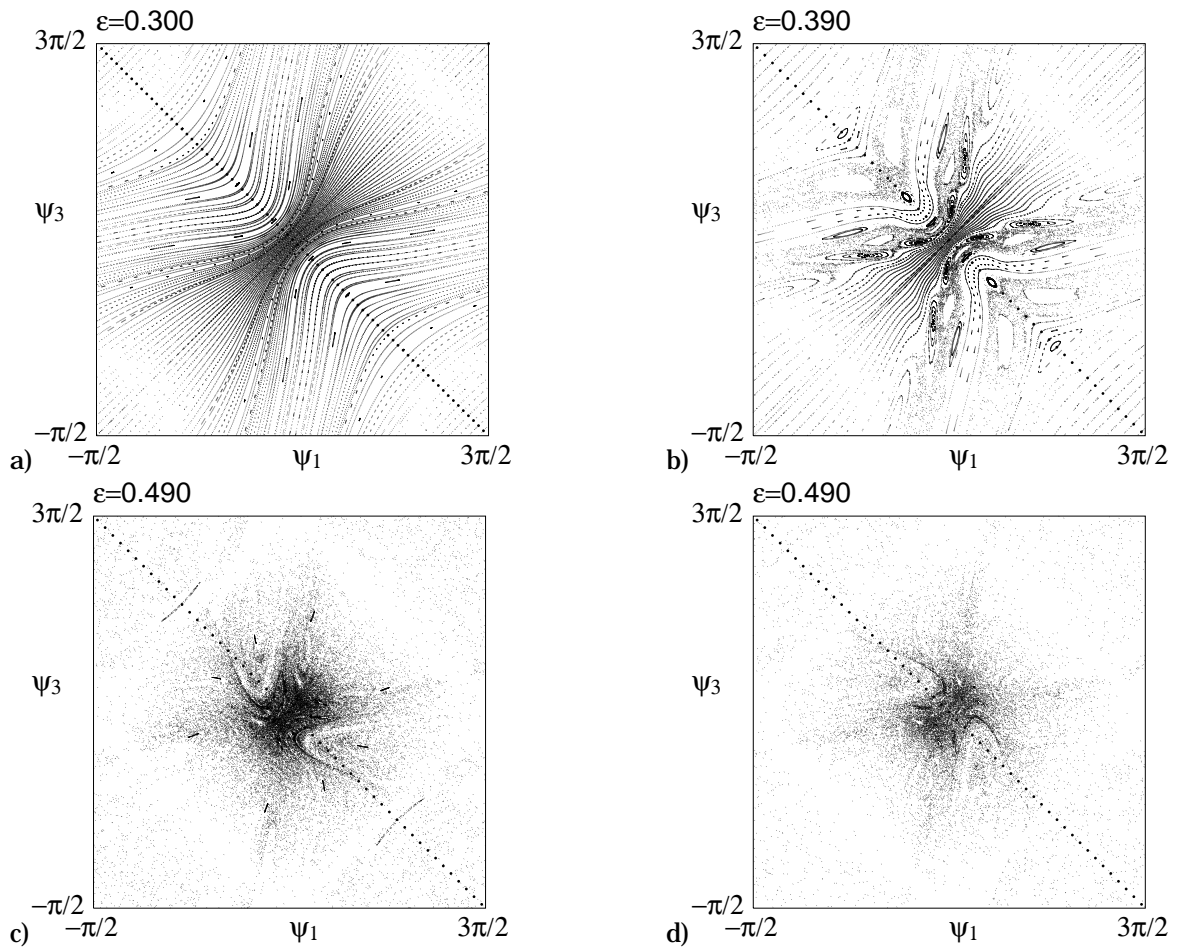


Figure 2.10: The Poincaré map for the system (2.19) for different values of coupling. The maps are constructed by choosing the initial conditions on the line  $\psi_1 + \psi_3 = \pi$  (filled circles) and plotting 2000 their iterations. (a)  $\varepsilon = 0.3$ , the quasiperiodic states dominate. (b)  $\varepsilon = 0.39$ : chaotic and quasiperiodic regimes coexist. The attractor and the repeller for  $\varepsilon = 0.49$  are shown in (c) and (d), respectively.

### 2.3. REVERSIBILITY OF REGULAR AND CHAOTIC REGIMES

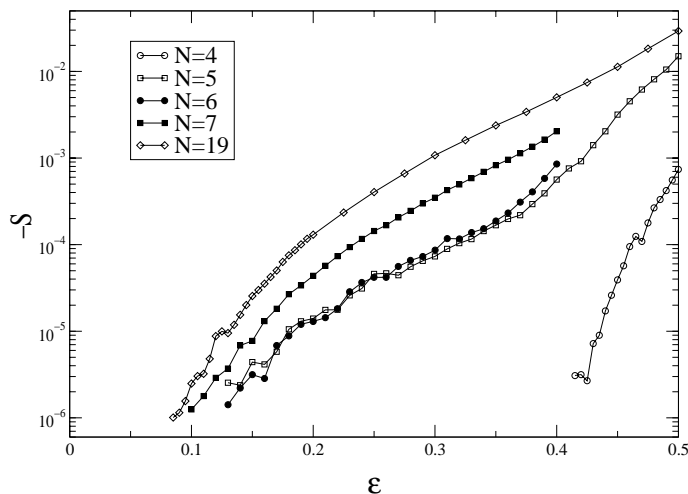


Figure 2.11: The average divergence of the phase volume for lattices of different sizes. The lowest values at  $|S| \approx 10^{-6}$  correspond to the remaining statistical uncertainty achieved after averaging over times as large as  $10^7$ . Up to this uncertainty, the threshold for the transition from the quasi-Hamiltonian to reversible behavior appears to lie at  $\varepsilon \approx 0.1$  for lattices with  $N > 4$ .

#### (iii) Chaotic dissipative dynamics:

As one can see from the detailed calculations of the mean divergence of phase volume (figure 2.11), for  $\varepsilon > 0.43$  the divergence is non-zero, although very small. Accordingly, we have to characterize the observed chaotic state as an attractor. Surely, there exists also the repeller symmetric to the attractor – it can be easily obtain via backward integration of the equations (2.19). We present the phase portraits of the attractor and the repeller in the figures 2.10c and 2.10d. From visual inspection of these pictures one may conclude that the attractor and the repeller “overlap”. However, according to the Birkhoff ergodic theorem [11], the invariant measures of these invariant sets should be mutually singular.<sup>‡</sup> The contradiction is resolved if one takes into account that although the attractor and the repeller look like possessing positive Lebesgue measure, in reality they are fractals having Lebesgue measure zero. Because the mean divergence of the phase volume is very small, the dimensions of these fractals are extremely close to 2, therefore it is difficult to distinguish them from quasi-Hamiltonian dynamics. Note that there exist reversible trajectories which are still non-wandering while being heteroclinic. The attractor and the repeller do not contain *FixR* but their closures do.

We emphasize that for some values of coupling we observed non-chaotic, periodic attractors in the system as shown in the figure 2.12. The situation appears to be similar to other cases of non-hyperbolic chaotic dynamics (e. g. in the Hénon map), where stable orbits with relatively short periods appear and disappear as a parameter is varied. Numerically, it is difficult to distinguish whether in these situations the chaotic attractor transforms to a chaotic saddle and the only attractor is the regular one, or there is a bistability “chaos - periodic orbit”.

<sup>‡</sup>We are thankful to D. Turaev for this remark.

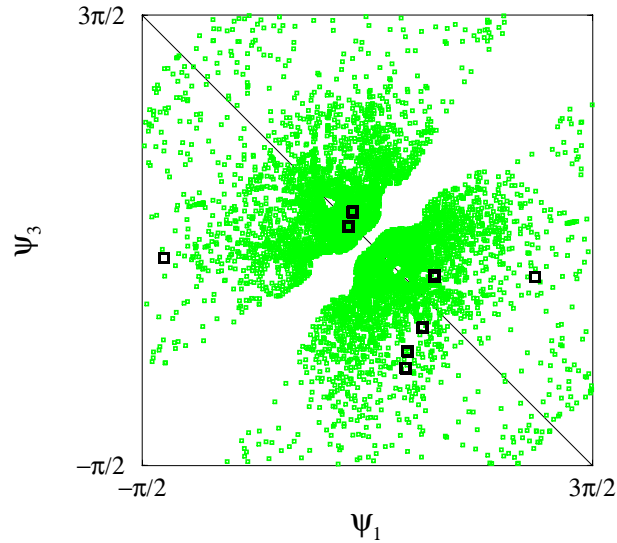


Figure 2.12: Stable periodic attractor,  $\varepsilon = 0.46$ . Transient chaotic state is shown in grey, integration time was  $10^6$ . Note that some points of the actually period 12 orbit nearly coincide, which hints that they were born from an orbit of a smaller period.

(iv) Clustering transition:

With increasing of the coupling, at  $\varepsilon \approx 0.604$  a pair of stable and unstable fixed points appears in the Poincaré map. On the stable periodic solution of system (2.19) the mean rotation frequencies of the variables  $\psi_3$  and  $\psi_1$  coincide, which corresponds to the appearance of the cluster (cf. Fig 2.1). The set  $Fix\mathbf{R}$  is now attracted to the stable orbit which is a global attractor of system (2.19), and the dynamics on this attractor is no more reversible.

### 2.3.6 Large number of oscillators

In the case of a large number of oscillators we can characterize the dynamics with averaged quantities like Lyapunov exponents, but it is rather difficult to reveal the topological structure in the phase space. Calculations of the Lyapunov exponents show that for small couplings  $\varepsilon$  they are coming in sign-symmetric pairs and the phase volume is conserved in average, i. e. the system is quasi-Hamiltonian. The dimension of the invariant set of the involution  $Fix\mathbf{R}$  is exactly  $[n/2]$  and thus is large enough to make reversible non-wandering orbits possible.

Numerically, it appears that the transition from quasi-Hamiltonian to dissipative dynamics for a large number of oscillators is not as abrupt as for  $N = 3$ , and does not coincide with the point of the first clustering, but is similar to the continuous transition described above for  $N = 4$ . This can be seen from the calculations of the average divergence of the phase space  $S$  (2.11) presented in the figure 2.11. Because of large statistical fluctuations we were not able to determine  $S$  with accuracy better than  $10^{-6}$ , and with this accuracy the threshold for the

transition lies at  $\varepsilon \approx 0.1$ . We expect that this threshold should be the same for every large chain length  $N$  because first clusters always appear at the ends of the chain and thus should not depend in a strong way on the number of oscillators in the middle of the chain. Due to high dimensionality of the system, we could not follow any topological transition in the structure of chaos at this point.

## 2.4 Destruction of reversibility

Obviously, the involution (2.16) which is responsible for the reversibility is based on the high symmetry in the lattice. This symmetry exists both due to the particular distribution of the frequencies  $\Omega_k$  ( $\mathbf{P}$ -symmetry) and the symmetry of the coupling function ( $\mathbf{Q}$ -symmetry). We demonstrate here that violations of these symmetries lead to non-reversible dynamics. For small lattice sizes properties of  $\mathbf{P}$ -symmetric solutions are discussed.

### 2.4.1 Non-uniform frequency distribution

Here we will demonstrate that quasi-Hamiltonian features disappear if the symmetry in the distribution of  $\Delta_k$  responsible for the  $\mathbf{P}$ -symmetry is broken. We start with the case of three oscillators.

(i) Three oscillators:

Given a general frequency vector  $\Delta = \begin{pmatrix} \Delta_1 \\ \Delta_2 \end{pmatrix}$  what would change in the behavior of the system? The system (2.6) reads now

$$\begin{cases} \dot{\psi}_1 = \Delta_1 - 2\varepsilon \sin \psi_1 + \varepsilon \sin \psi_2 \\ \dot{\psi}_2 = \Delta_2 - 2\varepsilon \sin \psi_2 + \varepsilon \sin \psi_1 \end{cases} \quad (2.20)$$

In the section 2.3.1 the substitution  $\psi_1 = x + y$  and  $\psi_2 = x - y$  was made. In the new variables  $x$  rotates ( $\dot{x} > 0, \forall x, y$ ) and  $y$  oscillates. A similar transformation is possible also if the frequency vector  $\Delta \not\sim \begin{pmatrix} 1 \\ 1 \end{pmatrix}$  is of general form  $\Delta = c_1 \begin{pmatrix} 1 \\ 1 \end{pmatrix} + c_2 \begin{pmatrix} 1 \\ -1 \end{pmatrix}$ . With the substitution  $x = ((c_1 - c_2)\psi_1 + (c_1 + c_2)\psi_2)/2$  and  $y = ((c_1 - c_2)\psi_1 - (c_1 + c_2)\psi_2)/2$  the equations (2.20) read

$$\begin{cases} \psi_1 = \frac{x+y}{c_1-c_2} \\ \psi_2 = \frac{x-y}{c_1+c_2} \end{cases}, \quad \text{and} \quad \frac{dy}{dx} = \frac{\dot{y}}{\dot{x}} = \frac{(c_2 + 3c_1) \sin \frac{x-y}{c_1+c_2} + (c_2 - 3c_1) \sin \frac{x+y}{c_1-c_2}}{2\varepsilon^{-1}(c_1^2 - c_2^2) - (c_1 + 3c_2) \sin \frac{x-y}{c_1+c_2} - (c_1 - 3c_2) \sin \frac{x+y}{c_1-c_2}} \quad (2.21)$$

The dynamics is reversible if  $dy/dx$  in the equation (2.21) is odd with respect to the rotating variable  $x$  (maybe shifted like in the equation (2.15)). This is the case in two situations. The first situation is given by  $\Delta \sim \begin{pmatrix} 1 \\ 1 \end{pmatrix}$ , i. e. natural frequencies  $\omega_k$  are distributed linearly.

CHAPTER 2. SYNCHRONIZATION VS. REVERSIBILITY

The situation  $\Delta \sim \begin{pmatrix} -1 \\ 1 \end{pmatrix}$  gives another degenerative case<sup>§¶</sup> with only periodic solutions in the whole region  $\varepsilon \leq \varepsilon_c = \frac{1}{3}$  as defined by the equation (2.9) (now denoting  $x = (\psi_2 - \psi_1)/2$  and  $y = (\psi_2 + \psi_1)/2$ ).

$$\frac{dy}{dx} = \frac{\sin y \cos x}{\varepsilon^{-1} - 3 \sin x \cos y} \tag{2.22}$$

If  $\Delta$  has both  $\begin{pmatrix} 1 \\ 1 \end{pmatrix}$  and  $\begin{pmatrix} -1 \\ 1 \end{pmatrix}$  components then the solutions are no more 1-periodic. We will analyze this general case with construction of the Poincaré map defined by the section  $x = \pi/2$ . This section is crossed by all trajectories because  $x$  is rotating at a sufficiently small  $\varepsilon$  (cf. equation (2.21)) for arbitrary  $c_1$  and  $c_2$ . Moreover, in the cases where all solutions are periodic,  $\Delta \sim \begin{pmatrix} 1 \\ 1 \end{pmatrix}$  and  $\Delta \sim \begin{pmatrix} -1 \\ 1 \end{pmatrix}$ , this section coincides with the invariant set  $Fix\mathbf{R}$  of the corresponding reversibility involution<sup>||</sup>.

Now we will analyze the one-dimensional function  $g(y)$  mapping the point from one Poincaré section  $\begin{pmatrix} \pi/2 \\ y \end{pmatrix}$  to the next Poincaré section point  $\begin{pmatrix} 2\pi+\pi/2 \\ g(y) \end{pmatrix}$ , so that e. g.  $g(y) = y$  would correspond to 1-periodic solutions, and  $g(\forall y) \neq y$  would mean that no simple 1-periodic solution exists.

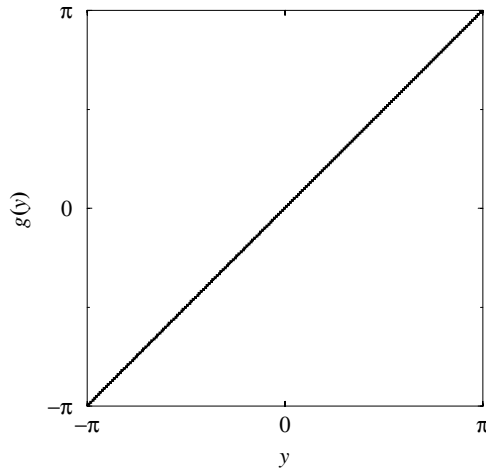


Figure 2.13: The Poincaré map with  $\Delta = \begin{pmatrix} 1 \\ 1 \end{pmatrix}$  or  $\Delta = \begin{pmatrix} -1 \\ 1 \end{pmatrix}$  at  $\varepsilon = 0.29 < \varepsilon_c$ ,  $f(\psi) = \sin \psi$ , is an identical map.

<sup>§</sup>This situation is reported in [107] to correspond to a typical arrangement of piano strings. Already in the Middle Age one noticed that a piano sounds better if instead of one string one would take three and slightly detune the middle one.

According to [107], in this case the horizontal oscillation modes are decaying much slower than vertical modes, which causes a typical aftersound. If the strings on the left and right of the middle one are detuned too then this effect disappears.

Horizontal modes of the three strings are weakly interacting and can be described with phase equations similar to equations (2.1) so that the slowness of their decay can be ascribed to this new effect of non-dissipativity of the symmetric solution with  $\Delta \sim \begin{pmatrix} -1 \\ 1 \end{pmatrix}$ .

<sup>¶</sup>We thank Prof. G. Pfister for attracting our attention to this example.

<sup>||</sup>Note that reversible trajectories always cross  $Fix\mathbf{R}$  transversally, i. e.  $\Psi \times K = 0$  for any vector of the tangential space at the crossing point  $\Psi_0$ ,  $K \in T_{\Psi_0}(Fix\mathbf{R})$ . The reason is that  $\mathbf{R}\Psi = -\Psi$  at the crossing point.

## 2.4. DESTRUCTION OF REVERSIBILITY

If all solutions are periodic then the map  $g(y)$  is identical,  $g(y) \equiv y$  (see figure 2.13) which is the case if  $\Delta \sim \begin{pmatrix} 1 \\ 1 \end{pmatrix}$  or  $\Delta \sim \begin{pmatrix} -1 \\ 1 \end{pmatrix}$ .

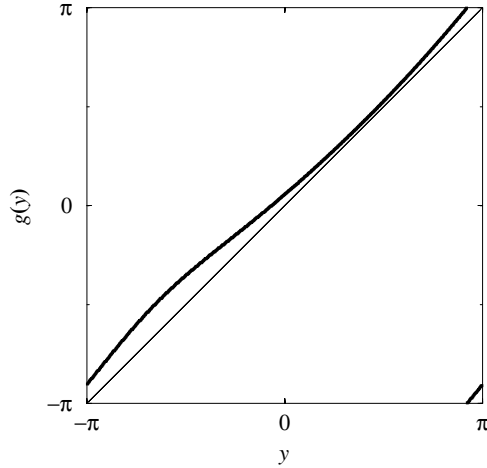


Figure 2.14: The Poincaré map,  $\Delta = \begin{pmatrix} 1 \\ 1 \end{pmatrix} + 0.01 \begin{pmatrix} -1 \\ 1 \end{pmatrix}$  at  $\varepsilon = 0.29 < \varepsilon_c$ .  $f(\psi) = \sin \psi$

In the case of the broken symmetry,  $\Delta = \begin{pmatrix} 1 \\ 1 \end{pmatrix} + c \begin{pmatrix} -1 \\ 1 \end{pmatrix}$ , we obtain the map from the figure 2.14 corresponding to a general circle map,  $y_{n+1} = g(y_n)$ . Therefore, Arnold tongues representing the stability regions in the plane of parameters  $(\varepsilon, c)$  are expected, which means the existence of a set of stability intervals in  $\varepsilon$ .

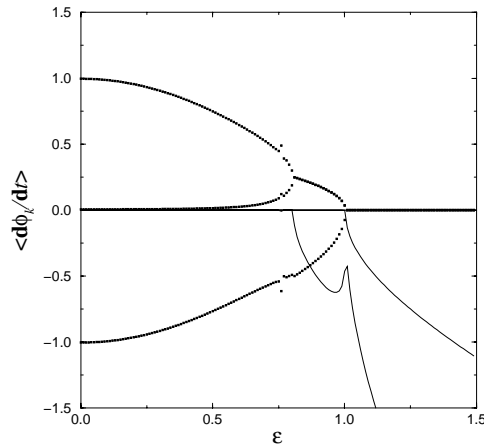


Figure 2.15: The synchronization diagram  $\Omega_k$  vs.  $\varepsilon$  (dots) and calculated Lyapunov exponents (lines) for  $\Delta = \begin{pmatrix} 1 \\ 1 \end{pmatrix} + 0.01 \begin{pmatrix} -1 \\ 1 \end{pmatrix}$ ,  $f(\psi) = \sin \psi$ .

In the figure 2.15 the synchronization diagram for  $\Delta = \begin{pmatrix} 1 \\ 1 \end{pmatrix} + 0.01 \begin{pmatrix} -1 \\ 1 \end{pmatrix}$  is plotted. The period-locking region around  $\varepsilon = 0.75$  is just one of many Arnold tongues which are clearly

seen in the zoomed figure 2.16.

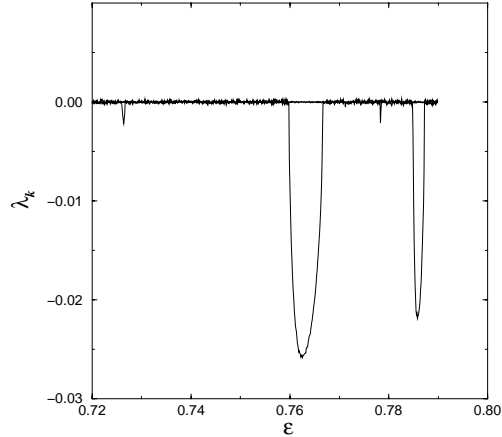


Figure 2.16: Lyapunov exponents for  $\Delta = \begin{pmatrix} 1 \\ 1 \end{pmatrix} + 0.01 \begin{pmatrix} -1 \\ 1 \end{pmatrix}$ , a closer look. The frequency locking region which was seen in the figure 2.15 reveals a fine structure of several (possibly infinitely many) Arnold tongues,  $f(\psi) = \sin \psi$ .

Thus in a chain of three oscillators one typically finds quasiperiodic trajectories with all three zero Lyapunov exponents and dissipative windows of periodic limit cycles (Arnold tongues).

(ii) Larger chains:

In general, the involution (2.16) requires that the frequency differences in (2.3) are symmetric but not necessarily equal.

$$\Delta_k = \Delta_{n-k}, \quad k = 1, \dots, n/2 \quad (2.23)$$

We illustrate this in the figure 2.17a. The phase volume here is conserved in average, and the dynamics remains reversible and quasi-Hamiltonian. Contrary to this, if we take a distribution of frequency differences that violates the symmetry (2.23), we obtain a strange attractor instead of quasi-Hamiltonicity (figure 2.17b). We emphasize, that also in this latter case the system is reversible under the  $\mathbf{P}$ -involution (2.18). The dimension of the invariant set of this involution is, however, too low (zero) to ensure reversibility of the dynamics.

We note that if the symmetry (2.23) is only slightly violated, the dynamics remains nearly quasi-Hamiltonian: the convergence of the phase space volume is small. In the chaotic case this means that the dimension of the attractor is close to the dimension of the phase space. In the periodic case like that in the figure 2.9 a weak dissipation means that the Poincaré map is a circle map close to the identity. It is known that in such maps a vast majority of states is quasiperiodic, i. e. they have zero Lyapunov exponents and are therefore not distinguishable from the quasi-Hamiltonian ones.



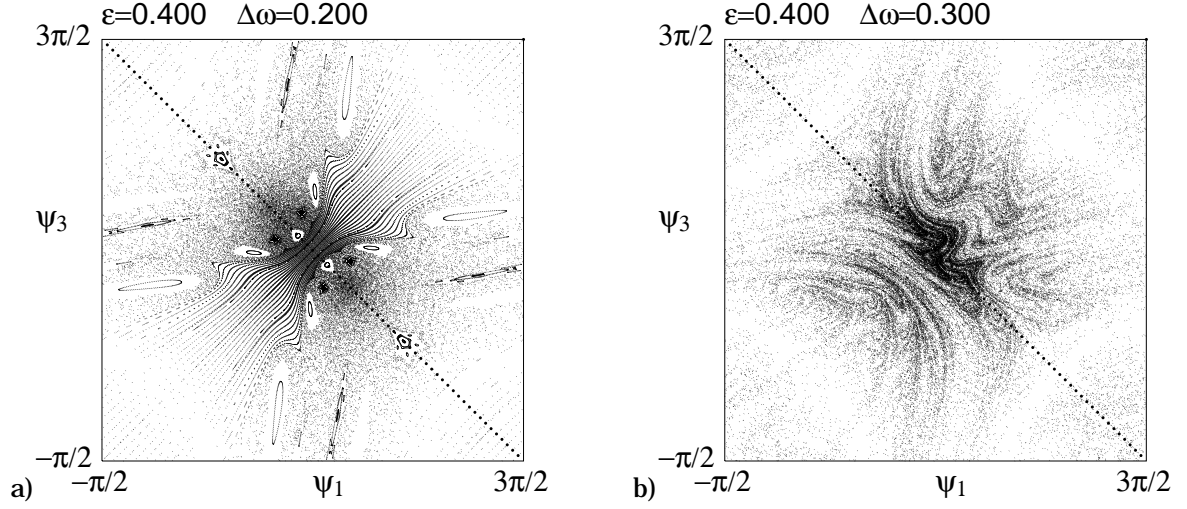


Figure 2.17: The dynamics of the system (2.3) with  $N = 4$ ,  $\varepsilon = 0.4$ . (a):  $\Delta_1 = \Delta_3 = 1$ ,  $\Delta_2 = 1.3$ . Here a violation of equality of frequencies that does not destroy involution (2.16) preserves quasi-Hamiltonian dynamics. (b):  $\Delta_1 = \Delta_2 = 1$ ,  $\Delta_3 = 1.2$ . The involution (2.16) is broken; the dynamics is dissipative with a strange attractor.

### 2.4.2 Non-symmetric coupling function

Here we demonstrate that violations of the function symmetry (2.18) lead to break of reversibility.

(i) Three oscillators:

Let us try different  $2\pi$ -periodic coupling functions  $f(\psi) = \sum(a_k \sin k\psi + b_k \cos k\psi)$ . As this  $f(x)$  is in general non-odd, the equations (2.1) now read as

$$\begin{cases} \dot{\Psi}_1 = 1 + \varepsilon(f(\Psi_2) + f(-\Psi_1) - f(\Psi_1)) \\ \dot{\Psi}_2 = 1 + \varepsilon(-f(-\Psi_1) + f(-\Psi_2) - f(\Psi_2)) \end{cases} \quad (2.24)$$

After performing the same substitution like in the equation (2.14),  $\psi_1 = x + y$  and  $\psi_2 = x - y$ , one obtains

$$\frac{dy}{dx} = \frac{(f(-y+x) + f(-y-x)) - \frac{1}{2}(f(y+x) + f(y-x))}{\varepsilon^{-1} - \frac{1}{2}(f(y+x) - f(y-x))} = \frac{2G_+(-y,x) - G_+(y,x)}{\varepsilon^{-1} - G_-(y,x)} \quad (2.25)$$

The functions  $G_{\pm}(u, v) = \frac{1}{2}(f(u+v) \pm f(u-v))$  are even/odd with respect to the second argument,  $G_{\pm}(u, v) = \pm G_{\pm}(u, -v)$ . The symmetry as from the case of  $f(\psi) = \sin \psi$  is present if the functions  $G_{\pm}(u, v + \frac{\pi}{2})$  are odd/even with respect to  $\frac{\pi}{2}$ , i. e.  $G_{\pm}(u, \frac{\pi}{2} + v) = \mp G_{\pm}(u, \frac{\pi}{2} - v)$ ,  $\forall u, v$ . The denominator would then be an even function and the numerator an odd one. For a generic  $2\pi$ -periodic function  $f(\psi) = \sum(a_k \sin k\psi + b_k \cos k\psi)$  holds

$$\begin{cases} G_+(u, v) = \frac{1}{2} \sum(a_k \sin k(u+v) + b_k \cos k(u+v) + a_k \sin k(u-v) + b_k \cos k(u-v)) \\ G_-(u, v) = \frac{1}{2} \sum(a_k \sin k(u+v) + b_k \cos k(u+v) - a_k \sin k(u-v) - b_k \cos k(u-v)) \end{cases}$$

## CHAPTER 2. SYNCHRONIZATION VS. REVERSIBILITY

or

$$\begin{cases} G_+(u, v) = \sum (a_k \sin ku + b_k \cos ku) \cos kv \\ G_-(u, v) = \sum (a_k \cos ku - b_k \sin ku) \sin kv \end{cases}$$

The oddness/evenness conditions for  $G_-(y, x)$ ,  $G_+(y, x)$ , and  $G_+(-y, x)$  have the same form, varying in the  $y$ -term only. E. g. for  $G_-(y, x)$  it reads as

$$G_-\left(u, \frac{\pi}{2} + v\right) + G_-\left(u, \frac{\pi}{2} - v\right) \stackrel{\forall x, y}{=} 0 = 2 \sum (a_k \cos ky - b_k \sin ky) \sin kx \cos \frac{k\pi}{2}$$

Thus every coupling function only consisting of odd harmonics ensures all the solutions to be 1-periodic like in the case  $f(\psi) = \sin \psi$ .

$$f(\psi) = a_1 \sin \psi + b_1 \cos \psi + a_3 \sin 3\psi + b_3 \cos 3\psi + a_5 \sin 5\psi + b_5 \cos 5\psi + \dots$$

In the figure 2.18 the influence of adding the next odd harmonics to the coupling function on the phase space diagram is shown.

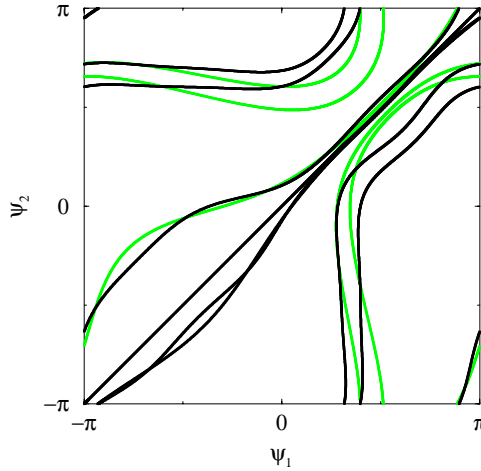


Figure 2.18: Numerical solutions of the equations (2.14) for different initial conditions and  $f(\psi) = 0.8 \sin \psi + 0.2 \sin 3\psi$  in  $\psi_1$ - $\psi_2$  diagrams, in grey the solutions for the same initial conditions and  $f(\psi) = \sin \psi$  are plotted,  $N = 3$ ,  $\varepsilon = 0.29$ .

If an even harmonics is present in the coupling function then the symmetry discussed above is broken. For the Poincaré map  $g(y)$  in the figure 2.19 this means the existence of two fixed points  $y = g(y)$ , one being stable and the other unstable. All the trajectories converge to a limit circle.

(ii) Larger chains:

Restricting ourselves to odd coupling functions  $f(\psi) = -f(-\psi)$  we see that the  $\mathcal{Q}$ -symmetry requires that  $f(\psi) = f(\pi - \psi)$ . The question whether there also exist non-odd functions delivering the symmetry  $\mathcal{Q}$  in the system (2.3) for an arbitrary lattice size could not be answered.

The odd coupling functions invariant under  $\mathcal{Q}$ -involution (2.18) are represented by a sine Fourier series with odd harmonics only. Such functions yield reversible dynamics; one exam-

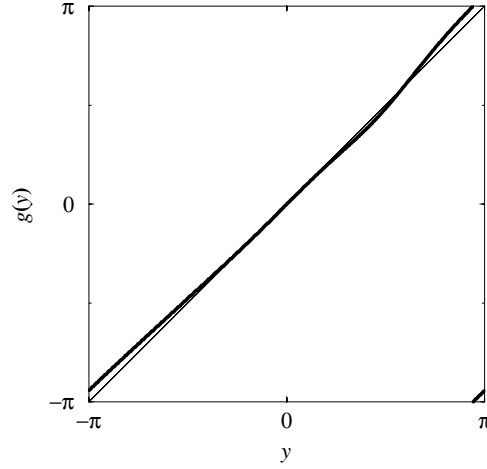


Figure 2.19: The Poincaré section map,  $\Delta = \begin{pmatrix} 1 \\ 1 \end{pmatrix}$  at  $\varepsilon = 0.29 < \varepsilon_c$ ,  $f(\psi) = 0.8 \sin \psi + 0.2 \sin 2\psi$ .

ple is presented in the figure 2.20a. If even harmonics in the Fourier series are present, the dynamics is dissipative as can be seen in the figure 2.20b.

### 2.4.3 On $P$ -symmetric solutions and their destruction

The reversibility of the systems is ensured by the product of the symmetries  $\mathbf{P}$  and  $\mathbf{Q}$ . The symmetry  $\mathbf{Q}$  ensures the reversibility and the symmetry  $\mathbf{P}$  ensures that the set of invariant points  $Fix\mathbf{R}$  of their product has a dimension which is high enough ( $[n/2]$ ). Then one can expect non-wandering typical trajectories in an ergodic set, that cross  $Fix\mathbf{R}$  and herewith establish quasi-Hamiltonian features on average over this ergodic set.

Besides such quasi-Hamiltonian ergodic sets there can exist other types of ergodic sets in the vicinity of  $Fix\mathbf{R}$  like quasiperiodic windows or ergodic sets of smaller dimensions. Here we want to illustrate this with discussing specific  $\mathbf{P}$ -symmetric solutions for small lattices.

The perturbation symmetry  $\mathbf{P}: \psi_k \mapsto \psi_{n-k}$  in the case of the coupling function  $f(\psi) = \sin \psi$  has the diagonal subspace  $\psi_k = \psi_{n-k}$  as an invariant set. For each of such pairs in the equation (2.6) we introduce new variables  $\xi_{\parallel k} = \xi_k = (\psi_k + \psi_{n-k})/2$ ,  $\xi_{\perp k} = \xi_{n-k} = (\psi_k - \psi_{n-k})/2$ . If the number of oscillators  $N$  is even ( $n$  is odd) then additionally is set  $\xi_{N/2} = \psi_{N/2}$ . The  $\mathbf{P}$ -invariant subspace is defined by  $\xi_{\perp k} = 0$ ,  $\forall k$ .

(i) Four oscillators:

Now we make this substitution in the chain of four oscillators with all  $\Delta_k = 1$  and  $f(\psi) = \sin \psi$ , i. e. in the case of the equation (2.19). Letting  $\xi_{\parallel} = \xi_1 = (\psi_1 + \psi_3)/2$ ,  $\xi_2 = \psi_2$ ,  $\xi_{\perp} = \xi_3 = (\psi_1 - \psi_3)/2$  one obtains from the equations (2.19)

$$\begin{cases} \dot{\xi}_1 = 1 + \varepsilon \sin \xi_2 - 2\varepsilon \sin \xi_1 \cos \xi_3 \\ \dot{\xi}_2 = 1 - 2\varepsilon \sin \xi_2 + 2\varepsilon \sin \xi_1 \cos \xi_3 \\ \dot{\xi}_3 = -2\varepsilon \sin \xi_3 \cos \xi_1 \end{cases} \quad (2.26)$$

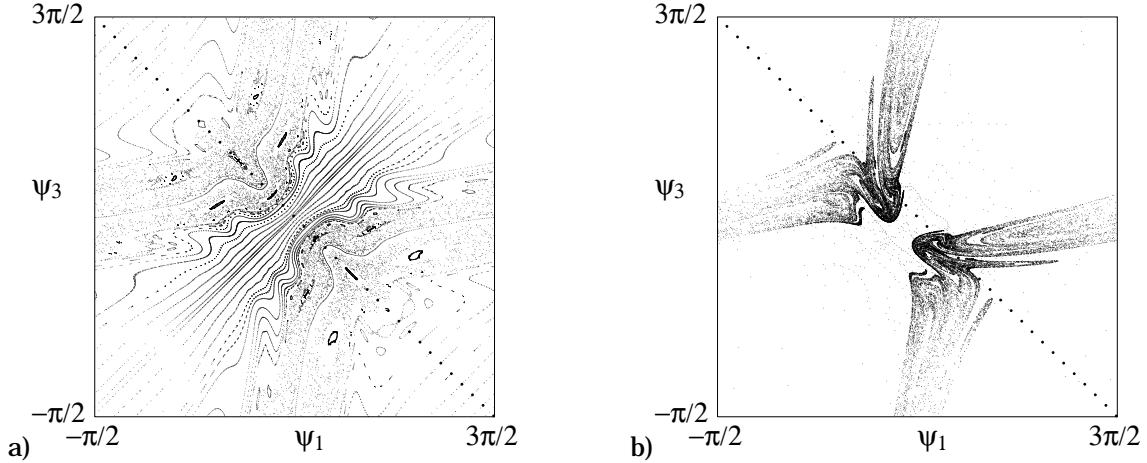


Figure 2.20: (a) The dynamics of system (2.3) with  $N = 4$ ,  $\Delta_k = 1$ ,  $\varepsilon = 0.35$  and  $f(\psi) = \sin \psi + 0.2 \sin 3\psi$  is reversible. (b) The same system as (a), but with a non-symmetric coupling function  $f(\psi) = \sin \psi + 0.2 \sin 2\psi$  and  $\varepsilon = 0.4$  has a strange attractor.

The linearized equation for the perturbations  $\delta$  of the  $\mathbf{P}$ -symmetric solution  $\xi_{\perp} = \xi_3 = 0$  reads

$$\begin{cases} \dot{\delta}_1 = \varepsilon \cos \xi_2 \delta_2 - 2\varepsilon \cos \xi_1 \delta_1 \\ \dot{\delta}_2 = -2\varepsilon \cos \xi_2 \delta_2 + 2\varepsilon \cos \xi_1 \delta_1 \\ \dot{\delta}_3 = -2\varepsilon \cos \xi_1 \delta_3 \end{cases} \quad (2.27)$$

The transversal Lyapunov exponent is then straightforward  $\lambda_{\perp} = \lambda_3 = -2\varepsilon \langle \cos \xi_1 \rangle$ . For  $\xi_{1,2}$  (which is equal to  $\psi_{1,2}$ ) holds

$$\begin{cases} \dot{\xi}_1 = 1 - 2\varepsilon \sin \xi_1 + \varepsilon \sin \xi_2 \\ \dot{\xi}_2 = 1 + 2\varepsilon \sin \xi_1 - 2\varepsilon \sin \xi_2 \end{cases} \quad (2.28)$$

This equation has the same form as the equation (2.4), with  $\Delta = \begin{pmatrix} 1 \\ 1 \end{pmatrix}$ ,  $A = \begin{pmatrix} -2 & 1 \\ 2 & -2 \end{pmatrix}$ ,  $F_k(\Psi) = \sin \psi_k$ , but it does not possess the reversibility symmetry.

As seen in the section 2.4.1, this equation corresponds in terms of the Poincaré map  $g(y)$  (with  $x = (\xi_1 + \xi_2)/2$ ,  $y = (\xi_1 - \xi_2)/2$ ) mapping one Poincaré section (which is defined here by  $x = 0$ )  $\begin{pmatrix} 0 \\ y \end{pmatrix}$  to the next one  $\begin{pmatrix} 2\pi \\ g(y) \end{pmatrix}$  to an invertible circle map, and one should expect Arnold tongues in  $\varepsilon$  where stable periodic solutions exist. One Lyapunov exponent, let it be  $\lambda_2$ , is always zero for non-constant solutions because the system is autonomous.  $\lambda_1$  shall be zero outside the Arnold tongues and negative within them. Through building the trace and averaging over time for the linearized version of (2.28) one obtains

$$\lambda_1 = \lambda_1 + \lambda_2 = -2\varepsilon(\langle \cos \xi_1 \rangle + \langle \cos \xi_2 \rangle) = -2\varepsilon \langle \cos \xi_2 \rangle + \lambda_{\perp}$$

In the figure 2.21 calculated Lyapunov exponents and their sum is shown. Beyond the Arnold tongues the dynamics in the  $\mathbf{P}$ -invariant plane is foliated by tori so that  $\lambda_1 = 0$ , among them there is one torus crossing the set  $\text{Fix}\mathbf{R}$  which ensures reversibility for all tori,  $\sum \lambda_k = 0$ .

## 2.4. DESTRUCTION OF REVERSIBILITY

Therefore all Lyapunov exponents are zero, the invariant plane  $\xi_{\perp} = 0$  is neutrally stable. Around the symmetric quasiperiodic solution  $\psi_1 = \psi_3$  other quasiperiodic solutions exist. Together they build a window of quasiperiodicity with  $\lambda_{\perp} = 0$  for initial conditions close to this plane.

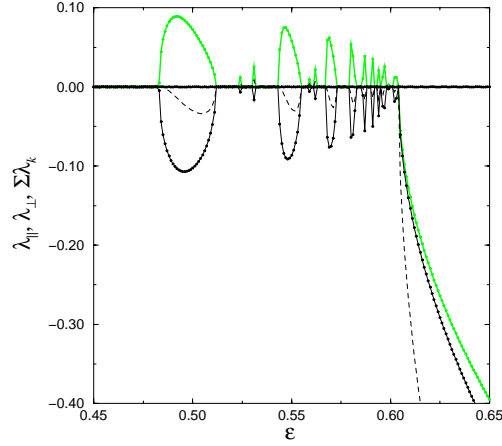


Figure 2.21: Numerical planar (black) and transversal (grey) Lyapunov exponents for the symmetric solution  $\psi_1 = \psi_3$  and their sum (dashed line).

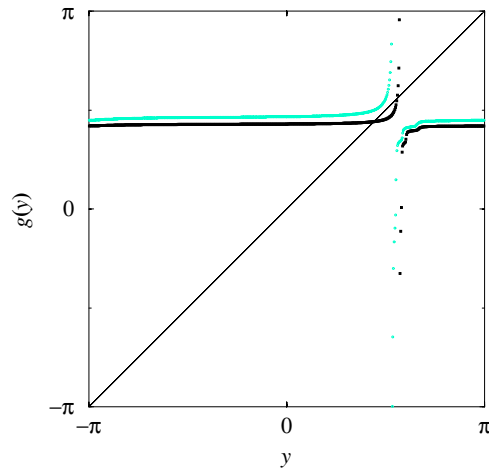


Figure 2.22: Tangent bifurcation of  $g(y)$ , in grey  $g(y)$  at  $\varepsilon = 0.6$ , in black  $g(y)$  at  $\varepsilon = 0.61$  above the bifurcation threshold.

Inside an Arnold tongue all trajectories on the  $\mathbf{P}$ -invariant plane converge to a periodic orbit. While stable in the invariant plane, this orbit is transversally unstable and represents a typical unstable saddle-type periodic orbit within chaos. In this case there cannot be any quasiperiodic windows around the  $\mathbf{P}$ -invariant plane, the sea of chaos involves this plane.

## CHAPTER 2. SYNCHRONIZATION VS. REVERSIBILITY

The sum of Lyapunov exponents is negative for such a plane-stable periodic orbit, the latter being then dissipative. However, there still exists the  $\mathbf{R}$ -symmetric trajectory with an inverted Lyapunov spectrum and diverging phase volume along it.

At the value of  $\varepsilon = \varepsilon_1 \approx 0.604$ , where first cluster arises, the map  $g(x)$  undergoes a tangent bifurcation, which is shown in the figure 2.22. There arises a  $\mathbf{Q}$ -symmetric pair of fixed points, one of them being both planarly and transversally stable and the other both planarly and transversally unstable. All the solutions converge then to the  $\mathbf{P}$ -symmetric plane. This ensures  $\psi_1(t) \rightarrow \psi_3(t)$  and means decreasing in the dimensionality of the motion from the three-dimensional to two-dimensional torus where no chaos can be present. All the  $\mathbf{P}$ -symmetric solutions converge to the periodic one corresponding to the fixed point of the map  $g(y)$ . Moreover, this periodic trajectory is oscillatory in  $\psi_1$ . This explains the arising of clusters, since for an oscillatory process the time average of its derivative is zero. The dimensionality is again reduced by one.

When clusters are present the system also demonstrates an exact intercluster synchronization, i. e.  $\psi_1(t) = \psi_3(t)$  after transients. In terms of the  $\mathbf{P}$ -symmetry it can be said that one subsystem  $\{\psi_k, k \leq [n/2]\}$  is exactly synchronized with the  $\mathbf{P}$ -symmetric subsystem  $\{\psi_{n-k}, k \leq [n/2]\}$ .

(ii) Five oscillators:

The situation with five oscillators ( $n = 4$ ) is interesting because the invariant set of the symmetry transform is still a plane which allows relative simple considerations. We proceed analogously to the case of four oscillators. With  $\xi_1 = (\psi_1 + \psi_4)/2$ ,  $\xi_2 = (\psi_2 + \psi_3)/2$ ,  $\xi_3 = (\psi_2 - \psi_3)/2$ ,  $\xi_4 = (\psi_1 - \psi_4)/2$  one can write for the  $\mathbf{P}$ -symmetric solutions ( $\psi_1 = \psi_4$ ,  $\psi_2 = \psi_3$ ):

$$\begin{aligned} \dot{\xi}_{\parallel} = \begin{pmatrix} \dot{\xi}_1 \\ \dot{\xi}_2 \end{pmatrix} &= \begin{pmatrix} 1 \\ 1 \end{pmatrix} + \varepsilon \begin{pmatrix} -2 & 1 \\ 1 & -1 \end{pmatrix} F(\xi) \\ \dot{\xi}_{\perp} = \begin{pmatrix} \dot{\xi}_3 \\ \dot{\xi}_4 \end{pmatrix} &= 0 \end{aligned}$$

Written in linearized form for perturbation, this gives

$$\begin{cases} \dot{\delta}_1 = -2\varepsilon\delta_1 \cos \xi_1 + \varepsilon\delta_2 \cos \xi_2 \\ \dot{\delta}_2 = \varepsilon\delta_1 \cos \xi_1 - \varepsilon\delta_2 \cos \xi_2 \\ \dot{\delta}_3 = \varepsilon\delta_3 \cos \xi_2 - 2\varepsilon\delta_4 \cos \xi_1 \\ \dot{\delta}_4 = -3\varepsilon\delta_3 \cos \xi_2 + \varepsilon\delta_4 \cos \xi_1 \end{cases}$$

Assuming one zero Lyapunov exponent  $\lambda_2 = 0$  one obtains

$$\begin{aligned} \lambda_1 + \lambda_2 &= -2\varepsilon \langle \cos \xi_1 \rangle - \varepsilon \langle \cos \xi_2 \rangle \\ \lambda_3 + \lambda_4 &= \varepsilon \langle \cos \xi_1 \rangle + \varepsilon \langle \cos \xi_2 \rangle \end{aligned}$$

Again, quasiperiodic solutions in the invariant plane  $\xi_3 = \xi_4 = 0$  are expected with  $\lambda_1 = 0$ , and there should be Arnold tongues with  $\lambda_1 < 0$  and a tangent bifurcation delivering the map  $g(y)$  a stable fixed point which corresponds to the synchronization to the first cluster. Calculated Lyapunov exponents in the plane are shown in black in the figure 2.23 together with the transversal Lyapunov exponents in grey. The dashed line represents the sum of all four exponents.

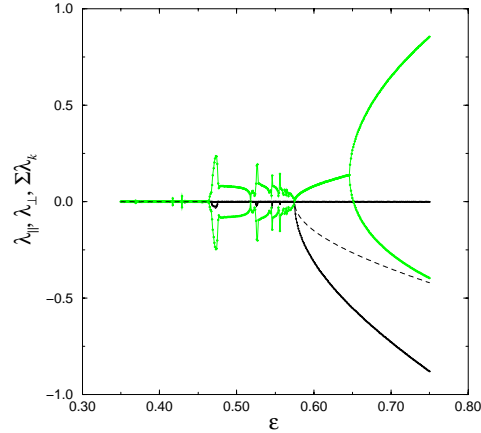


Figure 2.23: Five oscillators. Planar (black) and transversal (grey) Lyapunov exponents and their sum (dashed line) for the dynamics in the  $\mathbf{P}$ -invariant plane.

There are regions in  $\varepsilon$  where all exponents are zero. This means the possibility of existence of a window of quasiperiodicity around the invariant plane. Also there are intervals where every still quasiperiodic solution in the invariant plane is transversally a saddle-type trajectory with transversal Lyapunov exponents coming in the pair  $\pm\lambda$ . Like in the case of four oscillators this destroys the quasiperiodic window around the invariant plane which is then contained in the sea of chaos. Also here Arnold tongues with periodic saddle-type dissipative orbits in the plane are present.

At the value of  $\varepsilon_1 \approx 0.575$  corresponding the tangent bifurcation  $\Omega_1$  ( $\Omega_4$ ) first coincides with  $\Omega_2$  ( $\Omega_3$ ). But after  $\varepsilon_1$  up to the  $\tilde{\varepsilon}_1 \approx 0.732$  no clusters are observed, the system shows chaotic dynamics as seen from the figures 2.1 and 2.3.

Unlike the case of four oscillators the synchronization between the subsystems after appearance of the first cluster is not exact but exactly counterphase one. In the figure 2.24  $\Omega_1 = \Omega_4 = 0$  because  $\psi_1(t)$  and  $\psi_4(t)$  oscillate. But they do not only oscillate, they oscillate in an exact counterphase.

## 2.5 Summary

The extremely simple system of coupled phase oscillators demonstrates extremely rich dynamics. This can be already seen from the figures 2.1 and 2.3. Many regimes in large lattices are chaotic, so the clustering should be described as a transition inside chaos. In this work we focused on a particular peculiarity of the dynamics for very small couplings and demonstrated, that this dynamics is reversible.

This property is responsible for a rather unusual for dissipative systems quasi-Hamiltonian dynamics. Although the reversibility holds for any coupling, only when the clusters are absent the reversible trajectories appear to be dense in the ergodic sets; at large coupling they

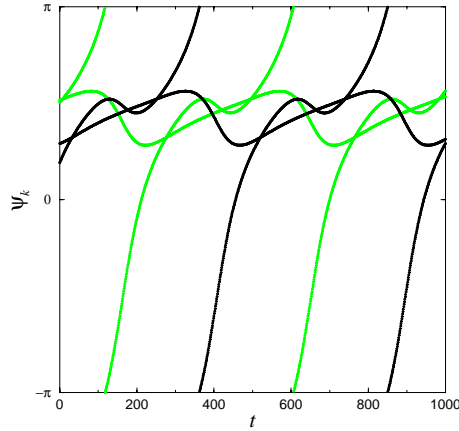


Figure 2.24: Time evolution of the system (2.6) in the two-clusters regime, five oscillators,  $\varepsilon = 0.8$ ,  $\psi_1$  and  $\psi_2$  in black are in counterphase to  $\psi_3$  and  $\psi_4$  in grey.

connect a repeller and an attractor, so that the observed dynamics on the attractor is dissipative.

In investigating the simplest non-trivial case of 4 coupled phase oscillators we have found a non-trivial transition from the quasi-Hamiltonian to dissipative dynamics. It can be characterized as a symmetry-breaking “chaos-chaos” transition, at which the mean contraction rate smoothly deviates from zero.

In discussing reversibility we have argued that the symmetry of the involution that gives rise to reversibility should be large enough. This requires not only the symmetry of the coupling function, but the symmetry of the natural frequencies as well. If the dimension of the invariant set of the involution is low, no reversible dynamics is observed. It would be interesting to apply these ideas to the systems of Josephson junctions, where the non-linear functions are known to have a high symmetry [104, 108].



## Chapter 3

# Transition to coherence in globally coupled maps

In this chapter we describe the transition to coherence in populations of dynamical systems coupled "every-to-every" via mean field. In the disordered state the mean field is constant up to statistical fluctuations, in the coherent state a non-trivial mean field arises. We show that this transition can be described in the framework of linear response theory as autogeneration in an amplifier circuit with feedback.

### 3.1 Introduction

The concept of the global coupling is the counterpart to the nearest-neighbor coupling representing short-range interactions. Speaking about globally coupled systems, one assumes that long-range interactions are present, they can be described as a type of interactions "every-to-every", or as the situation where an equal force is acting on every system in an ensemble, which is formed in its turn by individual dynamics of the systems in this ensemble. This force is often called mean field in resemblance with the notation of the mean field first introduced by Van der Waals [89], often it is not an approximation but arises naturally due to the nature of the problem. Prominent examples of globally coupled systems are arrays of Josephson junctions [39], multimode lasers [109], certain chemical reactions [54], interacting biological clocks [112], and models of neural activity [99].

In the context of coupled lattices [45, 47] a rich variety of dynamical phenomena was found, that seem to be typical for all globally coupled systems. With growing coupling a transition hierarchy from a completely disordered state to a completely ordered state is expected in globally coupled systems. At relatively large couplings that still are not large enough to ensure complete synchronization the effect of cluster formation has been found and extensively discussed [45, 113, 10, 80]. At very small coupling the effect of hidden coherence was found [46, 73, 74]. In this phenomenon the fluctuations of the mean field does not vanish in the thermodynamic limit. The mean field distribution seems to obey the central limit theorem, but not the law of large numbers.

In the language of non-linear Frobenius-Perron equation this means that the measure does not converge to a time-invariant limit in spite of the fact that the dynamical rules are autonomous. The mean field reveals a non-trivial asymptotic dynamics.

### 3.1.1 Formulation of the problem

We start with investigation of the transition to coherence in populations of globally coupled discrete time systems. Our basic model is an ensemble of  $N$  globally coupled chaotic maps

$$\begin{aligned} x_k(t+1) &= h(x_k(t), \varepsilon a(t)) \\ a(t) &= \frac{1}{N} \sum_{k=1}^N q(x_k(t)) \end{aligned} \quad (3.1)$$

Here  $\varepsilon$  is the coupling constant. Note that the coupling performs via the mean field  $a$  which is the average of some observable  $q(x)$ . We write the coupling in a general form, using arbitrary functions  $h(x, \varepsilon a)$  and  $q(x)$ . The only natural condition is that in the thermodynamic limit the mean field vanishes for  $\varepsilon = 0$ , i. e.  $\langle q(x) \rangle_0 = 0$ , where  $\langle \rangle_0$  denotes average over the stationary distribution of the map  $x \mapsto h(x, 0)$ .

This condition means that if  $\varepsilon = 0$  then individual systems in (3.1) are independent of each other, the mean field is constant in time up to statistical fluctuations due to the limited size of the ensemble. This constant mean field is assumed to be zero, i. e. it is assumed to be contained in the function  $h(x, \varepsilon a)^*$ .

With increasing  $\varepsilon$  the effect of the mean field  $a$  on individual systems becomes stronger and at some critical value  $\varepsilon_c$  the dynamics of individual systems reveal a certain coherence with each other so that arising of a non-trivial, i. e. time-dependent mean field is expected. Further in this section a theory of this transition [102] will be presented. This theory is based on general linear response theory (cf. [69]), similar ideas were developed for ensembles of noise-driven systems [101].

### 3.1.2 Finite-size effects

Assume that an ensemble with independently chosen initial conditions is prepared. The initial value of the mean field is proportional to  $\frac{1}{\sqrt{N}}$  with  $N$  being the number of systems in the ensemble. This small mean field can grow or decay with time, while one expects that for completely incoherent systems this value will remain small.

In the thermodynamic limit  $N \rightarrow \infty$  the effect of fluctuations due to the limited ensemble size should vanish. With this assumption the value of the mean field can be calculated by

---

\*Of course, a general ensemble of the form (3.1) does not have to produce a zero mean field if the systems are uncoupled,  $\varepsilon = 0$ , this trivial mean field can be any finite constant  $\bar{a}$ . With a formal continuation for  $\varepsilon \neq 0$  one can write with this trivial solution  $x_k(t+1) = h(x_k(t), \varepsilon \bar{a}(\varepsilon))$  to obtain a self-consistent trivial mean field  $\bar{a}(\varepsilon) = \frac{1}{N} \sum_{k=1}^N q(x_k(t))$ . With the substitution  $a(t) = \bar{a}(\varepsilon) + b(t)$  the equations (3.1) produce a zero mean field solution  $b = 0$  at  $\varepsilon = 0$  as well as for small  $\varepsilon \neq 0$ .

Unfortunately, in general the function  $\bar{a}(\varepsilon)$  does not have to be smooth (e. g. in structurally unstable systems). Nor it has to be unique (if multiple invariant states exist for  $\varepsilon > 0$ ).

averaging over phase space of an individual map.

$$a(t) = \langle q(x) \rangle = \int \rho_t(x) q(x) dx = \lim_{N \rightarrow \infty} \frac{1}{N} \sum_{k=1}^N q(x_k(t))$$

The evolution of the probability density is governed by the non-linear Frobenius-Perron equation (1.3). The effects of the limited ensemble size can be understood as small perturbations (of order  $\frac{1}{\sqrt{N}}$ ) of the thermodynamic limit state of the system. The question of arising of coherence in an ensemble of systems coupled through a mean field can therefore be answered in the limit of a very large ensemble size by studying the stability of the state  $a = 0$  in the framework of linear theory.

## 3.2 Linear stability analysis

In the thermodynamic limit  $N \rightarrow \infty$  the trivial mean field  $a = 0$  is a solution. In general one cannot guarantee that a solution at finite  $N$  exists that is close to this trivial solution so that finite-size effects only mean existence of fluctuations around  $a = 0$ . The question whether a linear response theory is possible at all for general chaotic systems has been intensively discussed in the last two decades [37, 84]. While such a theory should work for "good" chaotic systems, it is to be applied with care. Now we will introduce this linear stability theory for the state  $a = 0$ .

### 3.2.1 Breaking self-consistency condition

Let us take a closer look at the structure of the equations (3.1). They contain the mean field  $a(t)$  twice, the field acting on an individual system is defined in its turn by the state of all these systems. Another observation is that an individual system in the ensemble (3.1) experiences only the effect of the mean field, it has no other information about the dynamics of the other systems in the ensemble nor it knows their number.

Therefore the dynamics of this individual system remains unchanged if instead of the coupling through the mean field  $a = \frac{1}{N} \sum_{i=1}^N q(x_i(t))$  the system would be driven by an appropriate external force  $a_{in}$ . In particular, in the ensemble (3.1) the same mean field  $a_{out} = a_{in}$  would be generated. In other words, a proper input  $a_{in}$  ensures a proper output  $a_{out}$ .

Thus, the ensemble (3.1) can equally be written with using the self-consistency condition for the mean field as:

$$\begin{aligned} x_k(t+1) &= h(x_k(t), \epsilon a_{in}(t)) \\ a_{out}(t) &= \langle q(x(t)) \rangle \end{aligned} \tag{3.2}$$

$$a_{out}(t) = a_{in}(t) \tag{3.3}$$

Now we put aside the requirement of the self-consistency  $a_{out} = a_{in}$  to return to it later on. Instead of requiring (3.3) we will consider  $a_{in}(t)$  as a given (while unknown) function of time.

### 3.2.2 Linearization

After having broken the self-consistency the question of stability if the state  $a = 0$  is reduced to the question how the system (3.2) transforms an input signal  $a_{in}$ . In the disordered state this  $a_{in}$  is small. That is why one generally expects that the average response  $a_{out}$  of the ensemble (3.2) is also small and the linear stability theory can be applied. Then we can expand (3.1) around the trivial solution  $a = 0$ . Denoting  $h(x, 0) = f(x)$  and  $h'_{\epsilon a}(x, 0) = g(x)$  we obtain

$$\begin{aligned} x_k(t+1) &= f(x_k(t)) + \epsilon g(x_k(t))a(t) \\ a(t) &= \langle q(x(t)) \rangle \end{aligned} \quad (3.4)$$

Of course, the system (3.4) also has the trivial solution  $a = 0$ . As a linear response  $a_{out}$  of the system (3.1) to small perturbations  $a_{in}$  is expected one can equivalently analyze stability of the state  $a = 0$  in the systems (3.1) or (3.4).

Within the linear theory we will not be able to find the distant solutions of the system (3.1), i. e. the solutions that are far from  $a = 0$ , we will only find the critical value of the coupling at which the transition to coherence takes place.

### 3.2.3 On "good" and "bad" maps

It is known that the response to small perturbations can be singular as discussed above (e. g. [30, 37]). For instance, this happens in structurally unstable chaotic systems. In such systems, small changes of a parameter lead to a topologically nonequivalent dynamics, what can, e.g., been seen in the symbolic description or in the representation via unstable periodic orbits. Note, that to this class belong even many systems where chaos persists in the whole parameter range (e.g., the Lorenz attractor and the tent map), let alone such nonhyperbolic examples where small perturbation can lead to a periodic window (like in the logistic map). Response of the structurally unstable system is expected to be singular [30], what, in particular, can be seen from the fractal dependence of some statistical characteristics on a parameter [50].

We have argued that in order to ensure that the linear theory is valid the map (3.18) has to be "good" enough. Essentially, it should be structurally stable, i. e. adding a small perturbation should not change the topology of the attractor. The corresponding requirement has been formulated in [37]: the perturbation  $\mu g(x)a(t)$  should be such that it does not change the number of preimages of the map  $f(x)$ .

Note that it is not required here that the invariant measure of the perturbed map is close to the unperturbed one, we only need a smooth response of mean field that is an average over this measure. Under which condition a phase space average respond smoothly to a small perturbation of the underlying map deserves an independent research.

We proceed with the assumption that the map  $h(x, \epsilon a_{in})$  is structurally stable with respect to small perturbations  $a_{in}$ .

### 3.2.4 Ensemble as a linear filter

Equations (3.4) can be understood as input-output relations with the consistency condition (3.3)

$$\begin{aligned} x_k(t+1) &= f(x_k(t)) + \varepsilon g(x_k(t))a_{in}(t) \\ a_{out}(t) &= \langle q(x(t)) \rangle \end{aligned} \quad (3.5)$$

The system (3.5) transforms one function of time  $a_{in}(t)$  to another function of time  $a_{out}(t)$ . As a linear response is assumed the effect of transformation of every Fourier mode of  $a_{in}(t)$  can be analyzed separately. That is why we use now as test perturbations small periodic perturbations of the trivial state  $\varepsilon a = 0$ ,  $a_{in}(t) = \text{Re}\mu e^{i\omega t}$ ,  $\mu \ll 1$ . As the equations (3.5) are linear in  $a_{in}(t)$  the response is expected (under the same assumptions on the system to be structurally stable) to get asymptotically established at the same frequency proportionally to  $\mu$ :

$$a_{out}(t) = \mu \text{Re}K(\omega)e^{i\omega t} + o(\mu^2) \quad (3.6)$$

The complex constant  $K(\omega)$  corresponds to the well-known transfer function of a linear filter in the theory of analog processing (e.g. [69]). The ensemble after breaking the consistency can thus be understood as an amplifying device with the complex amplification coefficient  $K(\omega)$  at the frequency  $\omega$ .

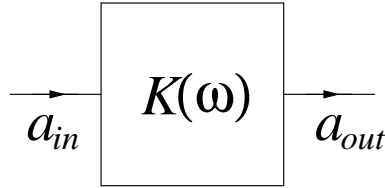


Figure 3.1: Linear amplifier analogy: a linear amplifying device is characterized by its complex transfer function  $K(\omega)$ .

### 3.2.5 Stability of a linear filter

Here the theory of linear circuits (e.g. [69]) needed in order to obtain the stability condition in the closed feedback loop is reminded. Given a general linear device with one input signal  $a_{in}(t)$  and one output signal  $a_{out}(t)$ , one can describe it through the linear ordinary differential equation

$$\sum_{k=0}^n \alpha_k \frac{d^k a_{out}}{dt^k} = \sum_{k=0}^m \beta_k \frac{d^k a_{in}}{dt^k} \quad (3.7)$$

With denoting the differentiation operator with  $\mathbf{D} = \frac{d}{dt}$  this equation takes the form

$$\alpha(\mathbf{D})a_{out} = \beta(\mathbf{D})a_{in} \quad (3.8)$$

$\alpha(\mathbf{D})$  and  $\beta(\mathbf{D})$  are polynomials in  $\mathbf{D}$  of the order  $n$  and  $m$  respectively. To solve this equation one uses the complex Laplace transform  $L$  which is defined by

CHAPTER 3. TRANSITION TO COHERENCE IN GLOBALLY COUPLED MAPS

$$\tilde{f}(p) = L\{f(t)\} = \int_0^{\infty} f(t)e^{-pt} dt \quad (3.9)$$

From a given Laplace transform  $\tilde{f}(p)$  its original can be restored with the inverse Laplace transform

$$f(t) = L^{-1}\{\tilde{f}(p)\} = \frac{1}{2\pi i} \int_{c-i\infty}^{c+i\infty} \tilde{f}(p)e^{pt} dp \quad (3.10)$$

The constant  $c$  is to be chosed in such a way that the integration contour lies to the right of all poles of  $\tilde{f}(p)$  in the complex plane. The Laplace transform is linear and its important property is that

$$L\{\mathbf{D}f(t)\} = pL\{f(t)\} - f(0) \quad (3.11)$$

Assuming zero initial conditions the equation (3.8) is read now

$$\alpha(p)\tilde{a}_{out}(p) = \beta(p)\tilde{a}_{in}(p) \quad (3.12)$$

From the convolution property of the Laplace transform, i. e.

$$L\left\{\int_0^t x(\tau)y(t-\tau)d\tau\right\} = \tilde{x}(p)\tilde{y}(p)$$

follows

$$\begin{aligned} a_{out}(t) &= \int_0^t h(\tau)a_{in}(t-\tau)d\tau \\ h(t) &= L^{-1}\{H(p)\} \\ H(p) &= \frac{\beta(p)}{\alpha(p)} \end{aligned} \quad (3.13)$$

The function of the complex variable  $H(p) = \beta(p)/\alpha(p)$  is called transfer function of the device described with the equation (3.7).

The device is stable by input if and only if

$$\int_0^{\infty} |h(t)| dt < \infty$$

In the language of the transfer function  $H(p)$  this implies two conditions:

- $n \geq m$ , i. e. the order or the polinomial  $\alpha(p)$  is not less than the order of  $\beta(p)$ .
- No poles of  $H(p)$  have positive real part.

Now we have to account for initial conditions which are generally non-zero. As the equation (3.8) is linear its solutions can be written as a superposition of the homogenous and the particular solutions:

## 3.2. LINEAR STABILITY ANALYSIS

$$\begin{aligned} a_{out}(t) &= A_{out}(t) + \int_0^t h(\tau) a_{in}(t-\tau) d\tau \\ \alpha(\mathbf{D})A_{out}(t) &= 0 \end{aligned} \quad (3.14)$$

The device is stable by initial conditions if and only if the effect of initial conditions asymptotically decays in time, i. e. if  $\lim_{t \rightarrow \infty} A_{out}(t) = 0$ .

After applying the Laplace transform to the homogenous equation  $\alpha(\mathbf{D})A_{out} = 0$  one obtains  $\alpha(p)\tilde{A}_{out}(p) + \gamma(p) = 0$ , where the polynomial  $\gamma(p)$  of order equal or less than that of  $\alpha(p)$  contains contributions of initial conditions on  $A_{out}$  and its derivatives due to the relation (3.11).

The asymptotic behavior of the homogenous solution  $A_{out}(t)$  is then obtained through the inverse Laplace transform

$$A_{out}(t) = \frac{1}{2\pi i} \oint \frac{\gamma(p)}{\alpha(p)} e^{pt} dp = \sum_k e^{p_k^* t} \text{Res} \frac{\gamma(p_k^*)}{\alpha(p_k^*)} \quad (3.15)$$

Here the sum goes over all complex roots  $p_k^*$  of  $\alpha(p)$  which are assumed to be simple. One sees that the device is stable by initial conditions if and only if all  $\text{Re} p_k^* < 0$ . If these conditions do not hold then the system responds singularly. Note that we cannot generally guarantee that the system (3.5) with broken feedback is stable by input and/or by initial conditions so that the whole linear theory will only work if it is the case (one can expect this for structurally stable maps as discussed above). If the system (3.5) does not respond singularly then asymptotically it responds to a small harmonic input  $a_{in}(t) = \mu e^{i\omega t}$  at the same frequency, which directly follows from (3.13):

$$a_{out}(t) = \int_0^t h(\tau) \mu e^{i\omega(t-\tau)} d\tau = \mu e^{i\omega t} \int_0^t h(\tau) e^{-i\omega\tau} d\tau$$

As  $\lim_{t \rightarrow \infty} \int_0^t h(\tau) e^{-i\omega\tau} d\tau = H(i\omega)$  it is valid asymptotically that

$$a_{out}(t) = \mu H(i\omega) e^{i\omega t}$$

That means that when calculating the linear response to a harmonic test input at a given frequency we are actually calculating

$$\varepsilon K(\omega) = H(i\omega) = \frac{\beta(i\omega)}{\alpha(i\omega)} \quad (3.16)$$

The fact that a system responds linearly to a harmonic input implies that the complex function  $K(\omega)$  does not have a pole (or, more exactly,  $\alpha(i\omega)$  does not have a root) for real  $\omega$ .

### 3.2.6 Stability of a feedback loop

From all what is said above it is now trivial to obtain the stability condition for the incoherent state  $a = 0$  in the ensemble (3.1). With the known transfer function  $H(p) = \frac{\beta(p)}{\alpha(p)} = H(-i\omega) = \varepsilon K(\omega)$  ( $p$  is purely imaginary because the input signal is harmonic) it is easy to

## CHAPTER 3. TRANSITION TO COHERENCE IN GLOBALLY COUPLED MAPS

write down the analog of the equation (3.8) by invoking the self-consistency of the mean field,  $a_{in} = a_{out} = a$ :

$$(\alpha(p) - \beta(p))\tilde{a}(p) = \alpha(p)(1 - \varepsilon K(\omega))\tilde{a}(p) = 0$$

Here there is no input in the system any more so that only instability by initial conditions is possible in the feedback loop. The onset of instability and, thus, of coherence in the ensemble of chaotic elements coupled through the mean field is given by the complex condition

$$\varepsilon K(\omega) = 1 \quad (3.17)$$

Note that there are actually two conditions, the condition on the imaginary part of the transfer function  $\text{Im}K(\omega) = 0$  gives the frequencies of autogeneration with which the critical coupling strength can be defined from the condition on the real part  $\varepsilon_c = \frac{1}{\text{Re}K(\omega)}$ .

### 3.3 Linear response of chaotic maps

So far the analysis was presented as if it were easy to calculate the average response of a chaotic system to a periodic external force which is, in fact, the most difficult part of the whole. Now we want to calculate this linear response of the ensemble of non-interacting maps defined on the unit circle to a small periodic driving  $\mu e^{i\omega t}$ .

We proceed assuming maps  $f_k(\cdot)$  from the ensemble (3.5) to be identical, structurally stable and chaotic. Then in the thermodynamic limit of a very large ensemble size  $N \rightarrow \infty$  averaging over ensemble can be replaced by averaging over the invariant measure of the individual map, which has the form

$$x(t+1) = \hat{f}(x(t)) = f(x(t)) + \mu g(x(t))a(t), \quad \text{with} \quad a(t) = e^{i\omega(t+\tau)} \quad (3.18)$$

The number  $\tau$  is an arbitrary phase constant. With this premise it is legitimate now to speak about response of an individual map to a harmonic perturbation.

The phase space averaged value of the contribution to the mean field from an individual map will oscillate at the frequency of the driving  $\langle q \rangle = \int \rho_t(x) q(x) dx = \mu \text{Re} K(\omega) e^{i\omega(t+\tau)}$ . Our goal is to find the variations of the probability distribution density in the first order in  $\mu \ll 1$ ,  $\rho_t(x) = \rho_0(x) + \mu \rho_1(x) e^{i\omega(t+\tau)} + o(\mu^2)$ . This can be done using different methods.

#### 3.3.1 Method 1: static response of the $p$ -iterate

Let us assume  $\omega = 2\pi q/p$ , i. e. the driving is  $p$ -periodic. Then the  $p$ -iterate of the map  $\hat{f}(\cdot)$  is autonomous, and the phase-averaged response of this  $p$ -iterate  $\hat{F} = \hat{f}^p$  to the driving  $\mu e^{i\omega(t+\tau)}$  will only depend on the phase  $\tau$ .

To define the linear response of the map (3.18) at the frequency  $\omega$  it is enough to define the static response of the  $p$ -iterate  $F(\cdot)$  of  $f(\cdot)$  to the perturbation with an appropriate function  $G(x) \sim e^{i\omega\tau}$ , i. e.  $\hat{f}^p(x) = (f + \mu g a_t)^p(x) = \hat{F}(x) = F(x) + \mu G(x) + o(\mu^2)$ .



### 3.3. LINEAR RESPONSE OF CHAOTIC MAPS

Assuming that the perturbation  $\mu G$  does not change preimages of  $F$  too much we can write the Frobenius-Perron equation for  $\hat{F}$  with the sum index running over preimages  $x_{\hat{m}}$  of  $x$  in the map  $\hat{F}$ :

$$\rho_0(x) + \mu\rho_1(x) + o(\mu^2) = \sum_{\hat{m}} \frac{\rho_0(x_{\hat{m}}) + \mu\rho_1(x_{\hat{m}}) + o(\mu^2)}{|F'(x_{\hat{m}}) + \mu G'(x_{\hat{m}}) + o(\mu^2)|} \quad (3.19)$$

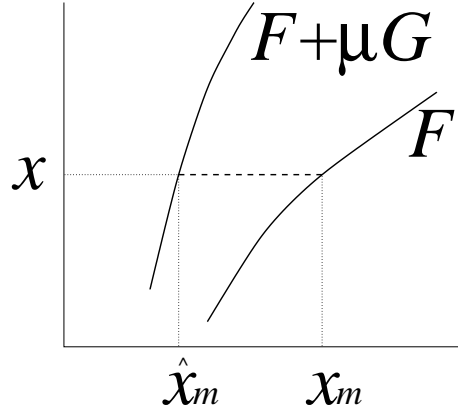


Figure 3.2: Shift of preimages up to the order of  $\mu$  of a point  $x$  in the map  $\hat{F} = F + \mu G$  as compared with the map  $F$ . This shift is smooth if the slope of every branch of  $F$  is non-zero at  $x_m(x)$ . If the slope is zero then an addition of a non-zero perturbation  $G$  causes a singular shift of preimages and/or change of their number. Therefore, not every possible perturbation functions  $G$  are allowing the linear response analysis.

Taking into account the shift of preimages of  $x$  in  $\hat{F}$  as compared to  $F$  up to the order of  $\mu$  ( $x = \hat{F}(x_{\hat{m}}) = F(x_m) \Rightarrow x_{\hat{m}} = x_m - \mu G'(x_m) / F'(x_m) + o(\mu^2)$ ) we can go over to the sum over preimages of the unperturbed map and extract the correction term  $\rho_1$ :

$$\rho_1(x) = \sum_m \frac{\text{sign} F'}{F'^2} (\rho_0 G \frac{F''}{F'} - \rho_0' G + \rho_1 F' - \rho_0 G') \Big|_{x_m} \quad (3.20)$$

Of course, the equation (3.20) is again of the Frobenius-Perron-type and may be not easy to solve analytically. However, this method has the advantage that it can be applied to analyze the response of individual (possibly stable)  $n$ -periodic orbits to the  $p$ -periodic driving just by analyzing the  $np$ -iterate of  $\hat{f}(\cdot)$ .

### 3.3.2 Method 2: spectral decomposition

Denoting the right hand side of (3.18) as  $F^t(x)$ , we write the Frobenius-Perron operator for the density  $\rho_t(x)$

$$\rho_{t+1}(x) = \int \delta(x - F^t(y)) \rho_t(y) dy \quad (3.21)$$

From this point on we restrict ourselves to maps on a unit circle and can now introduce the Fourier transform of the density  $\rho_t(x) = \sum \psi_t(k) e^{2\pi i k x}$  and obtain from (3.21) the corresponding

Frobenius-Perron operator in the Fourier space:

$$\begin{aligned}\Psi_{t+1}(k) &= \sum_{l=0}^{\infty} R_t(k, l) \Psi_t(l) \\ R_t(k, l) &= \int_0^1 e^{2\pi i l x - 2\pi i k F_t(x)} dx\end{aligned}\tag{3.22}$$

Taking into account that  $F^t(x) = \hat{f}(x) = f(x) + \mu g(x) e^{i\omega t}$  we can now write the spectral representation of the Frobenius-Perron equation (3.21) up to the first order in  $\mu$

$$R(k, l) = R^0(k, l) + \mu R^1(k, l) e^{i\omega t} + o(\mu^2)\tag{3.23}$$

where

$$\begin{aligned}R^0(k, l) &= \int_0^1 e^{2\pi i l x - 2\pi i k f(x)} dx \\ R^1(k, l) &= -2\pi i k \int_0^1 g(x) e^{2\pi i l x - 2\pi i k f(x)} dx\end{aligned}$$

Substituting this in (3.22) and writing  $\Psi_t(k) = \Psi^0(k) + \mu e^{i\omega t} \Psi^1(k) + o(\mu^2)$  we obtain the equation for the complex amplitude of the perturbation  $\Psi^1(k)$

$$e^{i\omega} \Psi^1(k) = \sum_{l=0}^{\infty} R^0(k, l) \Psi^1(l) + R^1(k, l) \Psi^0(l)\tag{3.24}$$

If all coefficients  $R^0(k, l)$  and  $R^1(k, l)$  of the Frobenius-Perron operator in the spectral representation can be found then one has to solve the algebraic equations (3.24) to obtain the oscillating correction term to the invariant density.

### 3.4 Transition to coherence in coupled Bernoulli maps

Here we will give an example of application of the linear response theory to an ensemble of particular chaotic maps.

#### 3.4.1 The system

To remind, we consider an ensemble of identical chaotic maps on a unit circle (3.4) which are coupled every to every through a mean field.

$$\begin{aligned}x_i(t+1) &= f(x_i(t)) + \varepsilon g(x_i(t)) a(t) \\ a(t) &= \frac{1}{N} \sum_{i=1}^N q(x_i(t))\end{aligned}$$

Individual uncoupled maps are taken here to be Bernoulli maps,  $f(x) = 2x \bmod 1$ , but the results should be general for structurally stable maps on a circle.

This map is a paradigmatic model of a chaotic systems while it admits relatively simple calculations. It is typically chaotic in the sense that if one writes a number from the interval  $[0, 1]$  as a binary fraction  $0.110010101111011010010\dots$  and takes a close number differing from

### 3.4. TRANSITION TO COHERENCE IN COUPLED BERNOULLI MAPS

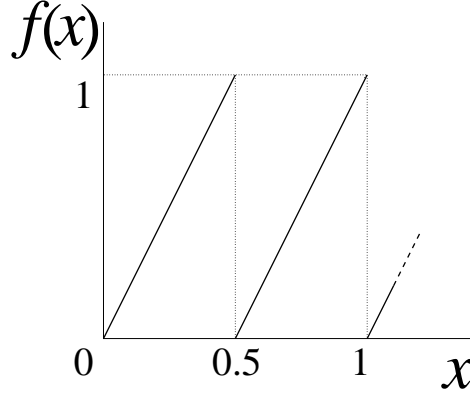


Figure 3.3: The Bernoulli map  $f(x) = 2x \bmod 1$ .

the first one in the digit  $n$  then the map generates diverging sequence of numbers. The distance between consequent images of the initially close numbers will grow to the order of one after  $n$  steps. The slope of this map is constant, the map has uniform invariant density and is structurally stable to small perturbations, i. e. the dynamics remains chaotic with its invariant density close to uniform.

In order to ensure that the number of preimages is not changed as discussed in [37] by the perturbation the perturbation function  $g(x) = \text{Re} \sum_{k=0}^{\infty} g_k e^{2\pi i k x}$  is introduced.

#### 3.4.2 Calculation of transfer function: method 1

Now our goal is to obtain the expansion of the invariant probability density  $\rho(x) = \rho_0(x) + \mu\rho_1(x) + o(\mu^2)$  in the perturbed system

$$x_{n+1} = \hat{f}(x_n) = f(x_n) + \mu g(x_n) a_n, \text{ with } a_n = \cos \omega(n + \tau) \quad (3.25)$$

This task reduces for  $p$ -periodic driving (i. e. if  $\omega = 2\pi \frac{q}{p}$ ) to the problem of finding out the first correction to the invariant density of the  $p$ -iterate of the map (3.25) when driven by a constant, with  $\hat{f}^p(x) = (f + \mu g a_n)^p(x) = \hat{F}(x) = F(x) + \mu G(x) + o(\mu^2)$  being now autonomous.

The equation (3.20) gives a Frobenius-Perron-like equation for this correction in terms of preimages of the  $p$ -iterate of the unperturbed map  $f(\cdot)$ , which is in our case the  $p$ -iterate of the Bernoulli map  $F(x) = f^p(x) = 2^p x \bmod 1$ .

The preimages  $x_m(x)$  of a point  $x$  defined by the  $p$ -iterate of the Bernoulli map are

$$x_m(x) = \frac{x + m}{2^p}, m = 0, 1, \dots, 2^p - 1 \quad (3.26)$$

Invariant density of the (unperturbed) Bernoulli map is uniform, i. e.

$$\begin{aligned} \rho_0(x) &= 1 \\ \rho'_0(x) &= 0 \end{aligned} \quad (3.27)$$

The slope of the  $p$ -iterate of the Bernoulli map is constant, i. e.

CHAPTER 3. TRANSITION TO COHERENCE IN GLOBALLY COUPLED MAPS

$$\begin{aligned} F(x) &= 2^p x \bmod 1 \\ F'(x) &= 2^p \\ F''(x) &= 0 \end{aligned} \tag{3.28}$$

The equation (3.20) for the correction term to the invariant density of the perturbed system is now read

$$\rho_1(x) = \sum_{m=0}^{2^p-1} 2^{-2p} \left( 2^p \rho_1 \left( \frac{x+m}{2^p} \right) - G' \left( \frac{x+m}{2^p} \right) \right) \tag{3.29}$$

To evaluate  $G'$  to be substituted into (3.29) we expand the derivative of the  $p$ -iterate  $\hat{F}$  of  $\hat{f} = f + \varepsilon g a_n$ :

$$\begin{aligned} \hat{F}'(x) = F'(x) + \mu G'(x) + o(\mu^2) &= \frac{d}{dx} \hat{f}^p(x) \\ &= \prod_{k=0}^{p-1} \left( f'(\hat{f}^k(x)) + \mu g'(\hat{f}^k(x)) a_k \right) \\ &= \prod_{k=0}^{p-1} f'(\hat{f}^k(x)) + \mu \sum_{l=0}^{p-1} \frac{g'(f^l(x)) a_l}{f'(f^l(x))} \prod_{k=0}^{p-1} f'(\hat{f}^k(x)) + o(\mu^2) \end{aligned}$$

The slope  $f'(\cdot)$  is the same at every point on the circle, so taking advantage of the Bernoulli map once again, we obtain with  $g(x \bmod 1) = g(x)$

$$G'(x_m) = 2^{p-1} \sum_{l=0}^{p-1} g'(2^{l-p}(x+m)) a_l \tag{3.30}$$

We will look for a solution of (3.29) with  $G'$  from (3.30) in the form

$$\rho_1 = \operatorname{Re} \sum c_k e^{2\pi i k x} \quad , \quad \text{with} \quad c_k = \int_0^1 \rho_1(x) e^{-2\pi i k x} dx$$

Now we compare coefficients at equal frequencies in the left and right sides of (3.29). As the invariant density is unique so it is sufficient to construct just one solution. Accordingly, we will set the coefficients to zero whenever possible.

We rewrite (3.29) as

$$\begin{aligned} \operatorname{Re} \sum_{k=0}^{p-1} c_k e^{2\pi i k x} &= \operatorname{Re} 2^{-p} \sum_{m=0}^{2^p-1} \sum_{k=0}^{\infty} c_k e^{2\pi i k \frac{x+m}{2^p}} - 2^{-p-1} \sum_{m=0}^{2^p-1} \sum_{l=0}^{p-1} g'(2^{l-p}(x+m)) \cos 2\pi \frac{q}{p} (l + \tau) \\ &= \operatorname{Re} A + \operatorname{Re} B \end{aligned} \tag{3.31}$$

Using the geometric sum  $\sum_{m=0}^{n-1} e^{2\pi i \frac{km}{n}} = \begin{cases} n & \text{if } k/n \in \mathbb{Z} \\ 0 & \text{if } k/n \notin \mathbb{Z} \end{cases}$  we receive:

### 3.4. TRANSITION TO COHERENCE IN COUPLED BERNOULLI MAPS

$$\begin{aligned}
A &= 2^{-p} \sum_{m=0}^{2^p-1} \sum_{k=0}^{\infty} c_k e^{2\pi i k \frac{x+m}{2^p}} = 2^{-p} \sum_{k=0}^{\infty} c_k e^{2\pi i k \frac{x}{2^p}} \sum_{m=0}^{2^p-1} e^{2\pi i k \frac{m}{2^p}} = \sum_{k=0}^{\infty} c_{2^p k} e^{2\pi i k x} \\
B &= -2^{-p-1} \sum_{m=0}^{2^p-1} \sum_{l=0}^{p-1} g'(2^{l-p}(x+m)) \cos 2\pi \frac{q}{p} (l+\tau) \\
&= -\sum_{l=0}^{p-1} 2^{-p-1} \cos 2\pi \frac{q}{p} (l+\tau) \sum_{k=0}^{\infty} 2\pi i k g_k \sum_{m=0}^{2^p-1} e^{2\pi i k 2^{l-p}(x+m)} \\
&= \sum_{k=0}^{\infty} e^{2\pi i k x} \left( -\sum_{l=0}^{p-1} 2^{p-l} \pi i k g_{2^{p-l}k} \cos 2\pi \frac{q}{p} (l+\tau) \right) \\
&= \sum_{k=0}^{\infty} e^{2\pi i k x} \left( -\sum_{l=1}^p 2^l \pi i k g_{2^l k} \cos 2\pi \frac{q}{p} (\tau-l) \right)
\end{aligned}$$

For coefficients  $c_k$  we obtain recursive relations which connect them with the spectral coefficients  $g_k$  of the perturbation function  $g(x)$

$$c_k = c_{2^p k} - \sum_{l=1}^p 2^l \pi i k g_{2^l k} \cos 2\pi \frac{q}{p} (\tau-l) \quad (3.32)$$

This equation should be read from larger values of  $k$  to smaller ones and the period  $p$  should be free to multiply with any integer together with  $q$  without any change in the result. Thus  $p$  can be assumed to be big enough for every limited  $k$  and the term  $c_{2^p k}$  can be neglected if the expansion  $g(x) = \text{Re} \sum g_n e^{2\pi i x n}$  is limited. A nonzero term  $g_n$  will contribute to the terms with  $2^l k = n$ .

$$\begin{array}{lll}
c_1 & \leftarrow & g_2, g_4, g_8, \dots \\
c_2 & \leftarrow & g_4, g_8, g_{16}, \dots \\
c_3 & \leftarrow & g_6, g_{12}, g_{24}, \dots \\
\dots & \dots & \dots
\end{array}$$

For example, if  $g(x) = \sin 4\pi x + \sin 8\pi x$ , i. e.  $g_2 = g_4 = -i$ , then the invariant density is

$$\begin{aligned}
\rho(x) &= 1 - \mu 2\pi \left( \cos 2\pi \frac{q}{p} (\tau-1) + 2 \cos 2\pi \frac{q}{p} (\tau-2) \right) \cos 2\pi x \\
&\quad - 4\mu \pi \cos 2\pi \frac{q}{p} (\tau-1) \cos 4\pi x + o(\mu^2)
\end{aligned} \quad (3.33)$$

From the equation (3.32) we now obtained the invariant density for the perturbed Bernoulli map at every time  $n + \tau$  (or just  $\tau$ ) in the form

$$\rho(x) = 1 + \mu \text{Re} \sum_{k=0}^{\infty} c_k(\tau) e^{2\pi i k x} + o(\mu^2) \quad (3.34)$$

Every coefficient  $c_k(\tau)$  is  $p$ -periodic in  $\tau$ ,  $c_k(\tau) \sim e^{i\omega\tau}$ . An average of an observable  $q(x) = \text{Re} \sum_{k=0}^{\infty} q_k e^{2\pi i k x}$  with driving frequency  $\omega = 2\pi \frac{q}{p}$  is:

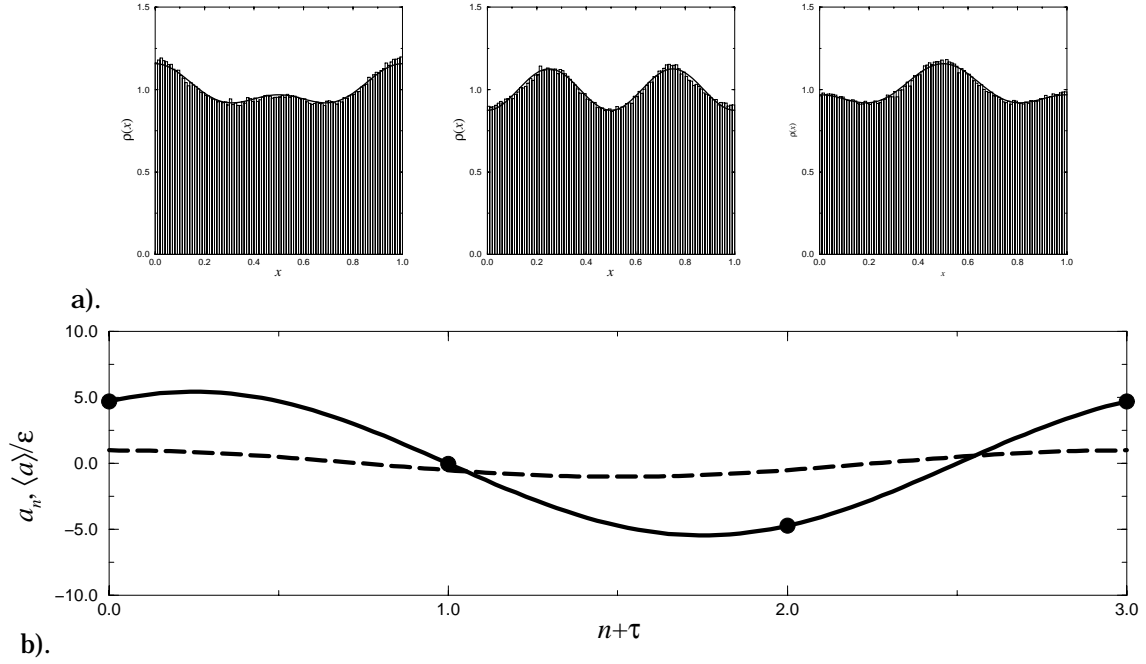


Figure 3.4: Modulation of the averaged response  $\langle q \rangle$  with the phase of the driving force  $a_n$ . a). Histogram of invariant density  $\rho = \rho_0 + \epsilon \rho_1 + o(\epsilon^2)$  of the 3-periodically driven system taken at different times  $(n + \tau)$ , here  $\tau = 0, 1, 2$ ,  $\epsilon = 0.01$ ,  $10^6$  points used. The observable is  $q(x) = \cos 2\pi x$ , the perturbation function  $g(x) = \sin 4\pi x + \sin 8\pi x$ . The thick lines are theoretically predicted density  $\rho(x) = 1 - 2\epsilon\pi \left( \cos 2\pi \frac{q}{p}(\tau - 1) + 2 \cos 2\pi \frac{q}{p}(\tau - 2) \right) \cos 2\pi x - 4\epsilon\pi \cos 2\pi \frac{q}{p}(\tau - 1) \cos 4\pi x$  at  $\tau = 0, 1, 2$ . b). External force  $a_n = \cos 2\pi \frac{1}{3}(n + \tau)$  (dashed) and  $\epsilon$ -normalized mean field response  $\frac{\langle q \rangle}{\epsilon}$ , amplification and phase shift effects are seen. Filled circles are observable averages  $a + \langle \cos 2\pi x \rangle$  calculated for  $\tau = 0, 1, 2$  from the above densities.

$$a_{out}(\tau) = \mu \sum_{k=0}^{\infty} \sum_{m=0}^{\infty} \int_0^1 \text{Re} q_k e^{2\pi i k x} \text{Re} c_k(\tau) e^{2\pi i m x} dx = \text{Re} \frac{\epsilon}{2} \sum_{k=0}^{\infty} \bar{q}_k c_k(\tau) = \text{Re} K(\omega) e^{i\omega\tau} \quad (3.35)$$

For example, with the observable defining the mean field set to be  $q(x) = \cos 2\pi x$  and the perturbation function  $g(x) = \sin 4\pi x + \sin 8\pi x$  (the modulation of the invariant measure with time for this choice of  $q(x)$  and  $g(x)$  is illustrated in the figure 3.4) the mean field response of the  $p$ -iterate of the map  $\hat{f}$  to the driving frequency  $\omega = 2\pi \frac{q}{p}$  results to

$$a_{out}(\tau) = \langle q(x) \rangle = -\mu\pi \cos \omega(\tau - 1) - 2\mu\pi \cos \omega(\tau - 2) = \text{Re} K(\omega) e^{i\omega\tau} \quad (3.36)$$

From (3.36) the complex transfer function follows

$$K(\omega) = -\pi (2e^{-i2\omega} + e^{-i\omega}) \quad (3.37)$$

### 3.4.3 Calculation of transfer function: method 2

Our starting point is the Frobenius-Perron equation in the spectral form (3.23). In the case of the Bernoulli map the corresponding Frobenius-Perron operators for the unperturbed map  $R^0(k, l)$  are

$$R^0(k, l) = \int_0^1 e^{2\pi i l x - 2\pi i k (2x \bmod 1)} dx = \delta_{l, 2k} \quad (3.38)$$

Here  $\delta_{k, n}$  is the Kronecker symbol. For the spectral components  $\psi^0(k)$  of the unperturbed Bernoulli map this gives  $\psi^0(k) = \psi^0(2k)$  so that the invariant density is uniform

$$\psi^0(k) = \delta_{0, k} \quad (3.39)$$

Also the operator  $R^1(k, l)$  is calculated straightforward to be

$$R^1(k, l) = -ik2\pi \int_0^1 g(x) e^{2\pi i l x - 2\pi i k (2x \bmod 1)} dx = -2\pi i k g_{2k-l} \quad (3.40)$$

Again,  $g_k$  is the spectral component of the perturbation function  $g(x)$ . Substituting (3.38), (3.39) and (3.40) in the equation (3.24) gives

$$e^{i\omega} \psi^1(k) = \psi^1(2k) - 2\pi i k g_{2k} \quad (3.41)$$

Writing down the expression for  $\psi^1(2^n k)$  and recalling that  $\lim_{n \rightarrow \infty} \psi^1(n) = 0$  if  $\rho_1(x)$  admits Fourier decomposition at all, one obtains

$$\psi^1(k) = -ik\pi \sum_{m=1}^{\infty} 2^m e^{-im\omega} g_{2^m k}. \quad (3.42)$$

Now we have to calculate the mean field as the average over the probability density:

$$\lim_{N \rightarrow \infty} \sum_{i=1}^N \frac{1}{N} q(x_i(t)) = \langle q(x(t)) \rangle = \int_0^1 \rho_t(x) q(x) dx$$

Substituting here the expression for the density

$$\rho_t(x) = \sum_k (\psi^0(k) + \mu e^{i\omega t} \psi^1(k)) e^{2\pi i k x} + o(\mu^2)$$

we obtain exactly like in the method 1:

$$\begin{aligned} \langle q \rangle &= \mu K(\omega) e^{i\omega t} \\ K(\omega) &= \sum_k q_{-k} \psi^1(k) \end{aligned} \quad (3.43)$$

$q_k$  is the Fourier harmonics of the function  $q(x)$

$$q_k = \int_0^1 q(x) e^{-2\pi i k x} dx$$

In deriving (3.43) we have taken into account that the unperturbed invariant density does not contribute to the mean field. In the particular case of Bernoulli map we obtain from (3.42),(3.43)

$$K(\omega) = \sum_{k=-\infty}^{\infty} \sum_{m=1}^{\infty} -ik\pi 2^m e^{-im\omega} g_{2^m k} q_{-k} \quad (3.44)$$

With  $g(x) = \sin 4\pi x + \sin 8\pi x$  and  $q(x) = \cos 2\pi x$  the equation (3.44) yields

$$K(\omega) = -\pi (2e^{-i2\omega} + e^{-i\omega}) \quad (3.45)$$

Of course, this coincides<sup>†</sup> with the result (3.37).

### 3.4.4 Transition points

Now we use the transfer function (3.45) and the stability condition (3.17) to define the critical coupling at which the transition to coherence in the ensemble (3.4) takes place.

First we define the frequencies of the most unstable modes, i. e. the autogeneration frequencies in the amplifier-feedback circuit:

$$\text{Im}K(\omega) = 0 \Leftrightarrow 2 \sin 2\omega + \sin \omega = 0 \Leftrightarrow \cos \omega = \begin{bmatrix} -1/4 \\ 1 \\ -1 \end{bmatrix}$$

With these frequencies we obtain the critical coupling strengths

$$\varepsilon \text{Re}K(\omega) = 1 \Leftrightarrow \varepsilon_c = \frac{\pi^{-1}}{2 - \cos \omega - 4 \cos^2 \omega} = \begin{bmatrix} 1/2\pi \\ -1/3\pi \\ -1/\pi \end{bmatrix} \quad (3.46)$$

The stability interval is herewith  $-1/3\pi = \varepsilon_{c2} < \varepsilon < \varepsilon_{c1} = 1/2\pi$ . The autogeneration frequencies are  $\omega_2 = 0$  and  $\omega_1 = \arccos(-1/4)$ .

---

<sup>†</sup>Both methods seem to be identical. In the method 1 one first obtains the Frobenius-Perron equation for the perturbation of the  $p$ -iterate of the map and then goes over to its spectral form while in the method 2 the Fourier transform is made in order to obtain the Frobenius-Perron equation for the perturbation of the invariant density.

In the relatively simple example of Bernoulli maps perturbed with "reasonable" functions  $g(x)$  these two ways are equivalent indeed and lead to the same recurrent relations between spectral coefficients. But there can be situations, where only one of these two steps is possible so that one would have to start with this possible step and try to advance after it in a different manner.

For instance, this is the case if there are stable  $n$ -periodic orbits. Their linear response to the driving at the frequency  $\omega = 2\pi q/p$  can be still calculated using the method 1, i. e. analyzing the  $np$ -iterate of the map.

Another argument is that the equation (3.20) is valid no matter whether  $\rho_1(x)$  admits simple spectral decomposition or not.



### 3.4.5 Numerics

An ensemble of  $10^6$  systems was simulated numerically. As an observable to visualize the transition to coherence the variance  $\langle a^2 \rangle$  of deviations of the mean field from the trivial state  $a = 0$  is used. In the disordered state this variance has to be of the order  $N^{-1}$ , where  $N$  is the size of the ensemble. The results are presented in the figure 3.5. They are in a good agreement with the theory.

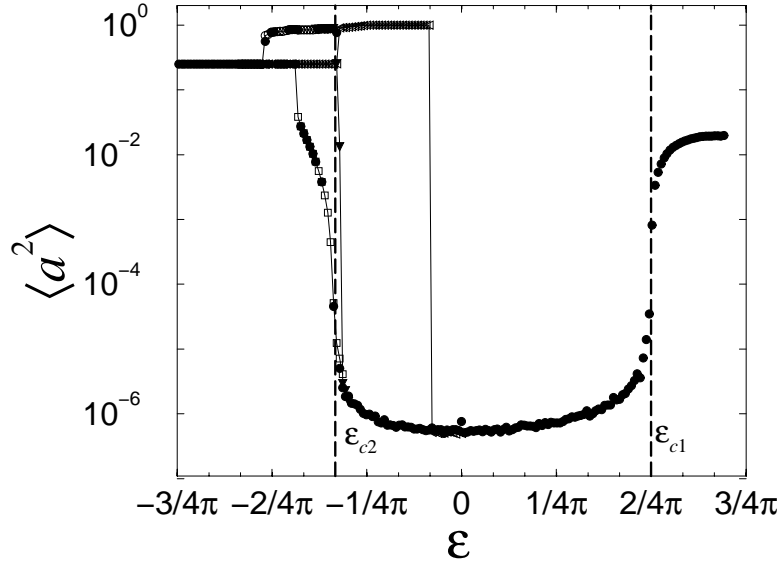


Figure 3.5: Transition to coherence in the ensemble of  $10^6$  globally coupled Bernoulli maps. Long-dashed lines shows the region of the theoretically predicted stability. Several invariant states exist for some values of  $\epsilon$ .

The transition to coherence occurs at  $\epsilon_{c1}$  and  $\epsilon_{c2}$  differently. At  $\epsilon_{c1}$  the frequency of auto-generation is non-zero, an oscillating mean field arises. At  $\epsilon_{c2}$  the frequency is zero, a shift of the mean field away from its zero state takes place. Both situations are illustrated in the figure 3.6.

### 3.4.6 Discrete Hopf bifurcation at $\epsilon_{c1}$

The transition at  $\epsilon_{c1} = 1/2\pi$  is generic in the sense that the autogeneration frequency in a feedback loop is typically non-zero. The corresponding bifurcation type is Neimark (discrete time Hopf) bifurcation. In the leading order one expects the amplitude of the mean field to scale as  $\sqrt{\Delta\epsilon}$ , with  $\Delta\epsilon = \epsilon - \epsilon_{c1}$ . In the figure 3.7 this scaling corresponds to the dashed line. One can argue that the expected scaling holds up to finite-size effects.

Another way to visualize the type of bifurcation at  $\epsilon_{c1}$  is to calculate the non-linear response function at the known autogeneration frequency  $\omega_1 = \arccos(-1/4)$ . The technique is the same, only the amplitude of the harmonic perturbation  $\mu$  is not small any more. Again, one is only interested in the response at the same frequency.

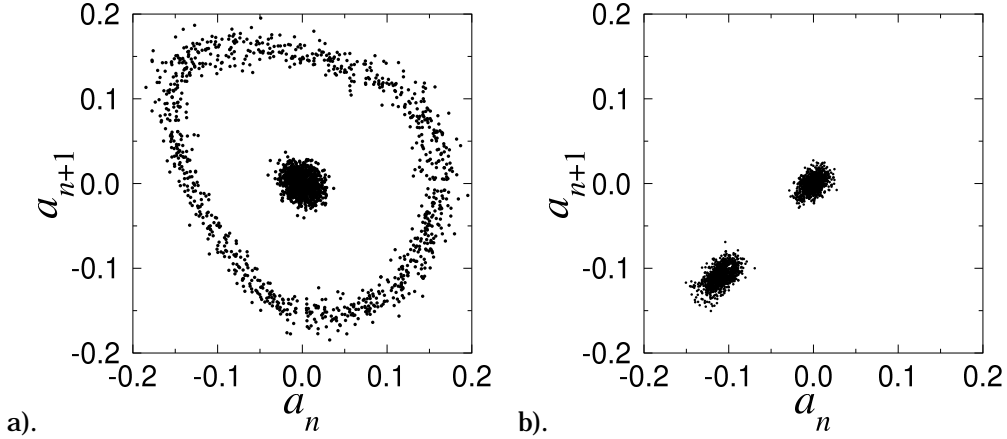


Figure 3.6: Different dynamics of the non-trivial mean field in the coherent regimes,  $N = 10^4$ . (a) The transition at  $\varepsilon_{c1}$ . In the disordered state at  $\varepsilon = 0.13$  the mean field vanishes up to finite-size fluctuations (a cloud around  $a_{n+1} = a_n = 0$ ); in the coherent state at  $\varepsilon = 0.18$  nearly periodic oscillations are observed. (b) The transition at  $\varepsilon_{c2}$  is one from a zero equilibrium point ( $\varepsilon = -0.08$ ) to a nearly constant mean field at  $\varepsilon = -0.13$ .

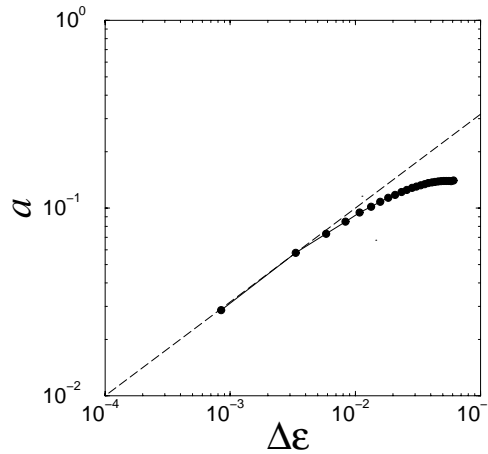


Figure 3.7: Scaling at  $\varepsilon_{c1}$ . The theoretically expected scaling is  $a \sim \sqrt{\Delta\varepsilon}$  (long-dashed line).

With this method one obtains a mapping from an input amplitude  $a_{in}$  to the output amplitude  $a_{out}$  at the given frequency and a given coupling strength  $\varepsilon$ . One sees immediately that  $a_{out}(0) = 0$  (no input means no output) and the slope of this mapping is proportional to the coupling constant  $\varepsilon$ . More exactly, the slope is equal to the product of  $\varepsilon$  and the modulus of the linear transfer function. At the transition point  $\varepsilon_{c1}$  the slope of the map exactly equals to one.

$$\frac{da_{out}}{da_{in}} = \varepsilon |K(\omega)|$$

At  $\varepsilon < \varepsilon_{c1}$  the map  $a_{out}(a_{in})$  (see figure 3.8) only has one stable fixed point  $a = a_{out} = a_{in} = 0$ . At  $\varepsilon > \varepsilon_{c1}$  the fixed point  $a = 0$  is unstable, and a small non-zero amplitude solution arises (a transcritical bifurcation). In the figure 3.8 formally the response to the "negative" amplitudes

### 3.4. TRANSITION TO COHERENCE IN COUPLED BERNOULLI MAPS

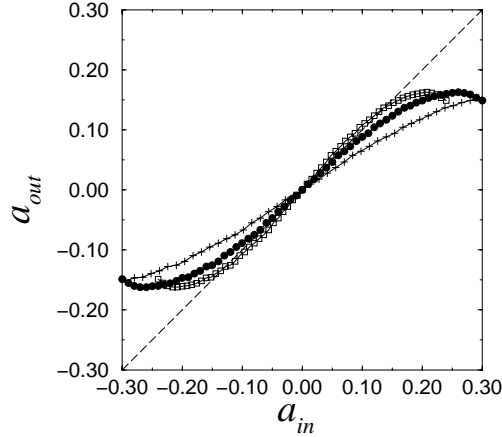


Figure 3.8: Non-linear response at the frequency  $\omega_{c1} = \arccos(-0.25)$ . With filled circles the non-linear response at  $\varepsilon = \varepsilon_{c1} = 1/2\pi$  is shown; squares correspond to the coherent state at  $\varepsilon = 1.4\varepsilon_{c1}$ ; plus signs correspond to the disordered state,  $\varepsilon = 0.8\varepsilon_{c1}$ . With the dashed line the invariant diagonal  $a_{out} = a_{in}$  is shown.

of  $a_{in}$  is drawn. In the Hopf bifurcation this negative branch is symmetric to the positive one, in general this is not always the case, to be seen later on.

The next-leading order in the expansion of the curve  $a_{out}(a_{in})$  around zero determines the scaling of the amplitude of the mean field with  $\Delta\varepsilon = \varepsilon - \varepsilon_{c1}$  as defined by the fixed point of the map  $a_{out}(a_{in}, \varepsilon)$ . Generally the quadratic order dominates so that close at a (transcritical) transition point holds

$$a = a_{in} = a_{out}(a_{in}, \Delta\varepsilon) = c_1 a_{in} + c_2 a_{in}^2 + o(a_{in}^2) \quad \text{with} \quad c_1 = 1 + \Delta\varepsilon + o(\Delta\varepsilon^2)$$

It follows straightforward for a non-zero solution

$$a \sim \sqrt{\Delta\varepsilon}$$

#### 3.4.7 Asymmetric subcritical bifurcation at $\varepsilon_{c2}$

This scenario fails to explain the transition at  $\varepsilon = \varepsilon_{c2}$ . The reason is that this transition takes place at zero frequency, to some extent it is a degenerate case due to the specific choice of the maps  $f(\cdot)$  (Bernoulli maps) and the perturbation function  $g(\cdot)$  in the ensemble (3.4).

In the language of the non-linear response the situation is illustrated in the figure 3.9 where the non-linear response functions at  $\varepsilon_{c2}$  and at two close values are calculated. One sees that the non-linear response function is not symmetric and at  $\varepsilon > \varepsilon_{c2} = -1/3\pi$  there are three self-consistent amplitudes. The zero-amplitude solution with  $a_{out} = a_{in} = 0$  and the distant solution with  $a_{out} = a_{in} \approx 1$  are stable (the diagonal is crossed from left-up to right-down), the solution in-between is unstable (the diagonal is crossed from left-down to right-up).

Note that the method of a non-linear response function at a given frequency only works for

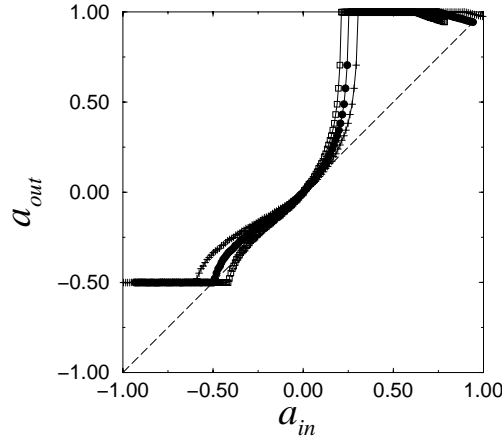


Figure 3.9: Non-linear static response (at the frequency  $\omega_{c2} = 0$ ). With filled circles the non-linear response at  $\varepsilon = \varepsilon_{c2} = -1/3\pi$  is shown; squares correspond to the coherent state at  $\varepsilon = 1.4\varepsilon_{c2}$ ; plus signs correspond to the disordered state,  $\varepsilon = 0.8\varepsilon_{c2}$ . With the dashed line the invariant diagonal  $a_{out} = a_{in}$  is shown.

small amplitudes. The distant solutions do not have to have the same frequency, at which the non-linear response function has been calculated. Therefore, existence of distant fixed points in the map  $a_{out}(a_{in})$  is not a proof but merely a hint on possible existence of self-consistent mean field solutions of large amplitudes and, probably, different frequencies.

At  $\varepsilon < \varepsilon_{c2} = -1/3\pi$ , i. e. in the coherent state, there are three stable solutions and two unstable solutions between them. We see that the transition at  $\varepsilon = \varepsilon_{c2} = -1/3\pi$  is subcritical. Due to absence of  $a \leftrightarrow -a$  symmetry the situation corresponds to the skewed subcritical bifurcation like that in the figure 3.10.

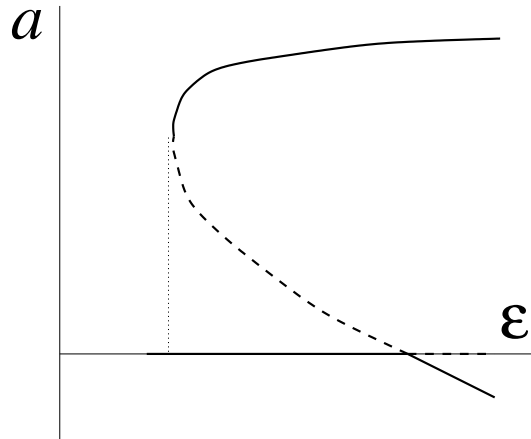


Figure 3.10: Subcritical pitch-fork bifurcation in absence of the symmetry  $a \leftrightarrow -a$ . A hysteretic transition is expected.

That is why we obtained one branch with small amplitudes near the transition,  $|\Delta\varepsilon| = |\varepsilon - \varepsilon_{c2}| \ll 1$ , and a number of distant solutions. Therefore, the trivial state  $a = 0$  is metastable, at least when close to the transition to coherence. This is also clearly seen in the figure 3.5.

### 3.4. TRANSITION TO COHERENCE IN COUPLED BERNOULLI MAPS

The branch of the small solution in the figure 3.10 has a well-defined slope, so that the scaling  $a \sim \Delta\varepsilon$  should be expected. This scaling is confirmed by the numerics in the figure 3.11.

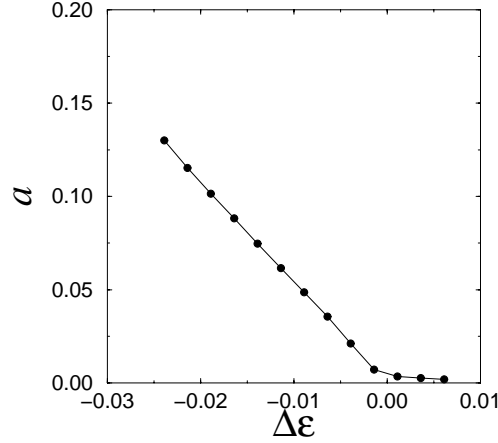


Figure 3.11: Scaling at  $\varepsilon_{c2}$  is linear,  $a \sim \Delta\varepsilon$ .

The stability of the distant solutions can be analyzed separately. Numerical experiments have shown that two different distant solutions can be obtained with different initial conditions (of course, because they are distant they do not have to be of zero-frequency).

One solution is a "one-cluster" solution. This means that all systems are synchronized to a fixed point solution  $x_k(t) = 0, \forall k$ . As the perturbation function  $g(x) = 0$  if  $x = 0$  so the mean field remains  $a = 1$  for all times. Of course, in an individual map this solution also exists but unstable. It becomes stable if the following condition is fulfilled

$$\left| \frac{dx_k(t+1)}{dx_k(t)} \right|_{x_k=0} < 1$$

Which gives the stability conditions

$$|2 + 12\pi\varepsilon| < 1 \quad \Rightarrow \quad \varepsilon \in \left[ -\frac{1}{4\pi}, -\frac{1}{12\pi} \right]$$

For  $\varepsilon < -1/4\pi$  the "one-cluster" solution does not exist but still there is a distant solution (cf. figures 3.5 and 3.9) as a continuation of the "one-cluster" solution, the structure of which is more complex and could not be described in a simple way. At least, it does not appear to be a cluster solution.

Another branch is the "two-cluster" solution, i. e.  $x_k = 1/3$  or  $x_k = 2/3$ . The points  $x = 1/3$  and  $x = 2/3$  are the period-two orbit of the Bernoulli map. Again, this is ensured because  $g(x) = \sin 4\pi x + \sin 8\pi x$  is zero if  $x = 1/3$  or  $x = 2/3$ . At both points the mean field has the value  $a(t) = -1/2$ .

The stability condition is now read

$$\left| \frac{dx_k(t+2)}{dx_k(t)} \right|_{x_k=\frac{1}{3}} = \left| (2 + \varepsilon g'(x)a(x)) \Big|_{x_k=\frac{1}{3}} \right| \left| (2 + \varepsilon g'(x)a(x)) \Big|_{x_k=\frac{2}{3}} \right| = (2 + 3\pi\varepsilon)^2 < 1$$

Every "two-cluster" solution (no matter how many systems are in the state  $x_k = 1/3$  and how many in the state  $x_k = 2/3$ ) is stable if

$$-\frac{1}{\pi} < \varepsilon < -\frac{1}{3\pi} \quad (3.47)$$

Note that apart of these two (numerically found) distant solutions also other solutions may exist but we did not find them in our simulations.

### 3.5 Extensions of the theory

The linear response approach has been adopted in analyzing the transition to coherence in globally coupled chaotic maps. This approach is quite general so that the above theory can be extended for similar problems. Below some generalizations are shortly discussed.

#### 3.5.1 Dynamics with additive noise

A straightforward generalization of the linear theory is including an additive noise in the dynamics. In this case the equation (3.4) is rewritten as

$$\begin{aligned} x_i(t+1) &= f(x_i(t)) + \varepsilon g(x_i(t))a(t) + \xi_i(t) \\ a(t) &= \frac{1}{N} \sum_1^N q(x_i(t)) \end{aligned} \quad (3.48)$$

Here  $\xi_i(t)$  are independent equally distributed random variables. The Frobenius-Perron equation (3.21) is generalized to this case by including the convolution of  $\rho$  with the probability density of  $\xi$  (e.g. [57]). In the Fourier space one simply multiplies the operators  $R^0$  and  $R^1$  in the case of the unperturbed (3.22) and perturbed (3.23) dynamics respectively with the characteristic function of noise

$$\tilde{R}(k, l) = w_k R(k, l)$$

Here  $\tilde{R}$ ,  $R$  are the operators  $R^0$  and  $R^1$  with and without noise, respectively, and  $w_k$  is the Fourier transform of the probability density  $W_\xi$  of the random noise

$$w_k = \int_{-\infty}^{\infty} W_\xi(x) e^{-2\pi i k x} dx$$

With this modification, all the linear response theory holds. Moreover, the presence of the fast decaying factor  $w_k$  regularizes the Frobenius-Perron equation, so that a non-singular solution for the response function can be expected even when the deterministic dynamics is structurally unstable, or even when in the deterministic dynamics periodic windows are present. In the particular case of Bernoulli maps, the final expression for the response function  $K$  (3.44) is modified to

$$K(\omega) = \sum_{k=-\infty}^{\infty} -ik\pi q_{-k} \sum_{m=1}^{\infty} 2^m e^{-im\omega} g_{2^m k} \prod_{l=0}^{m-1} w_{2^l k}$$

### 3.5.2 Complex dynamical dependence on the mean field

The linear response approach above can be also generalized to the case when the mean field has its own dynamics. Such a situation appears, e.g., in a series array of Josephson junctions coupled by means of an external load [110]. The junctions are coupled via the common current, which obeys an additional equation (for the RLC-load considered in [110] this is the equation of a driven damped linear oscillator).

Generally, the situation like that of the RLC-load means that there are more than two points in the circuit where the mean field  $a$  in some form (e.g. its derivatives) is present in the equations. This circuit is not a simple amplifier-feedback loop any more. As an illustration let us assume that there is an additional equation which governs the dynamics of the mean field.

$$\begin{aligned} x_k(t+1) &= h(x_k(t), \varepsilon a(t)) \\ \langle q \rangle &= \frac{1}{N} \sum_{k=1}^N q(x_k(t)) \\ a(t+1) &= \ell(a(t), \langle q \rangle) \end{aligned} \quad (3.49)$$

To apply the linear theory the equation (3.49) are linearized in  $a$  (still  $a = 0$  should be a solution, therefore  $\ell(0, \cdot) = \ell(\cdot, 0) = 0$ )

$$\begin{aligned} x_k(t+1) &= f(x_k(t)) + \varepsilon g(x_k(t))a(t) \\ \langle q \rangle &= \frac{1}{N} \sum_{k=1}^N q(x_k(t)) \\ a(t+1) &= \gamma_1 a(t) + \gamma_2 \langle q \rangle \end{aligned} \quad (3.50)$$

The first two equations in the system (3.50) describe the linear device which transfer function has to be defined. The third equation describes the inherent inertial dynamics of the mean field.

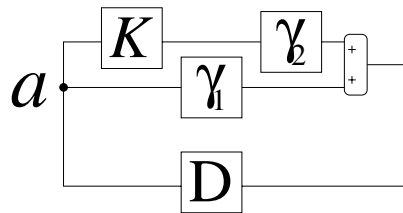


Figure 3.12: A circuit corresponding the equations (3.50) consists of a summator, a differentiating device, and three amplifiers with different amplification coefficients.

Again, one can consider this equations as a circuit with feedback as shown in the figure 3.12 and first break the feedback to define the transfer function  $K(\omega)$  in order to close it when the function  $K(\omega)$  is known. One calls the mean field in the first equation "input"  $a_{in}(t)$  and the average  $\langle q \rangle$  "output" of the second equation and the whole theory works so that linear response of  $\langle q \rangle$  to a small harmonic  $a_{in}$  can be defined.

The peculiarity is now that breaking of self-consistency can be done differently in the third equations. For instance, it can equally be understood as

$$a_{in}(t+1) = \gamma_1 a_{out}(t) + \gamma_2 \langle q \rangle \quad (3.51)$$

or

$$a_{out}(t+1) = \gamma_1 a_{out}(t) + \gamma_2 \langle q \rangle \quad (3.52)$$

These two interpretations of breaking of consistency are illustrated in the figure 3.13.

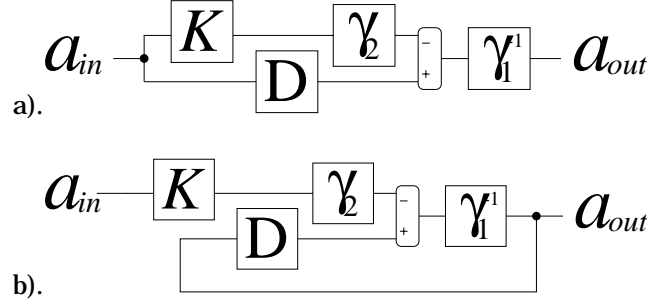


Figure 3.13: Different ways to break the self-consistency of the equations (3.50). a). Two inputs and one output as in the equation (3.51) b). One input and two outputs as in the equation (3.52).

In the case of the interpretation as given in the equation (3.51) the total transfer function  $K_{\Sigma}(\omega) = K_1(\omega)$  is asymptotically (i. e. zero initial conditions are assumed) calculated from

$$e^{i\omega} \tilde{a}_{in} = \gamma_1 \tilde{a}_{out} + \varepsilon \gamma_2 K(\omega) \tilde{a}_{in} \quad \Rightarrow \quad K_1(\omega) = \frac{e^{i\omega} - \varepsilon \gamma_2 K(\omega)}{\gamma_1} \quad (3.53)$$

With the interpretation from (3.52) this reads

$$e^{i\omega} \tilde{a}_{out} = \gamma_1 \tilde{a}_{out} + \varepsilon \gamma_2 K(\omega) \tilde{a}_{in} \quad \Rightarrow \quad K_2(\omega) = \frac{\varepsilon \gamma_2 K(\omega)}{e^{i\omega} - \gamma_1} \quad (3.54)$$

Invoking the self-consistency  $a = a_{out} = a_{in}$  gives in both cases

$$(-e^{i\omega} + \gamma_1 + \varepsilon \gamma_2 K(\omega)) \tilde{a} = 0 \quad (3.55)$$

The stability condition on  $\varepsilon$  is obvious

$$\varepsilon L(\omega) K(\omega) = 1 \quad \text{with} \quad L(\omega) = \frac{\gamma_2}{-\gamma_1 + e^{i\omega}} \quad (3.56)$$

Note that for general input  $a_{in}$  the linear device described by the transfer function  $K_1(\omega)$  from (3.53) can be unstable by input. Contrary to this, the device with  $K_2(\omega)$  from (3.54) is stable by input. Of course, this has no effect on the validity of the equation (3.55).

In general, if the dynamical equations of the ensemble have complex dynamical dependence on  $a$  then their linearization can be understood as a complex circuit of linear devices. Connections between groups of devices can be arbitrary broken so that every group has only one input and one output. After defining transfer functions of these groups the total stability of the circuit can be written by invoking the self-consistency as



### 3.5. EXTENSIONS OF THE THEORY

$$L(\omega)\tilde{a} = 0 \quad (3.57)$$

The function  $L(\omega)$  is independent of the choice how the self-consistency is broken. The stability by initial condition (there is no input in the equation (3.57)) is defined by the complex relation

$$L(\omega) = 0 \quad (3.58)$$

As an example let us consider the ensemble (3.4) with inertial dynamics of the mean field

$$a(t) = \gamma a(t-1) + \langle q(x(t)) \rangle$$

In this case  $L(\omega) = (1 - \gamma e^{-i\omega})^{-1}$  in the equation (3.56) with an obvious modification of the transition values  $\varepsilon_c$  and frequencies  $\omega$ . Namely, the frequencies are obtained from the imaginary part of  $L(\omega) = 1 - \varepsilon L(\omega)K(\omega) = 1 - \gamma e^{-i\omega} + \varepsilon\pi(2e^{-2i\omega} + e^{-i\omega}) = 0$  to be

$$\cos \omega = \begin{cases} -\frac{1}{4} + \frac{\gamma}{4\varepsilon_c\pi} \\ 1 \\ -1 \end{cases} \quad (3.59)$$

Here the frequency still depends on  $\varepsilon_c$ , one has to insert these frequencies (3.59) into  $\text{Re}L(\omega) = 0$  in order to resolve for  $\varepsilon_c$ . From this the transition points are

$$\varepsilon_c = \frac{(1 - \gamma \cos \omega)}{\pi(2 - \cos \omega - 4 \cos^2 \omega)} = \begin{cases} \frac{1}{2\pi} \\ \frac{\gamma-1}{3\pi} \\ -\frac{\gamma+1}{\pi} \end{cases} \quad (3.60)$$

This gives the explicit expression for the autogeneration frequencies

$$\cos \omega = \begin{cases} \frac{2\gamma-1}{4} \\ 1 \\ -1 \end{cases} \quad (3.61)$$

The inertial dynamics with a small  $\gamma$  of the mean field only affect the frequency but not the critical coupling at  $\varepsilon_{c1}$  and, on the contrary, it only affects the critical coupling but not the frequency at  $\varepsilon_{c2}$  (of course, this effect has no generality). The corresponding numerical simulations are presented in the figure 3.14.

If  $\gamma < -1/2$  then the mode with  $\cos \omega = -1$  (period-two oscillations) becomes more unstable than the mode  $\cos \omega = 1$  (zero frequency). The corresponding bifurcation diagram is presented in the figure 3.15. The difference of these two types of transitions at  $\varepsilon_{c2}$  is illustrated in the figure 3.16.

For  $\gamma < -1$  even the state at  $\varepsilon = 0$  is coherent. This corresponds to a divergent dynamics of  $a(t)$  (the modulus of the multiplier is larger than one) if interactions in the ensemble are absent,  $\varepsilon = 0$ . Note that there still exists the stability interval  $\varepsilon \in [-\frac{\gamma-1}{3\pi}, \frac{1}{2\pi}]$ , this means that coupling of a dynamical system with divergent dynamics with an ensemble of chaotic systems can stabilize it.

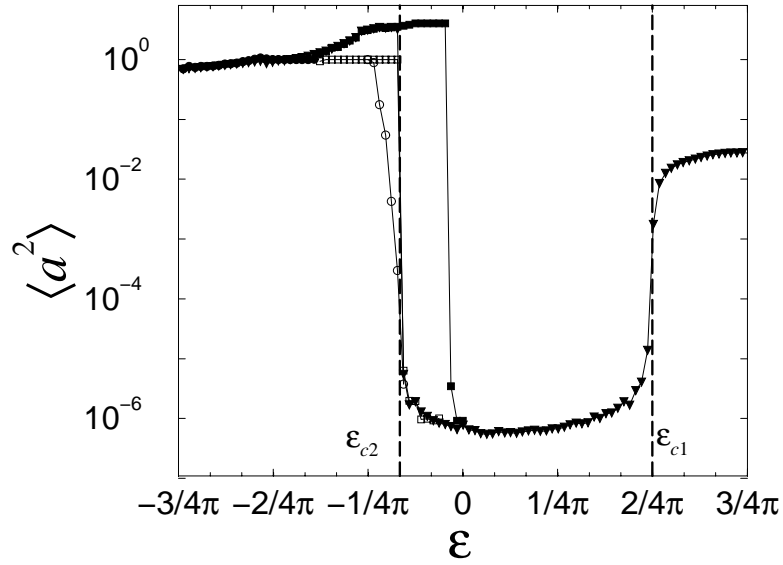


Figure 3.14: Transition to coherence in the ensemble of  $10^6$  coupled Bernoulli maps with an inertial mean field dynamics,  $\gamma = 1/2$ .

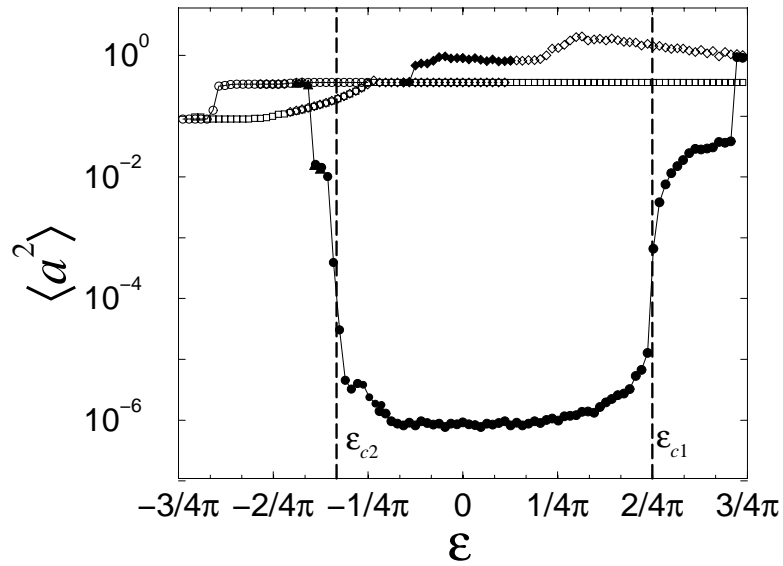


Figure 3.15: Transition to coherence in the ensemble of  $10^6$  coupled Bernoulli maps with an inertial mean field dynamics, an oscillatory transition at  $\varepsilon_{c2}$ ,  $\gamma = -2/3$ , note that even at  $|\varepsilon| \ll 1$  the trivial state  $a = 0$  is metastable.

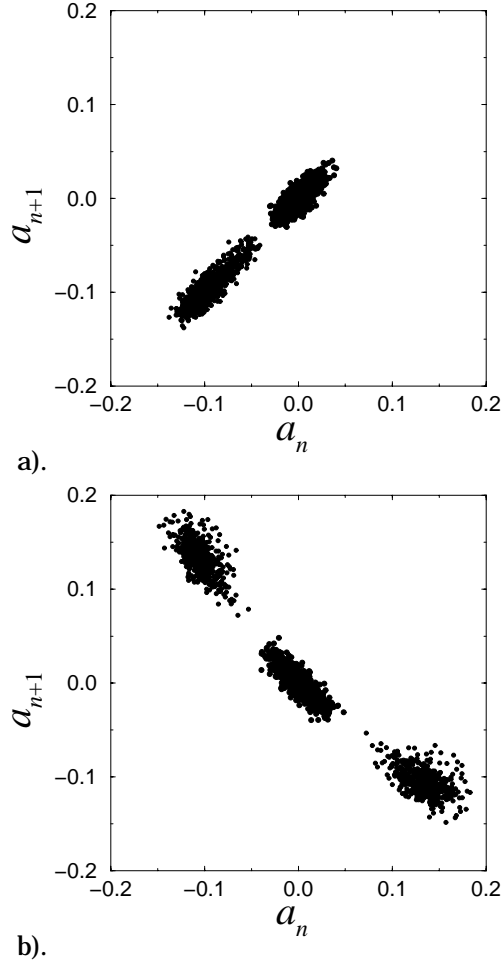


Figure 3.16: Different dynamics of the non-trivial mean field in the coherent regimes at  $\varepsilon < \varepsilon_{c2}$  with an inertial dynamics of the mean field. Ensemble size is  $N = 10^4$ . (a)  $\gamma = 1/2$ . In the disordered state at  $\varepsilon = 0.13$  the mean field vanishes up to finite-size fluctuations (a cloud around  $a_{n+1} = a_n = 0$ ); in the coherent state at  $\varepsilon = -0.07 < \varepsilon_{c2} = -1/6\pi$  nearly constant mean field is observed. (b)  $\gamma = -2/3$ . At  $\varepsilon = -0.13 < \varepsilon_{c2} = -1/3\pi$  the period of autogeneration is 2.

### 3.5.3 Ensembles of non-identical systems

Now assume that systems in the ensemble (3.1) are different

$$\begin{aligned} x_k(t+1) &= h_k(x_k(t), \varepsilon a(t)) \\ a(t) &= \frac{1}{N} \sum_{k=1}^N q(x_k(t)) \end{aligned} \quad (3.62)$$

Under which conditions does the linear theory still work?

In principle, if the ensemble still responds linearly to small periodic perturbations then it can be characterized by the transfer function  $K(\omega)$  and the transition to coherence can be analyzed in the same way as in the case of identical systems. Apparently, this holds if all the systems in the ensemble response linearly. In the thermodynamic limit  $N \rightarrow \infty$  we can proceed

### CHAPTER 3. TRANSITION TO COHERENCE IN GLOBALLY COUPLED MAPS

as if there were infinite number of systems of each kind. I. e. averaging over the ensemble can be replaced by averaging over invariant probability density of individual systems of each kind.

For each function  $h_k(x, \varepsilon a)$  a corresponding transfer function  $K_k(\omega)$  can be defined, the total transfer function is calculated as a superposition of contributions of each kind of systems. For instance, if some parameter  $r$  of systems in the ensemble is randomly distributed according to the probability distribution  $\Pi(r)$  then the total transfer function is

$$K(\omega) = \int K_r(\omega) \Pi(r) dr$$

Note that the condition that  $a_k = \langle q(x_k) \rangle = 0$  if  $\varepsilon = 0$  should be valid for all system is not required here. It is only required  $\sum a_k = 0$ . For a small harmonic driving all structurally stable systems are expected to respond at the same frequency.

As an example consider the situation that the ensemble (3.4) of Bernoulli maps is coupled with an ensemble of maps with a stable fixed point attractor. We take the simplest form of such a map giving  $\langle q(x) \rangle = \langle \cos 2\pi x \rangle = 0$ :

$$x(t+1) = \frac{1}{4} + k(x(t) - \frac{1}{4}) + \varepsilon a(t) \quad \text{with} \quad |k| < 1 \quad (3.63)$$

We assume that there are altogether  $N$  systems with the fraction  $Q$  of Bernoulli maps and the fraction  $1 - Q$  of the stable maps (3.63). The mean field is calculated by averaging over both fractions, i. e. just

$$a(t) = \frac{1}{N} \sum_{k=1}^N \cos 2\pi x_k(t)$$

The transfer function of the whole systems is

$$K(\omega) = QK_1(\omega) + (1 - Q)K_2(\omega) \quad (3.64)$$

The transfer function  $K_1(\omega)$  of the Bernoulli map fraction is given by the equation (3.45), the transfer function  $K_2(\omega)$  of the stable map fraction can be easily calculated with using the method 1 described in the section 3.3.1. The transfer function of the ensemble (3.63) at the frequency  $\omega = 2\pi q/p$  equals to the static response of the  $p$ -iterate of the map (3.63). As  $|k| < 1$  this  $p$ -iterate has a stable fixed point

$$\begin{aligned} x(t) - \frac{1}{4} = x(t+p) - \frac{1}{4} &= k^p(x(t) - \frac{1}{4}) + \varepsilon \sum_{k=0}^{p-1} k^{p-1-k} a(t+k) \\ &= k^p(x(t) - \frac{1}{4}) + \varepsilon e^{i\omega t} \sum_{k=0}^{p-1} k^{p-1-k} e^{i\omega k} \\ &= k^p(x(t) - \frac{1}{4}) + \varepsilon \frac{1 - e^{i\omega p} k^{-p}}{1 - e^{i\omega k} k^{-1}} k^{p-1} \end{aligned} \quad (3.65)$$

The complex shift of the fixed point of the  $p$ -iterate of the maps (3.63) driven at frequency  $\omega = 2\pi q/p$  is

$$\Delta x = \frac{\varepsilon}{e^{i\omega} - k}$$

### 3.5. EXTENSIONS OF THE THEORY

The transfer function as defined by the observable  $q(x) = \cos 2\pi x$  is given (with  $x_0 = 1/4$  being the fixed point of the unperturbed map) by

$$K_2(\omega) = \frac{1}{\varepsilon} q'(x_0) \Delta x = \frac{2\pi}{k - e^{i\omega}} \quad (3.66)$$

Substituting these transfer functions into the stability condition (3.17) gives for the imaginary and the real parts

$$\begin{aligned} \text{Im}K &= \pi \sin \omega \left( Q(4 \cos \omega + 1) + \frac{2(1-Q)}{k^2 - 2 \cos \omega + 1} \right) = 0 \\ \text{Re}K &= \pi \left( -Q(4 \cos^2 \omega + \cos \omega - 2) + 2(1-Q) \frac{k - \cos \omega}{k^2 - 2 \cos \omega + 1} \right) = \varepsilon_c^{-1} \end{aligned} \quad (3.67)$$

Thus there are four solutions:

(a) The zero frequency solution  $\cos \omega = 1$ . The corresponding critical coupling strength is

$$\varepsilon_c^a = -\frac{1-k}{\pi(2+Q(1-3k))} \quad (3.68)$$

This critical value is always negative for  $Q \in ]0, 1]$  and  $k \in ]-1, 1]$ .

(b) The period 2 solution  $\cos \omega = -1$ . The corresponding critical coupling strength is positive for  $Q \in [0, \frac{2}{3+k}[$  and negative for  $Q \in ]\frac{2}{3+k}, 1]$ .

$$\varepsilon_c^b = \frac{1+k}{\pi(2-Q(3+k))} \quad (3.69)$$

(c) Two more solutions given by

$$\cos \omega = \frac{1}{4} \left( \frac{k^2 + \frac{k}{2} + 1}{k} \left( 1 \pm \sqrt{1 + \frac{4k(1-Q)}{Q(k^2 + \frac{k}{2} + 1)^2}} \right) - 1 \right) \quad (3.70)$$

Of course, these solutions may not exist for some combinations of  $Q$  and  $k$  if either the argument of the square root is negative or the modulus of the right hand side exceeds 1. For the combinations of  $Q$  and  $k$  where they exist the critical value of the coupling is

$$\varepsilon_c^{c\pm} = \frac{1}{\pi Q \left( 2 - (k^2 + \frac{k}{2} + 1) \left( 1 \pm \sqrt{1 + \frac{4k(1-Q)}{Q(k^2 + \frac{k}{2} + 1)^2}} \right) \right)} \quad (3.71)$$

This critical coupling can be positive as well as negative. For different combinations of  $k$  and  $Q$  the critical value of  $\varepsilon$  is determined by different solutions  $\varepsilon_c^a$ ,  $\varepsilon_c^b$ , or  $\varepsilon_c^{c\pm}$ . To determine which solution is responsible for the transition to coherence we compare  $\varepsilon_c^a$ ,  $\varepsilon_c^b$ , and  $\varepsilon_c^{c\pm}$  at different  $Q$  and  $k$ . The two values of  $\varepsilon$ , one positive and one negative, with the smallest modulus will give the transition threshold.

Setting  $\varepsilon_c^a = \varepsilon_c^b$  gives  $Q = 2/(1+k^2) > 1$ ,  $k \in ]-1, 1[$ . This means that the solution  $\varepsilon_c^b$  is not relevant for the transition to coherence at negative  $\varepsilon$ . When calculating the condition  $\varepsilon_c^a = \varepsilon_c^c$  we take into account that this condition is an algebraic equation of the second order in  $Q$  and of the fourth order in  $k$  which has to admit a factorization. Indeed, for the combinations of  $Q$  and  $k$  which deliver  $\cos \omega = 1$  in (3.70) we already obtained the corresponding solution, which is linear in  $Q$  and quadratic in  $k$ , so that now we only have to look for the second factor, which

is linear in  $Q$  and quadratic in  $k$  too. With this approach from  $\varepsilon_c^a = \varepsilon_c^c$  follows

$$\left(5Q(1-k)^2 + 2(1-Q)\right)\left(Q(1-k)(2k+3) + 2(1-Q)\right) = 0 \quad (3.72)$$

The corresponding bifurcation curves lie in the  $(k, Q)$ -plane outside the area  $Q \in ]0, 1[$  and  $k \in ]-1, 1[$ . This means that it is the solution  $\varepsilon_c^a$  at zero frequency that determines the negative critical coupling at which the transition to coherence takes place.

Analogously, requiring  $\varepsilon_c^b = \varepsilon_c^c$ , one obtains

$$\left(-3Q(1+k)^2 + 2(1-Q)\right)\left(Q(1+k)(2k-1) + 2(1-Q)\right) = 0 \quad (3.73)$$

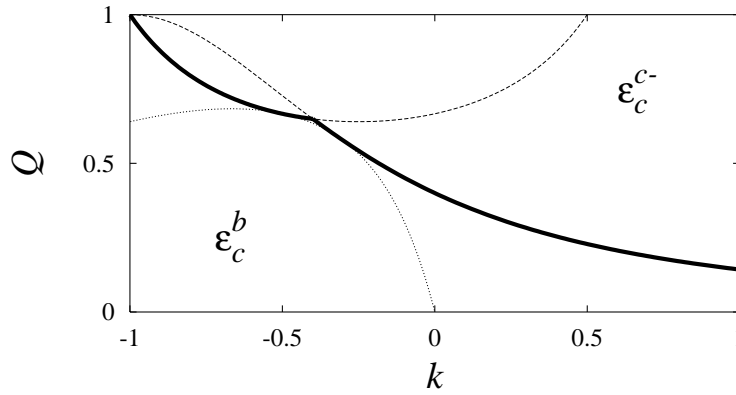


Figure 3.17: Parameter plane  $(k, Q)$ . Different regions for positive critical coupling values. Above the bold curve the transition value of the coupling is determined by  $\varepsilon_c^c$ , below it by  $\varepsilon_c^b$ , here the transition to coherence takes place with period 2. Below the dotted line no  $\varepsilon_c^c$  exists. Dashed lines correspond the condition  $\varepsilon_c^b = \varepsilon_c^c$ .

For positive critical coupling one obtains the bifurcation diagram presented in the figure 3.17. In the figures 3.18a and 3.18b the transitions for  $Q = 1/2$  and  $k = \pm 1/2$  are illustrated.

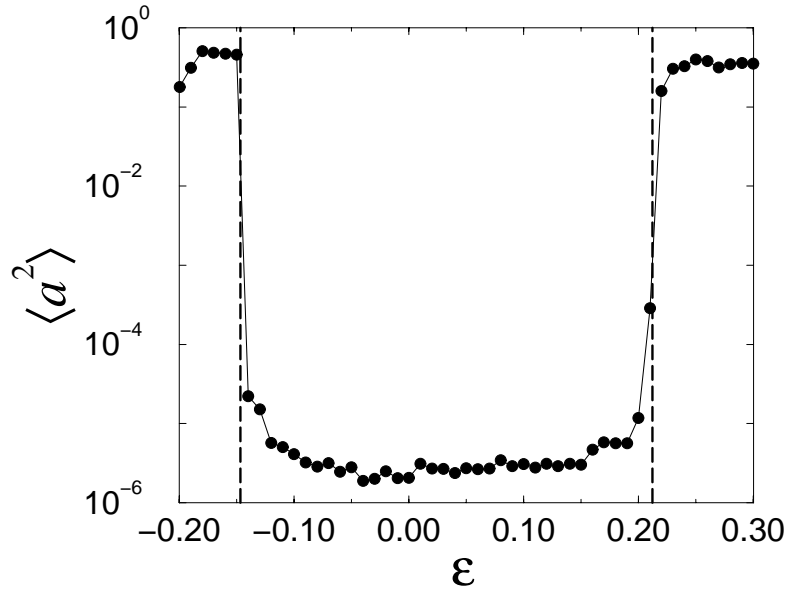
## 3.6 Possible further extentions

Here we want to give an outlook on some other possible extentions of the theory above that can be developed in future.

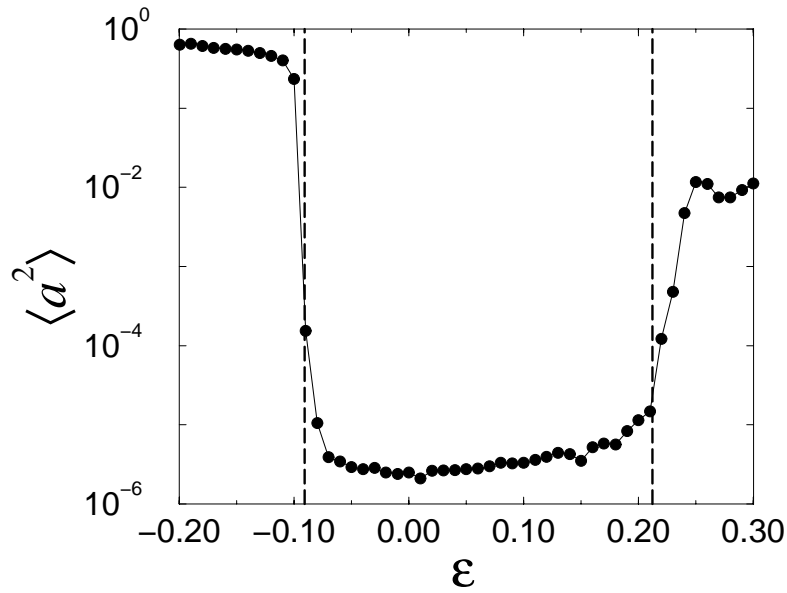
### 3.6.1 Structurally unstable systems

Amasingly, even if some systems are not structurally stable, the linear response approach should work, at least in some situations. For example, imagine the situation that an infinitely small harmonic input can stabilize a periodic orbit of the same period. Then the system (with parameter  $r$ ) will respond with a finite amplitude  $A_r(\omega)$  to this infinitesimal perturbation.

### 3.6. POSSIBLE FURTHER EXTENTIONS



a)



b)

Figure 3.18: Transition to coherence in an ensemble of Bernoulli maps coupled with an ensemble of stable maps, distant solutions are not shown.  $10^6$  systems in both ensembles,  $Q = 1/2$ , i.e. in each ensemble there are  $5 \cdot 10^5$  systems. The mean field observable is  $q(x) = \cos 2\pi x$ . With bold dashed lines the theoretical predictions are shown. (a)  $k = -1/2$ . The transition at the negative  $\varepsilon_c = -\frac{6}{13\pi}$  takes place at zero frequency, the transition at the positive  $\varepsilon_c = \frac{2}{3\pi}$  has the period 2. (b)  $k = 1/2$ . The transition at the negative  $\varepsilon_c = -\frac{2}{7\pi}$  takes place at zero frequency as well, the frequency of autogeneration at the positive  $\varepsilon_c = \frac{2}{3\pi}$  is  $\omega = \arccos(-\frac{3}{4})$ .

## CHAPTER 3. TRANSITION TO COHERENCE IN GLOBALLY COUPLED MAPS

Denoting the fraction of the systems in the ensemble responding singularly in this way to the driving with amplitude  $\varepsilon$  at frequency  $\omega$  through  $q(\omega, \varepsilon)$  we can write the output

$$\tilde{a}_{out}(\omega) = q(\omega, \varepsilon)A(\omega) + \varepsilon(1 - q(\omega, \varepsilon))K(\omega)\tilde{a}_{in}$$

Or, with self-consistency,

$$(1 - \varepsilon(1 - q(\omega, \varepsilon))K(\omega))\tilde{a} = q(\omega, \varepsilon)A(\omega) \quad (3.74)$$

The value  $A$  is obtained by averaging over all structurally unstable systems. In principle, no further assumptions have to be made on this  $A$ , it only has to be limited but does not have to be smooth.

Thus an ensemble with a small fraction  $q(\omega, \varepsilon)$  of systems responding singularly to a small harmonic perturbation at frequency  $\omega$  with amplitude  $\varepsilon$  shows small but finite mean field in the incoherent state if the device (3.74) is stable by input. The critical coupling  $\varepsilon_c$  and autogeneration frequency  $\omega_c$  are defined by the linear fraction only.

$$L(\omega) = 1 - \varepsilon(1 - q(\omega, \varepsilon))K(\omega) = 0 \quad (3.75)$$

To ensure correct integration one has to demand analyticity of  $q(\omega, \varepsilon)$ , at least in some vicinity of the roots of  $L(\omega)$ . The meaning of  $q(\omega, \varepsilon)$  is clear, it is the fraction of the systems locked in the Arnold tongue at the frequency  $\omega$ . At small  $\varepsilon$  the width of an Arnold tongue grows approximately linearly with  $\varepsilon$ . Therefore the effect of  $q(\omega, \varepsilon)$  on the stability of the linear fraction can be neglected if the transition to coherence is expected to take place at a small  $\varepsilon \ll 1$ .

In particular, this effect should be present in globally coupled Rössler oscillators. In [77] Arnold tongues for driven Rössler oscillators were calculated and found to reach very small  $\varepsilon$  values, down to  $\varepsilon \sim 10^{-2}$ . Ensembles of globally coupled Rössler oscillators have been studied and a transition to coherence with non-trivial mean field was found [76] to take place at about the same threshold of  $\varepsilon \sim 10^{-2}$ . In [105] the Arnold tongues in a driven Rössler system were found (at other parameter values) to exist at even smaller  $\varepsilon$ . It would be interesting to check in direct simulations whether the transition to coherence in an ensemble of non-identical Rössler oscillators takes place at larger  $\varepsilon$ , i. e. when a part of the systems are already locked in an Arnold tongue and respond singularly. This is the subject of the current work, the results will be reported elsewhere.

### 3.6.2 Continuous time systems

The approach of the linear response theory itself is independent of whether time is discrete or continuous. The linear response theory considers the ensemble of coupled chaotic systems as a linear device in analog signal processing, i. e. as a black box with given characteristics  $K(\omega)$ . This black box is given an input signal  $a_{in}(t)$  (in continuous time) and the output is read from the continuous time signal  $a_{out}(t)$ . What happens in interior of the black box does not concern the theoretical construction.



Therefore the only difference between the discrete time case and the continuous time case is at the stage of calculating the transfer function  $K(\omega)$ . Analyzing the Frobenius-Perron equation is to be replaced in the case of continuous time systems by analyzing Liouville or (if noise is present) Fokker-Plank equations. Of course, it is by far more difficult task.

In principle, two ways are still open to proceed. First, one could rely on numerics. As the fluctuations-dissipation theorem does not hold for general chaotic systems, the calculation of the transfer function has to be done by direct simulations [84]. Then the condition (3.17) gives the threshold of instability in the ensemble and the autogeneration frequency of the emerging macroscopic mean field.

In some cases simple analytic approximations of the linear response functions of continuous time chaotic systems can be made [84] using the shadow property of hyperbolic chaotic systems. The shadow property ensures that for every limited time interval there exists in the perturbed system a trajectory  $x$  which is  $\varepsilon$ -close to the unperturbed solution  $x_0$  in this time interval. The trick is to use this trajectory for averaging in the perturbed system. Unfortunately, the approximations like that in [84] give a good asymptotic description for small and large  $\omega$  but fail in the near of the peak in the power spectrum of the unperturbed dynamics. Thus the approach of analytic approximations can be useful if the autogeneration frequency lies far away from this peak.

That this can be the case we have already seen in the example of an inertial dynamics of the mean field in the previous section, where introducing the parameter of inertia  $\gamma$  changed the frequency of autogeneration so that this frequency could be tuned by changing  $\gamma$ .

### 3.7 Summary

Despite the dynamical equations (3.1) describing an ensemble of chaotic maps globally coupled through a mean field are not explicitly time-dependent there exist at a stronger coupling coherent states where the attractor do not possess a natural measure which is invariant in time. Instead, this measure (and the mean field calculated according to this measure) oscillates.

The transition can be analyzed by considering the supplementary problem of finding the first correction term of the natural measure of an individual system in the ensemble driven instead of mean field by a small harmonic external force at a given frequency. For structurally stable systems this response is expected to be linear so that the system can be linearized. By analyzing the linear response in the driven system the complex transfer function is defined, from the self-consistency condition on the input and output mean field the complex stability condition for the disordered state is defined. The transition to coherence can be described as a self-excitation in a linear amplifier with feedback. The frequency of autogeneration is derived from the condition on the imaginary part of the transfer function, the critical value of the coupling from its real part.

If the autogeneration frequency is not zero then the transition is a discrete Hopf bifurcation. If it is zero then the bifurcation can be subcritical and hysteretic due to existency of distant solutions (i. e. solutions with non-small amplitudes). This is the case in an ensemble

### CHAPTER 3. TRANSITION TO COHERENCE IN GLOBALLY COUPLED MAPS

of coupled Bernoulli maps which we could fully analyze as an example of an application of the linear theory.

The linear theory can be extended for the case of noisy dynamics, the case where there is an additional dynamical equation for the inherent dynamics of the mean field, the case of ensembles of non-identical systems, the case of continuous time systems, the case where some part of the systems in the ensemble are structurally unstable. The cases of continuous time systems and systems with structurally unstable fraction are especially intriguing, it would be interesting to investigate whether they admit a (partially) analytic treatment. In the case of continuous time systems one could make analytic approximations to the linear response function and proceed further with this approximation, which should work better if the autogeneration frequency lies far away of the mean peak in the power spectrum of an uncoupled individual system. If in the ensemble there is a structurally unstable fraction then we expect that the stability of the disordered state and the autogeneration frequency are determined by the linear fraction only. It would be worth trying to find this effect numerically.

# Résumé

In this work we studied synchronization phenomena in lattices of coupled dynamical systems. At small coupling strength the dynamics of an individual system in the lattice remains close to the dynamics in the unperturbed case but from some threshold on the systems reveal a certain coherence which can be seen in the dependence of some averaged quantity from the coupling strength.

We studied this transition to coherence in two different cases, for continuous time systems with nearest-neighbor coupling and for discrete time systems with global coupling. Since interacting oscillating continuous time systems can be described for a small coupling by closed phase equations a lattice of coupled phase equations with nearest-neighbor coupling was investigated. The coupling was implemented via coupling function such that for nearly coinciding dynamics of the systems it was equivalent to the dissipative coupling through the diffusion operator. In the case of discrete time systems an ensemble of chaotic maps globally coupled via mean field was investigated.

## *(i) Oscillator lattices with nearest-neighbor coupling, symmetries*

In the lattice of coupled oscillators described with the phase equations a hierarchical synchronization transition was observed. The observable was chosen to be the average rotation velocity, in absence of interactions all individual natural velocities are different. Generically the effects of clustering, i. e. successive grouping of oscillators into clusters of equal average velocities, and frequency locking are observed. For every limited lattice size there exists a critical coupling value above which a stable fixed point solution exists. This critical coupling can be calculated in the case of nearest-neighbor coupling for any lattice size, in the case of linearly distributed natural velocities it is quadratically diverging with increasing lattice size. In the thermodynamic limit no fixed point solution exists.

In the particular case of linearly distributed natural velocities also the effect of sensitive dependence of the average velocities from the initial conditions was found. This effect is explained with reversibility of the lattice. Reversibility means that there exists an involution which together with the time reversal leaves the equations of motion invariant. The solutions of a reversible system can be of two different types, either dissipative or what we called quasi-Hamiltonian. If a solution is typical for an ergodic set then the property of dissipativity or quasi-Hamiltonicity holds for the whole set.

## RESUME

A trajectory crossing the set of the invariant points of the reversibility involution is called reversible, if an ergodic set contains a reversible non-wandering trajectory then it is quasi-Hamiltonian, its properties resemble the properties of Hamiltonian systems. In particular, the Lyapunov exponents come in pairs of opposite signs, the phase volume is conserved on time average. In direct numerical simulations we found coexistent chaotic and quasi-periodic quasi-Hamiltonian ergodic sets. The mean velocity is the same for every initial condition from the chaotic ergodic set and different on every orbit from a quasi-periodic window, which explains the smeariness of the bifurcation diagrams.

In general reversible systems Quasi-Hamiltonian features are expected if the dimension of the invariant set of the reversibility involution is large enough, i. e. at least  $[(N - 1)/2]$ , with  $N$  being the size of the lattice. Then its images should cross it and one can expect the existence of periodic and, by continuity, non-wandering reversible trajectories.

At large coupling no quasi-Hamiltonian regimes are observed. The transition from the quasi-Hamiltonian to the dissipative dynamics is generally smooth and is a symmetry breaking chaos-chaos transition. The symmetric attractor of the system splits into an attractor-repeller pair. Despite both attractor and repeller appear to be dense in the phase space, it follows from the Birkhoff ergodic theorem that they have to be mutually singular. Therefore they have to be fractals of zero Lebesgue measure. For larger lattices the transition to the dissipative regime takes place at nearly same coupling strength. The reason is that the dynamics of the system is more sensitive on the ends of the chain and, therefore, the length of its middle part does not play any role.

The reversibility is caused by the specific symmetries of the coupling function and distribution of the natural frequencies. If these symmetries are violated the quasi-Hamiltonian features are destroyed.

Quasi-Hamiltonian behavior in the system constructed as dissipative shows importance of symmetries for synchronization phenomena in coupled complex systems. This behavior is characterized by a complicated topological structure of the phase space which should be understood in a better way in future. It is interesting to apply the concept of reversibility to arrays of coupled Josephson arrays where high symmetries ensuring reversibility are present.

### *(ii) Chaotic maps globally coupled via mean field*

In chaotic systems globally coupled via mean field a transition to coherence is observed, in the coherent states the dynamics of the individual systems remains chaotic but the mean field oscillates nearly periodic or fluctuates around a non-zero constant. In the disordered state the mean field is zero up to statistical fluctuations due to finite-size effects. The transition to coherence can be understood as the loss of stability by the trivial zero field state due

to fluctuations.

Because fluctuations are small on onset of transition, the study of stability can be made in a linearized system. This systems can be described as a linear amplifier with feedback. In order to completely solve the stability problem it is enough to calculate the linear response function of the amplifier without feedback describing the linear amplification coefficient at a given frequency. After defining the linear response of the systems without feedback, i. e. without the self-consistency of the mean field fluctuations the point of the transition to coherence is defined by the complex relation  $K = 1$ . From the imaginary part of this relation the frequency of the autogeneration is defined, from the real part one obtains the critical coupling strength on this frequency. This critical value does not need to be small.

To obtain a smooth linear response function the perturbation caused by the statistical fluctuations should be such that the number of preimages of the underlying maps is not changed for all points from the range of the map. To obtain the transfer function two approaches can be used.

*Method 1:* If the period of the fluctuations is rational  $q/p$  then the  $p$ -iterate of the initial map is autonomous with respect to the perturbation, the linear response to the perturbation with period  $p$  is equivalent to the static response of the  $p$ -iterate of the map. To define this static response the Frobenius-Perron-like equation is written for the first corrections to the invariant density of the unperturbed system.

*Method 2:* For maps on a unit circle the Frobenius-Perron operator can be rewritten in a spectral form. For the coefficient of the solution an infinite-dimensional rekursive system of algebraic equations has to be solved.

As an example an ensemble of Bernoulli maps was investigated, the transfer function was computed with both methods. The structure of bifurcations at positive and negative couplings was studied. The transition at positive coupling is a discrete time Hopf bifurcation with the characteristic square-root-scaling. At negative coupling an asymmetrical subcritical bifurcation takes place, there exist distant and close solutions with respect to the trivial zero state, the corresponding linear scaling of the close colution has been confirmed by the numerics.

The linear theory can be extended. Noisy terms can be incorporated into the spectral representation of the Frobenius-Perron operator. Considering inherent dynamics of the mean miel and ensembles of non-identical systems do not requires any reformulation of the linear theory, only the autogeneration condition is changed due to the different form of feedback loop.

Further progress can probably be done in future by extending the linear theory on continuous time systems and structurally unstable systems. In the case of continuous time systems the accent to be set on methods of defining linear response function. Existing methods are

## RESUME

not working well if the frequency of autogeneration is close to the peak of the power spectrum of the individual system. In the case of structurally unstable systems an interesting question could be to consider an ensemble of non-identical chaotic systems in which a small fraction of the systems respond singularly but no autogeneration takes place. This can be the case in globally coupled Rössler oscillators.

# Acknowledgements

The work presented in this thesis was done at the Institut für Physik der Universität Potsdam under the supervision of Prof. Dr. A. Pikovsky. I would like to thank Prof. Dr. A. Pikovsky for creating a challenging and inspiring scientific environment and for providing me with his endless support. His valuable guidance, creative suggestions, constructive criticism and constant encouragement during the whole work are unforgettable. His analytical perusal of the manuscript is highly acknowledged. My best acknowledgments go to Prof. Dr. U. Feudel, Prof. Dr. E. Mosekilde, and Prof. Dr. A. Pikovsky for their readiness to be referees of this thesis.

I appreciated enlightening discussions and fruitful cooperations I had with my colleagues. In particular, I am grateful to Prof. Dr. U. Feudel, Prof. Dr. W. Fuhrmann, Prof. Dr. J. Kurths, Prof. Dr. S. Kuznetsov, Prof. Dr. Yu. Maistrenko, Prof. Dr. G. Pfister, Prof. Dr. A. Pikovsky, Prof. Dr. A. Politi, Prof. Dr. S. Ruffo, Prof. Dr. D. Stauffer, Dr. M. Abel, Dr. V. Ahlers, Dr. B. Blasius, Dr. A. Demircan, Dr. O. Isaeva, Dr. W. Jansen, Dr. R. Hachenberger, Dr. I. Katzorke, Dr. W.-H. Kye, Dr. S. Kraut, Dr. A. Lerner, Dr. E. Neumann, Dr. E.-H. Park, Dr. O. Popovych, Dr. S. Popovych, Dr. M. Rosenblum, Dr. A. Sitz, Dr. S. Titz, Dr. D. Turaev, Dr. A. Witt, Dr. H.-L. Yang, Dr. A. Zaikin, Dr. M. Zaks, Dr. Chr. Ziehmann, Dr. R. Zillmer, and many others.

My thanks also go to members of the Sonderforschungsbereich 555 "Complex Nonlinear Processes", particularly to its principal organizers Prof. Dr. W. Ebeling, Prof. Dr. J. Kurths, Prof. Dr. L. Schimansky-Geier, and Prof. E. Scholl, for providing an excellent scientific infrastructure in Berlin and Potsdam and the Deutsche Forschungsgemeinschaft for its financial support of this investigation.

Thanks are also due to all the faculty staff for the technical assistance I was given throughout the project, especially I owe thanks to M. Dörrwand, B. Nader, and M. Path, who helped a lot in all the necessary official works during the period of my stay in Potsdam. I wish to thank Dr. I. Katzorke, Dr. V. Ahlers and J.-U. Tessmer for their efforts in maintaining our computer facilities.

I record my special thanks to all the members of the Institute for a pleasant working atmosphere and to all players, supporters, and sympatisants of the FC Torpedo Chaos 06 that ensured my sufficient fitness, especially during the hard time at the end of this project.

My indebtedness to my parents and to my wife Nathalie is beyond expression. Their love and affection and the smiles of my son Dan always stood by me as a long-lasting source of encouragement. Finally I am grateful to all my relatives and friends for all the rest.





# Bibliography

- [1] V. S. Afraimovich, V. I. Nekorkin, G. V. Osipov, and V. D. Shalfeev. *Stability, Structures and Chaos in Nonlinear Synchronization Networks*. World Scientific, Singapore, 1994.
- [2] T. Aoyagi and Y. Kuramoto. Frequency order and wave patterns of mutual entrainment in two-dimensional oscillator lattices. *Phys. Lett. A*, 155(6,7):410–414, 1991.
- [3] E. V. Appleton. The automatic synchronization of triode oscillator. *Proc. Cambridge Phil. Soc. (Math. and Phys. Sci.)*, 21:231–248, 1922.
- [4] V. I. Arnold. Small denominators. I. Mappings of the circumference onto itself. *Izv. Akad. Nauk Ser. Mat.*, 25(1):21–86, 1961. (In Russian); English Translation: AMS Transl. Ser. 2, v. 46, 213-284.
- [5] V. I. Arnold. Remarks on the perturbation problem for problems of Mathieu type. *Usp. Mat. Nauk*, 38(4):189–203, 1983. (In Russian); English Translation: Russ. Math. Surveys, 1983, v. 38, 215-233.
- [6] H. Atmanspacher, J. Kurths, H. Scheingraber, R. Wackerbauer, and A. Witt. Complexity and meaning in nonlinear dynamical systems. *Open syst. and inf. dyn.*, 1:269, 1993.
- [7] S. Y. Auyang. *Foundations of complex system theories*. Cambridge University Press, Cambridge, 1998.
- [8] P. Bak, C. Tang, and K. Wiesenfeld. Self-organized criticality. *Phys. Rev. A*, 38:364–374, 1988.
- [9] M. Bakhtine. *Le Marxisme et la philosophie du langage*. Éditions de Minuit, Paris, 1977.
- [10] N. J. Balmforth, A. Jacobson, and A. Provenzale. Synchronized family dynamics in globally coupled maps. *CHAOS*, 9(3):738–754, 1999.
- [11] G. D. Birkhoff. On the periodic motions of dynamical systems. *Acta Math.* (reprinted in *MacKay and Meiss 1987*), 50:359, 1927.
- [12] I. I. Blekhman. *Vibrational mechanics*. Nauka, Moscow, 1994. (in Russian).
- [13] B. Boashash. Estimating and interpreting the instantaneous frequency of a signal. *Proc. of the IEEE*, 80(4):520–568, 1992.

## BIBLIOGRAPHY

- [14] A. A. Bogdanov. *Essays in tektology: the general science of organization*. Intersystems publications, Seaside CA, 1984.
- [15] R. Bowen and D. Ruelle. The ergodic theory of axiom-A flows. *Inventiones Mathematicae*, 29:181, 1975.
- [16] Y. Braiman, W. L. Ditto, K. Wiesenfeld, and M. L. Spano. Disorder-enhanced synchronization. *Physics Letters A*, 206:54–60, 1995.
- [17] A. H. Cohen, Ph. J. Holmes, and R. H. Rand. The nature of the coupling between segmental oscillators of the lamprey spinal generator for locomotion: a mathematical model. *J. Math. Biology*, (13):345–369, 1982.
- [18] I. P. Cornfeld, S. V. Fomin, and Ya. G. Sinai. *Ergodic Theory*. Springer, New York, 1982.
- [19] A. Crisanti, G. Paladin, and A. Vulpiani. *Products of Random Matrices in Statistical Physics*. Springer, Berlin, 1993.
- [20] M. de Sousa Vieira, A. J. Lichtenberg, and M. A. Lieberman. Self synchronization of many coupled oscillations. *Int. J. of Bifurcation and Chaos*, 4(6):1563–1577, 1994.
- [21] A. Denjoy. Sur les courbes définies par les équations différentielles à la surface du tore. *J. Math. Pures Appl.*, 11:333–375, 1932.
- [22] B. Van der Pol. On relaxation oscillation. *Phil. Mag.*, 2:978–992, 1926.
- [23] N. E. Diamant and A. Bortoff. Nature of the intestinal slow-wave frequency. *Am. J. Physiol.*, 216(2):301–307, 1969.
- [24] R.K. Dodd, J.C. Eilbeck, J.D. Gibbon, and H.C. Morris. *Solitons and Nonlinear Wave Equations*. Academic Press, London, 1982.
- [25] W. Ebeling. *Chaos und Cosmos: Prinzipien der Evolution*. Springer, Berlin-Heidelberg-Oxford, 1994.
- [26] J.-P. Eckmann and D. Ruelle. Ergodic theory of chaos and strange attractors. *Rev. Mod. Phys.*, 57:617–656, 1985.
- [27] W. Bodmer (Ed.). *Mathematical and statistical aspects of DNA and protein sequence analysis*. Philosophical transactions of the Royal Society of London, Ser: B. 1310, London, 1994.
- [28] M. Eigen and P. Schuster. *The hypercycle*. Springer, Berlin, 1979.
- [29] G. B. Ermentrout and N. Kopell. Frequency plateaus in a chain of weakly coupled oscillators, I. *SIAM J. Math. Anal.*, 15(2):215–237, 1984.
- [30] S. V. Ershov. Is a perturbation theory for dynamical chaos possible? *Phys. Lett. A*, 177:180–185, 1993.

## BIBLIOGRAPHY

- [31] H. Fujisaka and T. Yamada. A new intermittency in coupled dynamical systems. *Prog. Theor. Phys.*, 74(4):918–921, 1985.
- [32] H. Fujisaka and T. Yamada. Stability theory of synchronized motion in coupled-oscillator systems. IV. Instability of synchronized chaos and new intermittency. *Prog. Theor. Phys.*, 75(5):1087–1104, 1986.
- [33] D. Gabor. Theory of communication. *J. IEE London*, 93(3):429–457, 1946.
- [34] P. Glansdorff and I. Prigogine. *Thermodynamic theory of structure, stability and fluctuations*. Wiley-Interscience, London, 1971.
- [35] A. F. Glova, S. Yu. Kurchatov, V. V. Likhanskii, A. Yu. Lysikov, and A. P. Napartovich. Coherent emission of a linear array of CO<sub>2</sub> waveguide lasers with a spatial filter. *Quantum Electronics*, 26(6):500–502, 1996.
- [36] P. Grassberger and I. Procaccia. Dimensions and entropies of strange attractors from a fluctuating dynamics approach. *Physica D*, 13:34–54, 1984.
- [37] S. Großmann. Linear response in chaotic states of discrete dynamics. *Z. Phys. B*, 57:77–84, 1984.
- [38] J. Guckenheimer. Isochrons and phaseless sets. *J. Math. Biology*, 1:259–273, 1975.
- [39] P. Hadley, M. R. Beasley, and K. Wiesenfeld. Phase locking of Josephson-junction series arrays. *Phys. Rev. B*, 38:8712–8719, 1988.
- [40] H. Haken. *Advanced synergetics*. Springer-Verlag, Berlin, 1983.
- [41] F. A. Hayek. *Studies in philosophy, politics and economics*. Wiley, London-Chicago-Toronto, 1967.
- [42] B. Hu and Zh. Zheng. Phase synchronizations: transitions from high- to low-dimensional tori through chaos. *Int. J. Of Bif. and Chaos*, 10(10):2399–2414, 2000.
- [43] Ch. Huygens. *Œvres Complètes*, volume 15. Swets & Zeitlinger B. V., Amsterdam, 1967.
- [44] M. A. Jaglom and I. M. Jaglom. *Wahrscheinlichkeit und Information*. Dt. Verlag der Wissenschaften, Berlin, 1984.
- [45] K. Kaneko. Clustering, coding, switching, hierarchical ordering and control in network of chaotic elements. *Physica D*, 41:137–172, 1990.
- [46] K. Kaneko. Globally coupled chaos violates the law of large numbers but not the central-limit theorem. *Phys. Rev. Lett.*, 65:1391–1394, 1990.
- [47] K. Kaneko, editor. *Theory and Applications of Coupled Map Lattices*. John Wiley & Sons, Chichester, 1993.
- [48] A. Katok and B. Hasselblatt. *Introduction to the Modern Theory of Dynamical Systems*. Cambridge University Press, 1995.

## BIBLIOGRAPHY

- [49] A. I. Khinchin. *Mathematical foundations of statistical mechanics*. Dover Publ., Inc., New York, 1949.
- [50] R. Klages and J. R. Dorgman. Simple maps with fractal diffusion coefficients. *Phys. Rev. Lett.*, 74(3):387–390, 1995.
- [51] A. N. Kolmogorov. Eine neue metrische invariante transitiver dynamischer systeme und automorphismen von lebesque-Räumen (in russ.). *Dokl. Akad. Nauk SSSR*, 119:861, 1958.
- [52] A. N. Kolmogorov. Über die entropie zur zeit eins als metrische invariante von automorphismen (in russ.). *Dokl. Akad. Nauk SSSR*, 124:754, 1959.
- [53] N. Kopell and G. B. Ermentrout. Symmetry and phase locking in chains of weakly coupled oscillators. *Comm. Pure Appl. Math.*, 39:623–660, 1986.
- [54] Y. Kuramoto. *Chemical Oscillations, Waves and Turbulence*. Springer, Berlin, 1984.
- [55] W.-H. Kye and D. Topaj. Attractor bifurcation and on-off intermittency. *Phys. Rev. E*, 63:045202(R), 2001.
- [56] P. S. Laplace. *A philosophical essay on probabilities*. Wiley, New York, 1917.
- [57] A. Lasota and M. C. Mackay. *Probabilistic Properties of Deterministic Systems*. Cambridge University Press, Cambridge, 1985.
- [58] R. W. Leven, B.-P. Koch, and B. Pompe. *Chaos in dissipativen Systemen*. Akademie-Verlag, Berlin, 1989.
- [59] A. J. Lichtenberg. *Phase space dynamics of particles*. Wiley, New York, 1969.
- [60] N. Luhmann. *Soziale Systeme*. Suhrkamp, Frankfurt am Main, 1988.
- [61] A. N. Malakhov. *Fluctuations in Self-Oscillatory Systems*. Nauka, Moscow, 1968. (In Russian).
- [62] I. G. Malkin. *Some Problems in Nonlinear Oscillation Theory*. Gostechizdat, Moscow, 1956. (In Russian).
- [63] J. Milnor. On the concept of attractor. *Commun. Math. Phys.*, 99:177–195, 1985.
- [64] V. I. Oseledec. A multiplicative ergodic theorem for lyapunov characteristic numbers for dynamical systems. *Trans. Moscow Math. Soc.*, 19:197–231, 1968.
- [65] E. Ott. *Chaos in Dynamical Systems*. Cambridge Univ. Press, Cambridge, 1992.
- [66] G. Paladin and A. Vulpiani. Anomalous scaling laws in multifractal objects. *Phys. Rep.*, 156:147–225, 1987.
- [67] P. Panter. *Modulation, Noise, and Spectral Analysis*. McGraw–Hill, New York, 1965.
- [68] C. S. Peirce. *Collected papers*. Harvard University Press, Cambridge MA, 1932.

## BIBLIOGRAPHY

- [69] A. A. Pervozvansky. *Automatic control theory*. Nauka, Moscow, 1986. (in Russian).
- [70] Ja. B. Pesin. Lyapunov characteristic exponents and ergodic properties of smooth dynamical systems with an invariant measure. *Sov. Math. Dokl.*, 17:196, 1976.
- [71] A. Pikovsky, M. Rosenblum, and J. Kurths. *Synchronization. A Universal Concept in Nonlinear Sciences*. Cambridge University Press, Cambridge, 2001.
- [72] A. S. Pikovsky. Phase synchronization of chaotic oscillations by a periodic external field. *Sov. J. Commun. Technol. Electron.*, 30:85, 1985.
- [73] A. S. Pikovsky and J. Kurths. Collective behavior in ensembles of globally coupled maps. *Physica D*, 76:411–419, 1994.
- [74] A. S. Pikovsky and J. Kurths. Do globally coupled maps really violate the law of large numbers? *Phys. Rev. Lett.*, 72(11):1644–1646, 1994.
- [75] A. S. Pikovsky and J. Kurths. Roughening interfaces in the dynamics of perturbations of spatiotemporal chaos. *Phys. Rev. E*, 49(1):898–901, 1994.
- [76] A. S. Pikovsky, M. G. Rosenblum, and J. Kurths. Synchronization in a population of globally coupled chaotic oscillators. *Europhys. Lett.*, 34(3):165–170, 1996.
- [77] A. S. Pikovsky, M. G. Rosenblum, G. V. Osipov, and J. Kurths. Phase synchronization of chaotic oscillators by external driving. *Physica D*, 105:219–238, 1997.
- [78] A. S. Pikovsky, M. G. Rosenblum, M. A. Zaks, and J. Kurths. Phase synchronization of regular and chaotic oscillators. In H. G. Schuster, editor, *Handbook of Chaos Control*, pages 305–328. Wiley-VCh, 1999.
- [79] A.S. Pikovsky, M.G. Rosenblum, and J. Kurths. Phase synchronization in regular and chaotic systems. *Int. J. of Bifurcation and Chaos*, 10(11):2291–2306, 2000.
- [80] O. Popovych, Yu. Maistrenko, and E. Mosekilde. Loss of coherence in a system of globally coupled maps. *Phys. Rew. E*, 64:026205, 2001.
- [81] I. Prigogine and I. Stengers. *Order out of chaos*. Heinemann, London, 1984.
- [82] L. R. Rabiner and B. Gold. *Theory and Application of Digital Signal Processing*. Prentice–Hall, Englewood Cliffs, NJ, 1975.
- [83] J. Rayleigh. *The Theory of Sound*. Dover Publ., New York, 1945.
- [84] C. Reick. Analytic approximation to linear response functions of chaotic systems. In *Computational Physics Nonlinear Dynamical Phenomena in Physical, Chemical and Biological Systems. Proc. of th 3rd IMACS Int. Conf. on Comput. Phys., Lyngby, Denmark, 1-4 Aug. 1994*, pages 209–214. IMACS (Rutgers Univ.), Piscataway, NJ, USA, 1994.
- [85] L. Ren and B. Ermentrout. Phase locking in chains of multiple-coupled oscillators. *Physica D*, 143(1-4):56–73, 2000.

## BIBLIOGRAPHY

- [86] J. A. G. Roberts and G. R. W. Quispel. Chaos and time-reversal symmetry. Order and chaos in reversible dynamical systems. *Physics Reports*, 216:63–177, 1992.
- [87] M. Rosenblum, A. Pikovsky, and J. Kurths. Phase synchronization of chaotic oscillators. *Phys. Rev. Lett.*, 76:1804, 1996.
- [88] M. Rosenblum, A. Pikovsky, and J. Kurths. From phase to lag synchronization in coupled chaotic oscillators. *Phys. Rev. Lett.*, 78:4193–4196, 1997.
- [89] J. S. Rowlinson and J. D. Van der Waals. *On the continuity of the gaseous and liquid states, Studies in statistical mechanics XIV, in: J. L. Lebowitz (Ed.)*. North Holland, Amsterdam, 1988.
- [90] D. Ruelle. An inequality for the entropy of differentiable maps. *Bol. Soc. Bras. Math.*, 9:83–87, 1978.
- [91] D. Ruelle. *Zufall und Chaos*. Springer, Berlin, 1993.
- [92] M. Schroeder. *Fractals, Chaos, and Power Laws*. Freeman, New York, 1991.
- [93] W. Seifritz. *Wachstum, Rückkopplung und Chaos*. Hanser, München, 1987.
- [94] M. B. Sevryuk. *Reversible Systems*. Springer Lecture Notes in Mathematics, v. 1211, Berlin, 1986.
- [95] C. E. Shannon. *The mathematical theory of communication*. Urbana, Univ. of Illinois Press, 1972.
- [96] C. E. Shannon. *Shannon, Claude Elwood: collected papers*. IEEE Computer Soc. Press, New York, 1993.
- [97] J. G. Sinai and E. Vul. Hyperbolicity conditions for the Lorenz model. *Physica D*, 2:3, 1981.
- [98] M.J.T. Smith and R.M. Mersereau. *Introduction to Digital Signal Processing. A Computer Laboratory Textbook*. Wiley, New York, 1992.
- [99] H. Sompolinsky, D. Golomb, and D. Kleinfeld. Cooperative dynamics in visual processing. *Phys. Rev. A*, 43:6990–7011, 1991.
- [100] R. L. Stratonovich. *Topics in the Theory of Random Noise*. Gordon and Breach, New York, 1963.
- [101] S. H. Strogatz and R. E. Mirollo. Stability of incoherence in a population of coupled oscillators. *J. Stat. Phys.*, 63(3/4):613–635, 1991.
- [102] D. Topaj, W.-H. Kye, and A. Pikovsky. Transition to coherence in populations of coupled chaotic oscillators: a linear response approach. *Phys. Rev. Lett.*, 87:074101, 2001.
- [103] D. Topaj and A. Pikovsky. Reversibility versus synchronization in oscillator lattices. *submitted to Physica D*.

## BIBLIOGRAPHY

- [104] K. Y. Tsang, S. H. Strogatz, and K. Wiesenfeld. Reversibility and noise sensitivity in globally coupled oscillators. *Phys. Rev. Lett.*, 66:1094–1097, 1991.
- [105] T. E. Vadivasova, A. G. Balanov, O. V. Sosnovtseva, D. E. Postnov, and E. Mosekilde. Synchronization in driven chaotic systems: Diagnostics and bifurcations. *Phys. Lett. A*, 253(1-2):66–74, 1999.
- [106] L. von Bertalanffy. *General system theory*. Braziller, Berlin-Amsterdam, 1968.
- [107] G. Weinreich. Coupled piano strings. *J. Acoust. Soc. Am.*, 62:1474, 1977.
- [108] K. Wiesenfeld. Noise, coherence, and reversibility in Josephson arrays. *Phys. Rev. B*, 45(1):431–435, 1992.
- [109] K. Wiesenfeld, C. Bracikowski, G. James, and R. Roy. Observation of antiphase states in a multimode laser. *Phys. Rev. Lett.*, 65:1749–1752, 1990.
- [110] K. Wiesenfeld and J. W. Swift. Averaged equations for Josephson junction series arrays. *Phys. Rev. E*, 51(2):1020–1025, 1995.
- [111] A. T. Winfree. Biological rhythms and the behavior of populations of coupled oscillators. *J. Theor. Biol.*, 16:15–42, 1967.
- [112] A. T. Winfree. *The Geometry of Biological Time*. Springer, 1980.
- [113] F. Xie and H. A. Cerdeira. Coherent-ordered transition in chaotic globally coupled maps. *Phys. Rev. E*, 54(4):3235–3238, 1996.
- [114] T. Yamada and H. Fujisaka. Intermittency caused by chaotic modulation. I. Analysis with a multiplicative noise model. *Prog. Theor. Phys.*, 76(3):582–591, 1986.
- [115] H. L. Yang, Z. Q. Huang, and E. J. Ding. Attractor bifurcation and on-off intermittency. *Phys. Rev. Lett.*, 77:4899, 1996.
- [116] Z. G. Zheng, G. Hu, and B. Hu. Phase slips and phase synchronization of coupled oscillators. *Phys. Rev. Lett.*, 81(24):5318–5321, 1998.

